THE UNIVERSITY OF MANITOBA

CONTRIBUTIONS TO STATISTICAL PROCESS CONTROL TOOLS

by

Keoagile Thaga

A Thesis

Submitted to the Faculty of Graduate Studies

in Partial Fulfillment of the Requirements for the Degree of

Doctor of Philosophy

Department of Statistics

Winnipeg, Manitoba

December, 2003

THE UNIVERSITY OF MANITOBA

FACULTY OF GRADUATE STUDIES

*****

COPYRIGHT PERMISSION

CONTRIBUTIONS TO STATISTICAL PROCESS CONTROL TOOLS

BY

Keoagile Thaga

A Thesis/Practicum submitted to the Faculty of Graduate Studies of The University of Manitoba in partial fulfillment of the requirement of the degree

Of

DOCTOR OF PHILOSOPHY

Abstract

Single univariate and multivariate control charts capable of quickly detecting small and large changes in the process location and/or spread are proposed. We develop these charts under the normality assumption for both independent and autocorrelated processes. These charts are compared among themselves and to other single charts in the literature using their out-of-control average run length by first adjusting their control limits so that the compared charts have the same in-control average run length.

We propose two univariate cumulative sum (CUSUM) charts and two multivariate charts; one CUSUM chart and one Shewhart-type chart. These four charts are designed based on the assumption that a process being monitored will produce measurements that are independent and identically distributed over time when only the inherent sources of variability are present in the system. Two more charts are developed for autocorrelated processes by first fitting a times series model and then monitoring the residuals. The observations are represented by a first-order autoregressive process plus a random error model.

We also assess the performance of an attributes chart for high yield processes. The chart based on Poisson approximation is recommended based on its comparability to the binomial chart for these processes.

Acknowledgments

I am greatly indebted to two special people whose influence shaped this thesis, my advisors Dr. Smiley W. Cheng and Dr. Brian D. Macpherson. I thank them for their guidance and invaluable academic and financial support. In particular, I learned the spirit and persistence required to produce outstanding academic research from them. I would also like to thank my committee members Dr. F. A. Spiring who discussed with me a couple of research ideas, Dr. J. Pai and my external examiner Dr. D. C. Montgomery for their valuable contributions. I would like to also thank my sponsor and employer, the University of Botswana for the financial support.

One special person who deserves my acknowledgement is my former officemate Dr. Y. M. Chang who introduced me to Matlab and Latex softwares. Without him I wouldn't have achieved this. I would also like to acknowledge those professors in the Department of Statistics for imparting much useful knowledge.

Unspeakable joy chokes me ecstatically when I try to utter thanks to my family. Thanks to my loving wife Portia who took all my family responsibilities. Thanks to my beautiful children, Anita, Ketshepile, Neo and Tlotlo for their sacrifices. I love you guys. May God bless us.

I would like to dedicate this PhD. thesis to my wife Mrs. Portia Emzo Thaga, my late father Mr. Thaga and my mother Mrs. Nkhabe Thaga. These are the people who made me what I am. The completion of this work was solely due to their steadfast love, support, encouragement and inspiration. The whole Thaga and Manthe families deserve special thanks for their support.

Table of Contents

List of Tables

List of Figures

Chapter 1

Introduction

1.1 Overall View

In business, the main objective of the producer or service provider is to produce goods and services that satisfy the customers' increasing demand for high quality goods and services. However, it is not possible to produce goods that are always exactly identical, even if they are produced under the same environmental conditions. Variability is inevitable. Variability can only be described in statistical terms and thus statistical methods play an integral part in quality improvement efforts. Control charts are basic and most powerful tools in statistical process control (SPC) and are widely used for monitoring quality characteristics of a process. A process can be defined as *a set of causes and conditions that repeatedly come together to transform inputs into outcomes.* These inputs include such things as raw materials, machinery, people and information while outcomes include, among others, products, services and behavior. There are two types of data used for quality assessment, namely, attributes data and variables data. Variables data follow a continuous scale which measures the numerical magnitude of a characteristic such as weight and length, while attributes data denote the presence or absence of a property related to a characteristic or characteristics. Such a property may address the existence of the characteristic (for example, cracks) or its magnitude relative to a specification (for example, high resistance). In this thesis we investigate the quality improvement techniques for both variables data and attributes data.

The variability experienced in a process can be classified into two classes, the assignable (special) cause and the natural (common) cause of variation. The common cause of variation is the variation in the process that is due to chance or cannot be attributed to any one specific cause. This variation is present in every process. The assignable cause of variation is the variation in the process that is caused by changes in the factors involved in the production process such as machine wear, controller fatigue and other factors that can be controlled. The process is said to be in statistical control if only common cause variation is present and out of control if an assignable cause of variation is also present. The main objective of quality control is to quickly detect the presence of assignable causes of variation so that corrective action can be taken to remove them. Control charts have an outstanding history of being credited with a good ability to carry out this task by discriminating between situations where only common causes of variation are affecting the process outcome and situations where assignable causes are also present.

Before the introduction of control charts, mechanisms like division of labor and job specialization were used to try to improve quality of goods and services. In that era, large industries employed full-time inspectors whose main job was to keep defective items from reaching the consumers. Quality control was merely quality inspection rather than quality improvement. The use of statistical methods for quality improvement started in the 1920's through the introduction of statistical control charts. Besides control charts, several other statistical techniques such as design of experiments and acceptance sampling have been used to improve process quality.

The statistical point of view of improving quality is different from that of management. While production managers understand improving quality as producing goods that are identical, statisticians accept that variability is inevitable, and that quality improvement entails reduction of variability by monitoring the process itself. Several statistical methods including among others designed experiments, acceptance sampling and control charts have been used in an effort to improve the performance of production processes.

The first control charts were developed by Walter Shewhart ([88]), and ever since, several new charts have been developed in an effort to improve these Shewhart control charts' ability to detect a shift of the process from a target value. The statistical control chart, generally with 3σ action limits and 2σ warning limits, is the longest established statistical form of graphical control. The control chart statistics are plotted by simply plotting time on the horizontal axis and a quality characteristic on the vertical axis. A quality characteristic is said to be in an in-control state if nearly all points falls within the acceptance region of the chart and out of control if the statistic plots outside the acceptance region. Shewhart ([88]), suggested that control charts can be used: (i) to define the goal or standard for a process that the management might strive to attain; (ii) as an instrument for attaining that goal, and (iii) to serve as means of judging whether the goal has been met.

Sir Ronald Fisher introduced the technique of design of experiments in the 1920's. There has been an increasing trend in the application of design of experiments for quality improvement especially in the US chemical industry. In fact, Montgomery ([70]) attributes the growth and quality of this industry to design of experiments. Design of experiment methods are statistical techniques used to set up efficient experiments designed to evaluate the effect of a change of one or more process factors on the performance of the product. Taguchi and Wu ([94]) developed a simple design of experiments tool that attracted the attention of many manufacturing engineers. This consists of setting up a robust design of the process that makes the process robust to environmental factors and other factors that are difficult to control.

It is very difficult to define or measure quality, Montgomery ([70]), summarized the components of quality as follows:

- Performance (whether the product can do the job it is designed to perform?)
- Reliability (how often does the product fail?)
- Durability (how long does the product last?)
- Serviceability (how easy is it to repair the product?)
- Aesthetics (what does the product look like?)
- Features (what does the product do?)
- Perceived quality (what is the reputation of the company or its product?)
- Conformance to standards (is the product made exactly as the designer intended?)

As technology improved, the customer's demand for better quality increased, and most of the processes experienced small shifts from their nominal values which the Shewhart charts failed to detect quickly. Therefore a search for new charts that could quickly detect these small shifts with lower false alarm rates than the Shewhart charts with runs rules was undertaken. One of the charts developed as a result of that search was the cumulative sum (CUSUM) control chart developed by Page [80]. This technique plots the cumulative sums of deviations of the sample values from a target value against time. Another chart developed as an effort to improve the control charting procedure is the exponentially weighted moving average

(EWMA) control chart introduced by Roberts [85]. An EWMA chart takes previous observations into consideration when plotting the statistics. These two charts are more effective when monitoring processes experiencing small persistent shifts in the process than the Shewhart charts.

The above mentioned control charts are leading charts for process monitoring even though there are several other charts in the literature. The Shewhart charts have proved to be particularly effective when the quality characteristics are independent and identically distributed and follow a normal distribution. Control chart theory is based on the realization that, no two items are identical. Control charts are credited with the ability to tell the operator when to leave a process alone and when to take action to correct an unwanted situation. When using control charts, substantial improvements in quality of products and services are often observed as well as reduction in spoilage, rework and unnecessary work stoppage and process adjustments.

However, these commonly used control charts have some limitations. Firstly, they perform very well if the underlying distribution of the quality characteristic is normal and the observations are independent and identically distributed over time. In some situations, this might not be true and the control charts in particular the Shewhart chart will not be appropriate. Secondly, the Shewhart chart is not effective in detecting small shifts in the process while the CUSUM and EWMA charts are not effective in detecting some types of large shifts. Finally, in some situations, shifts may occur in both process mean and standard deviation and most of the charting procedure require running two charts concurrently which may be cumbersome and time-consuming.

1.2 Scope and Objective

The scope of this thesis includes SPC methods that can be applied to cases where the process measurement follows a normal distribution when the process is in control. We develop control charts for cases where process measurements are independently distributed over time and for process measurements that are serially correlated. We restrict ourselves to stationary data which is assumed to be generated by a first order autoregressive plus random error model. This model is frequently encountered in practice. We also discuss control charts for attributes data for cases where the number of nonconforming items are in the order of parts-per-million.

The major objective of this thesis is to develop single control charts that simultaneously monitor both the process location and the variability by using a single plotting variable. These charts are capable of quickly detecting both small and large shifts in the process location and spread and are also capable of handling cases of varying sample sizes and efficiently monitoring autocorrelation processes.

1.3 Thesis Outline

Chapter 2 introduces the reader to the principles of SPC through discussion of some literature on SPC. It introduces three main control charts, the Shewhart chart, the CUSUM chart and the EWMA chart. These charts are used in quality control for independent processes and autocorrelated processes for both univariate and multivariate processes. The chapter concludes by discussing some limitations of these charts particularly in monitoring serially correlated observations, monitoring process where assignable causes of variation cause simultaneous shifts in both location and spread as well as interpretation of an out-of-control signal when using multivariate charts.

In Chapters 3 and 4 two single CUSUM charts are developed and their performance studied. It turns out that these charts are sensitive to both small and large shifts in the process mean and/or standard deviation. These charts are applicable in cases where the process measurements follow a univariate normal distribution and measurements are not serially correlated.

Chapters 5 and 6 present new control charts for the mean vector and covariance matrix. A multivariate single CUSUM chart is presented in Chapter 5. This chart quickly detects both small and large shifts in the mean vector and covariance matrix. A Shewhart-type single multivariate chart is presented in Chapter 6. This chart is particularly effective in detecting large shifts in the process parameters.

Chapters 7 and 8 present control charts for monitoring processes that are serially correlated. Chapter 7 presents a single CUSUM chart while Chapter 8 presents a single Shewhart-type chart. These charts are developed by fitting a time series model to the data and calculating the residuals which will be monitored for detecting shifts in the process mean and/or standard deviation. We assess the effect of autocorrelation on the performance of control charts for models that are assumed to follow a first order autoregressive model plus random error.

In Chapter 9, we present control charts for attributes data for the case where the number of nonconforming items are measured in the order of parts-per-million. We show that the chart based on the normal approximation does not perform well in this case due to the asymmetric nature of the binomial distribution when the fraction of nonconforming items p is very small. A chart based on a Poisson approximation does not significantly differ from a chart based on the original binomial random variables.

In Chapter 10, we present the conclusions of our research findings as well as suggestions for future research.

1.4 Notations

The notations below are used throughout the thesis.

CUSUM	Cumulative sum
EWMA	Exponentially weighted moving average
SPC	Statistical process control
CL	Center line
UCL	Upper control limit
LCL	Lower control limit
ARL	Average run length
n_i	i^{th} sample size
n	Equal sample size
m	Number of samples taken from a process
μ	Process mean
$\boldsymbol{\mu}$	Process mean vector
σ^2	Process variance
σ	Process standard deviation
$\boldsymbol{\Sigma}$	Process covariance matrix
$\lvert\boldsymbol{\Sigma}\rvert$	Determinant of the process covariance matrix
ρ	Correlation coefficient between two quality characteristics
ARL_0	In control average run length
$\Phi(\cdot)$	Standard normal cumulative distribution function
$\Phi^{-1}(\cdot)$	Inverse of standard normal cumulative distribution function
$H_v(\cdot)$	Chi-square distribution function with v degrees of freedom
$H_{v,\delta}(\cdot)$	Noncentral chi-square cumulative distribution function with v degrees of freedom and noncentrality parameter δ
$X \sim N(\mu, \sigma^2)$	A random variable X follows the normal

	distribution with mean μ and variance σ^2
$X \sim \chi^2_v$	A random variable X follows the chi-square distribution with v degrees of freedom
$X \sim \chi^2_{v,\delta}$	A random variable X follows a noncentral chi-square with v degrees of freedom and noncentrality parameter δ
$\chi^2_{\alpha,v}$	Percentage point of the chi-square distribution with v degrees of freedom
X_{ij}	Measurement of a quality characteristic on the j^{th} observation in the i^{th} sample
$\boldsymbol{X}_{ij}$	A k×1 vector of measurements of quality characteristics
$\bar{X}_i$	i^{th} sample mean
S_i^2	i^{th} sample variance
S_{12}	Sample covariance between two quality characteristics
S_n	Sample covariance matrix
$\bar{\bar{X}}$	Grand sample mean
$\bar{S}$	Grand sample standard deviation
a	A multiplier of a step-shift in the process mean
b	A multiplier of a step-shift in the process standard deviation
k	CUSUM reference value
h	CUSUM decision interval
$\bar{n}$	Average sample size
d_2	An R control chart constant
c_4	An S control chart constant
$C+$	An out of control signal due to increase in the process mean
$C-$	An out of control signal due to decrease in the process mean
$S+$	An out of control signal due to increase in the process standard deviation
$S-$	An out of control signal due to decrease in the process standard deviation

$B{+}{+}$	An out of control signal due to increase in both process mean and standard deviation
$B{+}{-}$	An out of control signal due to increase in process mean and a decrease in the standard deviation
$B{-}{+}$	An out of control signal due to decrease in the process mean an increase in the standard deviation
$B{-}{-}$	An out of control signal due to decrease in both process mean and standard deviation
max	maximum
SS	Sum of squares
p	Number of quality characteristics
r	Radius
$Var(\cdot)$	Variance function of a univariate distribution
$E(\cdot)$	Mean function of a distribution
T^2	Hotelling's test statistic
AR(1)	First order autoregressive process
MA(1)	First order moving average process
ε_t	Random error at time t
σ_ε^2	Variance of the random error term ε_t
ϕ	Autoregressive parameter
ξ	Process mean for an autoregressive process
μ_t	The mean at time t
α_t	Normal random variables in an autoregressive process
σ_α^2	Variance of α_t
ψ	Proportion of process variance due to μ_t
B	Backshift operator
θ	Moving average parameter

MSE	Mean square error
ATS	Average time to signal
MCAP	Maximum cumulative sum for autocorrelated process
ARMA(1,1)	First order autoregressive moving average
Q chart	Quesenbery chart
F^{-1}	Inverse of the Poisson cumulative distribution function
$B(x_i; n, p)$	The binomial cumulative distribution function
V^+	An out of control signal due to a shift in the covariance matrix
M_i	Single charts plotting statistic
$\boldsymbol{\mu}_G$	Good mean vector
$\boldsymbol{\mu}_B$	Bad mean vector
D	Noncentrality parameter
c chart	A control chart for number of nonconformities
np chart	A control chart for number of nonconforming items

Chapter 2

Literature Review

2.1 Statistical Quality Control

Quality has always been an integral part of all products and services. Engineers and producers have a common goal, which is to design and produce goods that are not expensive to produce and at the same time very durable and attractive to the consumer.

In the early production era, that is before the 1920's, quality of goods was judged through the eye of the producer. As production industry expanded, the work of quality assessment was delegated to top company management who had the task of assessing quality by physically comparing all products to see if they are identical. During the industrial revolution and industrial boom, high volume of goods were produced and the visual inspection of individual items became an expensive and time consuming task. This necessitated investigations on ways of improving quality and finding effective methods of quality assessment. In an effort to improve quality, Frederick Taylor suggested the principle of division of labor and work specialization (Montgomery [70]). This resulted in an increase in production as well as an improvement in the quality of goods.

The growth in industrial production overburdened inspectors and called for some standard quality control mechanisms to be developed. During that era, inspection was done on all products; and items not meeting the manufacturer's requirement were excluded from the shipment, while only those meeting requirements were shipped. Quality monitoring was concentrated on the final product, this made it difficult or impossible to notice faults in the production process itself. This resulted in many items being rejected as not conforming to some set standards. One of the major disadvantages of the physical examination was that no form of variability in the products was measured.

In the 1920's, an active search for alternative and effective methods of process monitoring was mounted. Several quality practitioners realized that there always exist some forms of variability in the process. They acknowledged that variability can only be described in statistical terms and thus statistical methods would play an integral part in quality improvement efforts. Dr. Walter Shewhart ([88]) proposed the use of statistical control charts for quality monitoring. These charts are the present day Shewhart control charts, namely the X-bar, R and S charts for variables data and p, np, c and u charts for attributes data. The quality control chart procedure emphasizes the improvement of quality by monitoring the process rather than correcting defects in the final product. Control charts that are used to define what is meant by an in control state are referred to as *Phase I* charts. The charts that are then used in the second phase to monitor the process are referred to as *Phase II* charts. The introduction of these control charts promoted the concept of sampling inspection as an alternative to 100 percent inspection. Control charts did not gain popularity immediately due to their complexity and the failure by engineers to recognize their importance in quality improvement. They were mainly used at the Bell Telephone Laboratories where Shewhart first introduced them.

During and after the World War II, demand for goods was very high. This resulted in formation of new and large industries and employment of semiskilled and unskilled workers. Emphasis was on meeting the customer's demand and not on quality, this resulted in a high volume of products not meeting the customer's expectations and thus a lot of goods being returned for rework or replacement. The experience learned in the manufacturing industry necessitated the use of statistical techniques for quality control and quality improvement. These included control charts, acceptance sampling and design of experiments. Several organizations such as the American Society for Quality Control, formed in 1946, engaged in promotion of statistical quality control techniques through different forms of training and publications.

Statistical quality control gained popularity in Japanese industry during the 1950's through Dr. Edward E. Deming's training programs and emphasis on Total Quality Management (TQM). TQM applies the quality concept not only on the production floor but to all departments involved in the production process. These include among others, management, planning, purchasing, sales and even accounting departments. He emphasizes the concept of "do it right the first time" in order to reduce rework costs.

The control charting procedure recognizes as a fact that, in any production process, a certain amount of variability will always be present. This variability can be classified into two classes, the variability due to chance and variability due to some causes. The variability due to chance is caused by a combination of small amount of noise from several uncontrollable factors in the process. This variability cannot be removed without a major revision of the whole process. When a process is operating in the presence of this form of variability only, the process is said to be in statistical control. It is usually not within the power of the operator to influence the effect of these unassignable causes (as Shewhart called them) of variation on the process. The reduction of this form of variability is the responsibility of the top management as it may require a total overhaul of the process.

The form of variability that is of more interest in control charting procedures is the variability caused by either internal or external factors such as machine setting, operator error, raw material and other factors that can be controlled. The presence of this type of variability represents an unacceptable level of process performance and results in an out-of-control state. When this is signaled, the cause should be identified and eliminated from the process. Since the removal of these causes does not require revision of the process, the operator is usually instructed to identify and remove them. The control chart procedure is used to discriminate between situations where only unassignable causes are affecting the process outcome and situations where there are also assignable causes of variation present.

It is therefore important for both managers and operators to understand the process behavior so that they can know when to take action and when to leave the process alone. Failure to take relevant action can result in losses for the company. It is usually very expensive to reduce unassignable causes of variation and management is often reluctant to take such actions. Snee ([89]) pointed out that,

> *"Deming and his colleagues point out that managers typically treat all problems as due to assignable cause variation, when in fact, more than 85% of problems are due to defects in a system (unassignable cause variation), which only management can change. The result is that management spends too much time 'fire-fighting', solving the same problem again and again because the system was not changed"*

As Montgomery ([70]) stated, the statistical theory employed in control charts is the theory of hypothesis testing. The null hypothesis being that the process is in a state of statistical control, while the alternative is that the process is operating out of control. If the sample mean plots outside the control limits, we say the process is out of control. The difference is that in hypothesis testing, we first check the validity of assumptions, while control charts are used to detect departures from an assumed state of statistical control. Another difference is that in hypothesis testing, once a decision to accept the null hypothesis is reached, no further testing is carried out, while in process monitoring, when the hypothesis of in control is accepted, the process is continually monitored throughout the production process.

Like any other testing procedures, control chart decisions are subject to type I and type II errors. Type I error occurs when the control chart issues an out-of-control signal when the process is in control. This, in control charting language, is called the false alarm or the producer's risk. Type II error occurs when the control chart plots all values within the control limits when in fact the process is out of control. This is called the consumer's risk. When charting, we usually fix the probability of type I error and want to minimize the probability of type II error.

2.2 Shewhart Control Chart

The control chart is based on the idea that if the process is in a state of statistical control, the outcomes are predictable. Based on previous observations, it is possible to determine the probability that future observations will fall within some given sets of limits. The basic Shewhart control chart plots quality characteristics on the vertical axis and the sample number on the horizontal axis. It assumes that quality characteristics are independent and identically distributed and follow a normal distribution. Included in the chart are, the center line which represents the nominal value, the upper control limit which is a line at a distance of three standard deviations above the target value and a lower control limit which is at a distance of three standard deviations below the process target value. If a point falls beyond these three-sigma limits, the chart has produced a signal that the process is out of control, otherwise the process is deemed to be in control. These limits are associated with the magnitude of the variability of the process when only common causes are present. When the process is in control, we expect the plotted points to show a random pattern within the limits and if points behave in a nonrandom manner, even though plotting within the limits, we should be suspicious that the process is operating in an out-of-control state. Shewhart chose the 3-sigma limits so that the false alarm rate may be as low as one in every 370 samples so as to avoid unnecessary process stoppage. Basically, the Shewhart charts are used for determining whether a process has achieved a state of statistical control and for maintaining current control of a process.

The X-bar control chart is used for monitoring and assessing the process mean while R and S control charts are used to monitor and assess the process variability. Montgomery ([70]) suggested that, when dealing with quality characteristics for variables data, we should always monitor the process mean and process variability. The ($\bar{X}$, R) charts have historically been used on the manufacturing floor due to their simplicity while the ($\bar{X}$, S) charts are used by the data analysts in the quality assurance department due to their statistical appeal.

Shewhart control charts only use information about the process contained in the last plotted point and thus ignore any information given by the entire sequence of points. This makes the chart insensitive to small shifts in the process. As production technology improved over time, most of the changes in the process parameters tend to be small and the Shewhart chart proved to be not good enough to detect these changes effectively.

To overcome the weakness of the original Shewhart charts, several authors such as Moore [72], Page [77] and Weindling, Littauer and Tiago [100] and Nelson [76], suggested certain supplementary runs rules which were also suggested by the Bell company and used at Western Electric. They suggested running the Shewhart charts with the usual 3-sigma limits called the action limits together with the 1-sigma and 2-sigma limits called the warning limits. Some of these sensitizing rules are listed below. The process is deemed to be out of control if:

(i) One or more points plots outside the action limits.

(ii) Two of three successive points fall outside the 2-sigma limits on the same side of the center line.

(iii) Four of five successive points fall outside the 1-sigma limits on the same side of the center line.

(iv) Eight successive points fall on the same side of the center line.

(v) Six points in a row steadily increasing or decreasing.

(vi) Fifteen points in a row plots within 1σ limits.

(vii) Fourteen points in a row alternating up or down.

(viii) Eight points in a row in both sides of the center line with none within 1σ limits.

(ix) An unusual or nonrandom pattern in the data.

(x) One or more points near the warning or action limits.

The idea behind the use of these runs rules is to increase the sensitivity of the Shewhart charts by combining the evidence of the current sample with that of previous samples (Barnard [4]). These rules substantially improve the performance of the Shewhart charts in the sense that it could detect smaller shifts in the mean. However, these rules made the Shewhart charts produce a high level of false alarm signals (Champ and Woodall [14]).

Several control charts were introduced in an effort to improve or supplement the Shewhart chart. Among these are the CUSUM control charts and the EWMA control charts. Another chart proposed to take into consideration information from several successive results is the Arithmetic Running Means chart (Ewan [33]). In this chart, the mean of the last k results is calculated and plotted against time. When a new result is obtained, the mean of the most recent k result is re-calculated and thus removing the earliest result in the computation. Lack of control will be indicated by a running mean falling outside a single control limit.

2.3 Exponentially Weighted Moving Average Control Chart

The EWMA chart was first developed by Roberts ([85]), in an effort to produce a chart that could quickly detect small shifts in the process mean with a low false alarm rate. An EWMA chart is constructed by attaching weights to the observations in the sample. The EWMA chart gives the greatest weight to the most recent observation and then decreasing weights to all previous observations in geometric progression from the most recent to the first. It is sometimes called a Geometric Moving Average (GMA) control chart. The EWMA chart is used extensively in time series modelling and forecasting for processes with gradual drift (Box, Jenkins and Reinsel [7]). For processes which are essentially white noise (random variation) with periodic shifts in mean level, the EWMA scheme is useful for monitoring the process and alerting the user that a shift has occurred (Crowder [28]).

The design parameters of the EWMA charts are a multiple of sigma (L) used in determining the control limits and a smoothing operator (λ). The constant λ, determines the rate of decay of the weights and hence the amount of information obtained from the historical data. A combination of these parameters is determined by an in-control average run length desired in the process. This chart can be viewed as a weighted average of all past and current observations making it insensitive to the normality assumption which is an important assumption for the application of the Shewhart chart.

For a random variable x_i at sample number or time i with variance σ^2, the EWMA control chart statistic is defined as

$$z_i = \lambda x_i + (1 - \lambda) z_{i-1}$$

The EWMA chart is constructed by plotting these z_i values on the vertical axis against the sample numbers or time on the horizontal axis. Included in the chart are the center line which represent the target value, two lines at a distance of L-sigma below and above the center line, where sigma is the standard deviation of the z_i's. When the process is in control, the EWMA, Shewhart and CUSUM control charts are roughly equivalent in their ability to monitor departures from the target. However, the EWMA chart provides a forecast of where the process will be in the next instance of time. It thus provide a mechanism for dynamic process control (Hunter [43]).

The EWMA chart suffers from the disadvantage of being unable to quickly detect large and temporary shifts in the process parameters as compared to the Shewhart chart. Several authors have conducted research on this chart in an effort to try to make it more sensitive to both small and large shifts in the process parameters and also easy to use in industry. These include among others, Crowder [27], Chantraine [18] and Hunter [43]. Lucas and Saccucci ([62]) introduced some enhancements to the EWMA chart. These included the fast initial response to make the chart more responsive to initial out-of-control conditions and a combined Shewhart-EWMA control chart that is more sensitive to both small and large shifts in the process mean. They also introduced a robust EWMA chart to provide extra protection against outliers in the process.

Wortham and Ringer ([107]) and Sweet ([93]), proposed EWMA charts for monitoring the process variance and for simultaneously monitoring both process mean and variability respectively. Crowder and Hamilton ([29]) used the log transformation to develop an EWMA chart for monitoring increases in the process variance. They showed that the EWMA chart performs better than the Shewhart chart for detecting small increases in the process standard deviation.

2.4 Cumulative Sum Control Chart

One of the charts developed in an effort to supplement the Shewhart chart is the CUSUM control chart which was first developed by Page ([80]). This chart has been widely used to monitor the quality of continuous manufacturing processes. This technique plots the cumulative sums of deviations of the sample values from a target value against time. An important feature of the CUSUM chart is that, it incorporates all the information in the sequence of sample values . This makes the CUSUM chart more sensitive to even smaller shifts in the process mean. The CUSUM charts are highly recommended by Marquardt ([65]) for use in industry. This is because they can detect small changes in the distribution of a quality characteristic and thus maintain tight control over a process. Bissell ([5]) reviewed the use of CUSUM charts for both variables data and attributes data. They provided tables and nomograms that can be used facilitate the application of CUSUM charts.

There are two types of the CUSUM procedures, the tabular CUSUM procedure and the V-mask CUSUM procedure. The V-mask procedure operates by using a mobile V-shaped mask to decide whether a shift has occurred. The mask is in the shape of a V placed sidewise ($>$) with its vertex placed a fixed distance from the last plotted CUSUM point. If all previous values lie within the two arms of the V-mask, the process is in control, otherwise, the process is said to be out of control. The other type of the CUSUM procedure is the tabular CUSUM. The chart using the tabular CUSUM procedure is constructed by to plotting CUSUM values against time, while adding two lines a distance of h above and below the target value. The h value is called the decision interval. The tabular form makes use of two cumulative sums, the upper CUSUM accumulates positive deviations of the sample values from a target value while the lower CUSUM accumulates negative deviations of the sample values from a target value.

Montgomery ([70]) strongly discourages the use of V-mask procedure because of the following reasons:

(i) being a two-sided scheme, the V-mask is not very useful in one-sided process monitoring problems;

(ii) the useful fast initial response (FIR) feature proposed by Lucas and Crosier ([60] and [61]) cannot be applied to the V-mask;

(iii) it is not clear how far backwards the arms of the V-mask should extend, this complicates interpretation of the V-mask.

We agree with Montgomery's assertion and we only propose new schemes for the tabular CUSUM chart in this thesis.

If there is no assignable cause variation, the two-sided CUSUM chart is a random walk with mean zero. If the process shifts, a trend will develop either upwards or downwards depending on the direction of the shift and in this situation a search for the assignable cause of variation should be undertaken. The magnitude of a change can be determined from the slope of the CUSUM chart and a point at which a change first occurred is the point where a trend first developed. The ability to detect a point at which changes in the process parameters began makes the CUSUM chart a valuable tool for use where high volumes of goods are produced within a short period of time.

The design parameters of the tabular CUSUM chart are the decision interval, h and the reference value k. The reference value k is usually chosen to be one-half δ, where δ is the smallest shift, measured in units of the standard error that is considered large enough to be quickly detected by the chart. The decision interval is the action limit of the CUSUM chart, it is normally set by choosing an in control average run length together with the minimum allowable shift of the process. A combination of h and k can be determined to give the desired average run length.

More research has been carried out investigating the performance of the CUSUM chart. Gibra ([35]) and Woodall ([105]) gave a brief review of literature on CUSUM charts. Lucas and Crosier ([61]) recommended using the headstart to make the CUSUM chart quick to detect an initial out-of-control condition. Page ([78] and [79]), Ewan ([33]) and Duncan ([32]) stated that the CUSUM chart may be too sensitive to small shifts in the process mean in some applications. Gibra ([35]) states that the CUSUM chart should not be used or should be used with greater thought when some slack in the process is permissible because the chart will falsely issue an out-of-control signal. Ewan ([33]) suggested that two or more V-masks should be used simultaneously to improve the sensitivity of the V-mask CUSUM chart to large shifts in the mean. Lucas ([59]) and Bissell ([6]) have also proposed changes in the shape of the V-mask near its vertex. Lucas ([58]) recommended combining the Shewhart and CUSUM charts so that the combined chart can be more sensitive to both small and large shifts in the process mean.

Shewhart pointed out that it is not enough to monitor only the process mean; the process variability is just as important in quality control and must be monitored. This point of view is perhaps even more appropriate today in light of the Taguchi emphasis on improving quality by reducing noise variation (Hawkins [38]). Several CUSUM charts for monitoring process variability have been suggested. Hawkins ([39]), suggested a CUSUM chart based on $\sqrt{|X_t/\sigma|}$, which is approximately normally distributed if measurements of a quality characteristic X_t follows a normal distribution with mean 0 and variance σ^2. Box and Ramirez ([8], [9] and [10]) proposed CUSUM charts for process variability based on $(X_t - \mu)^2$, where μ is the process mean. Chang and Gan ([17]) proposed using the CUSUM chart based on the logarithmic transformation (to base e) of the sample variance, to monitor the process variance.

2.5 Autocorrelated Process Control Charts

The control charts discussed above are designed under the assumption that a process being monitored will produce measurements that are independent and identically distributed over time when only the inherent sources of variability are present in the system. However, in some applications, the assumption of independent observations is not realistic. For instance, measured variables from tanks, reactors and recycle streams in chemical processes show significant serial correlation (Harris and Ross [37]). In some instances, the dynamics of the process will induce correlations in observations which are closely spaced in time. If the sampling interval used for process monitoring in these applications is short enough for the process dynamics to produce significant correlation, then this correlation can have very serious effects on the properties of standard control charts developed under the independence assumption, (see Maragah and Woodall [64], VanBrackle and Reynolds [96], Lu and Reynolds [55] and [56] and Runger, Willemain and Prabhu [86]). If there is correlation among observations, the process mean is not constant. It may be more realistic to assume that the process mean is continually wandering even when the process is in control.

Positive autocorrelation in observations can result in severe negative bias in traditional estimators of the standard deviation. This bias produces control limits that are much tighter than desired. Lu and Reynolds ([55]), observed that tight control limits, combined with autocorrelation in the observations plotted, can result in an average false alarm rate much higher than expected. This will result in effort being wasted searching for unavailable special causes of variation in the process. This can also result in loss of confidence in the control charts and practitioners may abandon their use. Corrective action taken after the false alarms can also introduce variability into the process and make the control chart less effective and very expensive to use. Negative autocorrelation can lead to wider control limits which makes the chart insensitive to shifts in the process mean. It is therefore very important to take autocorrelation among observations into consideration when designing a process monitoring scheme, in particular control charts, in order to maximize full benefit from their use.

Maragah and Woodall ([64]), observed that autocorrelation is a source of variability. They proposed that if a process is being controlled to a target value and the cause of the autocorrelation can be found and removed from the process, then it should be. The effect of autocorrelation has been studied for several types of control charts. Vasilopoulos and Stamboulis ([98]) have studied the modification of $\bar{X}$ control chart limits in the presence of data correlation within samples. Maragah and Woodall ([64]), studied the effect of autocorrelation on the retrospective X-chart. Johnson and Bagshaw ([48]), Atienza; Tang and Ang ([3]), Lu and Reynolds ([55]), and others studied the effect of autocorrelation on the CUSUM charts. Lu and Reynolds ([56]), studied the effect of autocorrelation on the EWMA control charts.

The studies mentioned above used several methods, such as simulation, asymptotic approximation and, direct calculation, to evaluate properties of the control charts. A conclusion that can be drawn from these studies is that correlation between observations has a significant effect on the properties of the control charts.

Recently, new control charts have been proposed for dealing with autocorrelated data. Two approaches have been advocated for dealing with this phenomenon. The first approach uses standard control charts on original observations, but adjust the control limits and methods of estimating parameters to account for the autocorrelation in the observations (see, VanBrackle and Reynolds [96], Lu and Reynolds [56]). This approach is particularly applicable when the level of autocorrelation is not high.

A second approach for dealing with autocorrelation fits time series model to the process observations. The procedure forecasts observations from previous values and then computes the forecast errors or residuals. These residuals are then plotted on standard control charts, because the residuals are independent and identically distributed normal random variables when the process is in control, when the fitted time series model is the same as the true process model and the parameters are estimated without error. (see, Alwan and Roberts [2]; Montgomery and Mastrangelo [71]; Wardell, Moskowitz, and Plante [99]; Lu and Reynolds [57]; and Runger, Willemain and Prabhu [86]). Control charts based on residuals seem to work well when the level of autocorrelation is high. When the level of autocorrelation is low, forecasting is more difficult and residual charts are not very effective at detecting process changes.

The second approach is more appealing due to the following reasons:

(i) it takes advantage of the fact that the process is correlated and allow forecasts of future quality;

(ii) it is based on the assumption that the residuals are random so the traditional statistical process control tools can be used;

(iii) the chart can be used to detect any assignable cause including change in the time series structure;

(iv) the chart is easy to construct;

(v) unlike other methods for dealing with correlated data that have been limited to AR(1) or MA(1) time series models, the method can be applied to any type of time series model;

(vi) the method is often more effective in detecting shifts in the process mean than more traditional control charts when the underlying process is ARMA(1,1) (Wadell, Moskowitz, and Plante [99]).

The control charts discussed above were developed for monitoring the process mean. However in the production process many special causes of variation can affect both process mean and process variability. This problem also arises in the case of monitoring autocorrelated processes even though there has been little work published in the control chart literature on this problem. MacGregor and Harris ([63]) developed the exponentially weighted moving variance control charts for monitoring variability for autocorrelated processes. These charts are useful when only individual observations are collected. One of their charts is based on an exponentially weighted mean square deviation from the target and another one is based on an exponentially weighted moving variance.

Lu and Reynolds ([57]) developed EWMA control charts for monitoring the variance of an autocorrelated process. They used the logarithms of the squared residuals to develop the EWMA chart. They also showed some results for the Shewhart chart for residuals.

2.6 Multivariate Control Charts

There are many situations in which the overall quality of an item is determined by several (say p) correlated quality characteristics and we wish to test whether the process is in statistical control. For example, a chemical process may be a function of temperature and pressure both of which need to be monitored carefully, the performance of a machine used in the process may depend on its age and the time since the last maintenance check. In fact, multivariate situations where process performance is determined by many correlated variables are common in industry. The product/item is considered to be in statistical control if all critical product characteristics are simultaneously in control. To monitor the quality of such products, several control charts have been suggested. One such suggestion is to run p univariate control charts one for each component of the product. Since in most cases these components of the product are correlated, individual control charts disregard this correlation structure and may give misleading results.

Hotelling ([42]) proposed a new control chart for multivariate data based on his statistic known as the Hotelling's T^2 statistic. This statistic is a scalar that combines information from the dispersion and mean of several variables. The underlying probability distribution of these p quality characteristics is assumed to be multivariate normal with mean vector $\boldsymbol{\mu}$ and covariance matrix $\boldsymbol{\Sigma}$. Healy ([41]) proposed a multivariate CUSUM chart for the mean vector when the mean shifts from a known target value to a known out-of-control value. Crosier ([26]) proposed two multivariate CUSUM charts. One chart makes use of the Hotelling's T statistic to form a CUSUM of T statistics. The other procedure forms a CUSUM vector directly from the observations. Lowry and Woodall ([54]) and Prabhu and Runger ([81]) proposed some multivariate EWMA control charts. Woodall and Ncube ([106]) suggested operating p one-sided or two-sided univariate CUSUM schemes simultaneously to detect a shift in the mean vector of a p-variate normal distribution. Recently, Khoo and Quah ([50]) proposed a multivariate control charts for short runs based on individual measurements and subgroup data.

The multivariate control chart initially did not receive much attention due to their complexity. However, due to the increasing use of computers in many industries application of these charts is receiving more attention and some practitioners now refer to them as Shewhart charts even though Shewhart had nothing to do with them.

Most of the research on multivariate charts is focused on monitoring the process mean vector. However some recent work has proposed control charts for monitoring changes in the process variability. Alt and Smith ([1]) suggested the Shewhart-type control chart for the covariance. Healy ([41]) proposed a CUSUM chart for detecting changes in covariance from Σ_0 to $C\Sigma_0$ where $C > 0$. Chan and Zhang ([15]) proposed multivariate CUSUM charts for the covariance. These charts are based on the projection pursuit technique and are also effective in a low volume or short-run environment. Chan and Zhang ([15]) proposed a CUSUM chart based on the likelihood ratio which is only applicable when the subgroup size is larger than the number of the quality characteristics measured per item. Yeh, Lin, Zhou and Venkataaramani ([110]) using the idea of probability integral transformation, proposed a multivariate EWMA chart for detecting changes in $|\Sigma_0|$, the determinant of the variance-covariance matrix. Wierda ([101]) proposed a multivariate control chart hierarchically using the likelihood ratio test. Prins and Mader ([82]) suggested that for grouped data, the T^2 chart can be paired with a chart that displays a measure of variability within the subgroups for all the analyzed characteristics. This is analogous to the $(\bar{X}, S)$ or $(\bar{X}, R)$ charts for univariate processes.

2.6.1 Interpretation of an Out-of-Control Signal

There are some difficulties associated with the use of multivariate control charts. These difficulties include among others: that the value displayed on the chart is unitless and hence is not related to the units of measurement of the monitored variables. The other difficulty is that the user does not know which particular quality characteristic(s) caused the out-of-control signal when the T^2 statistic exceeds the upper control limit. Furthermore, a multivariate control chart can issue an out-of-control signal when either or both of the individual variables are out of control and or when the relationship between the two variables changes relative to the historical structure. It is therefore important to eliminate the collinearity between observations in the historical data before constructing a control chart.

One method for investigating which quality characteristic(s) have shifted is a method that uses the principal component analysis (see Jackson and Morris [46], Jackson [44] and [45]). The T^2 statistic is decomposed into a sum of independent squared principal components which are linear combinations of the original variables. The principal components are examined to see why the process is out of control. However, the principal component approach is not very effective due to their lack of ease of interpretation. Kourti and MacGregor ([52]) proposed an approach based on normalized principal components scores. The T^2 is expressed in terms of those normalized scores of the multinormal variables. When an out-of-control signal is issued the normalized score(s) with high values are detected and contribution plots are used to find the variable(s) responsible for the signal. A contribution plot indicates how each variable involved in the calculation of that score contributes to it. Mason, Tracy, and Young ([67]), Mason, Champ, Tracy, Wierda and Young ([68]) decompose the T^2 statistic into p independent components each of which provide information on the variables that significantly contribute to an out-of-control signal. Using univariate charts to supplement the multivariate chart for monitoring the variance based on the generalized sample variance is suggested by Lowry and Montgomery ([53]).

Woodall and Ncube ([106]) proposed running p charts each at level α and conclude that the process is out of control if any of these charts signals. However, the overall probability of producing a false alarm for these p charts combined is not the same as the that of a chart that plots all the characteristics together. Wierda ([101]) stated that it is not satisfactory to use the joint distribution to obtain probability of false alarm for p control charts in such a way that the overall probability is equal to α since the quality characteristics depend on each other. Therefore when quality characteristics are correlated, the information of one characteristic should be used to evaluate the value of the other. Prins and Mader ([82]) recommended that individual univariate charts could be run at the same time with a multivariate control chart even though the individual charts will not detect shifts due to correlation structure.

2.7 Simultaneous Control Charts

Most of the Shewhart, CUSUM and EWMA control charts discussed in the literature monitor the process location and spread separately. Two control charts, one for the mean and the other for the process variability, are run concurrently. This practice requires more resources such as quality control practitioners, time and other resources. Recently, more effort has been committed to designing control charts that can simultaneously monitor both process mean and variability. Such charts are called single control charts. Some of the main difficulties encountered in this endeavor include designing a single chart that is effective for both small and large shifts in both parameters, designing a chart that is simple to use and interpret, and designing a chart that can immediately indicate whether the mean is out of control, the variability is out of control or both, as well as the direction of the shift when an out-of-control signal is issued.

White and Schroeder ([103]) first introduced the use of one control chart to monitor both process mean and variability. This chart was developed using resistant measures and a modified box plot display. Domangue and Patch ([31]) developed some omnibus EWMA schemes based on the exponentiation of the absolute value of the standardized sample mean of observations, capable of simultaneously detecting shifts in the process mean and process standard deviation. These charts are sensitive to shifts in the process mean and/or variability. However, it is not possible to identify the parameter that has shifted. Hawkins ([38]) suggested plotting the two statistics on the same plot using different plotting symbols. This produces a chart that is somewhat complicated to interpret and is congested with many plotting points on the same chart. For multivariate processes, Spiring and Cheng ([91]) developed a single chart that plots both process mean and standard deviation on the same chart. This chart also plots two variables in the same chart.

In recent years, attention has been devoted to developing single control charts that use only one plotting character for both process mean and standard deviation on a single chart. Such charts should be able to issue an out-of-control signal and identify the parameter(s) that has shifted. Cheng and Li ([24]) proposed a single variable T control chart that measures the proximity of the observations to the target value (center) and the variability of the process. The T chart suffers from the weakness of not being able to tell which parameter has shifted.

Chao and Cheng ([19]) developed a single control chart called the semicircle control chart. This is actually an improvement to Van Nuland's ([97]) circle technique. This chart uses a semicircle to plot a single plotting character to indicate the position of the mean and standard deviation by plotting the two parameters against each other. This chart is able to show which parameter has shifted from its target value. The disadvantage of this chart is that it loses track of the time sequence of the plotted points.

Chen and Cheng ([21]) developed a single Shewhart-type control chart called the Max chart. This chart plots the maximum absolute values of the standardized mean and standard deviation. It is capable of simultaneously monitoring the process mean and variability, it further shows which parameter has shifted as well as the direction of the shift. This chart performs like the combined Shewhart charts for the mean and standard deviation (*i.e.* the combined $\bar{X}$) and S charts. Chen, Cheng and Xie ([22] and [23]) and Xie ([108]) proposed several EWMA control charts that simultaneously monitor the process mean and standard deviation. These charts have, in addition to the advantages enjoyed by the Max chart, the capability of quickly detecting small shifts in the process.

There has been no attempt to the best of our knowledge to develop single CUSUM charts. We are proposing some single univariate and multivariate CUSUM chart for monitoring both process location and spread for the cases of independent and autocorrelated processes.

2.8 Average Run Length

The average run length (ARL) of a control chart is often used as a measure of performance of the chart. The ARL of the chart is the average number of points that must be plotted before a point plots above or below the control limits. If this happens, the chart issues an out-of-control signal indicating the presence of assignable cause(s) of variation in the process. When there is a significant change in the process, it is desirable to have a low ARL so that the change can be detected quickly. When the process is in control, it is desirable to have a large ARL so that the false alarm rate produced by the chart is low.

A chart that has low out-of-control ARL with the same or higher in control ARL as its competitors is said to be more efficient in monitoring the process. For comparison of charts in this thesis, we adjust the chart's control limits so that the compared charts will have the same in control ARL and then compare their out of control ARL's for changes in the mean alone, standard deviation alone and for changes in both mean and standard deviation. We are aware of the objection to using the ARL as a way to compare charts since only a fraction of the behavior of the control chart is reflected by the size of the ARL. We believe that it would be better to investigate the distribution of the run length, however, the ARL is widely used in the literature to compare different control charts since the amount of production is proportional to the ARL.

When there is a change in the process, the ARL is usually computed under the assumption that this change is present at the time the chart is started. However, in practice, a change in the process may occur after the chart has been running for some time. In this case, it would be appropriate to look at the time from the change in the process to the time of the first signal by the chart. This time has been frequently measured using the steady-state run length distribution. The steady-state run length distribution is the distribution of the number of samples from the change to the process until the occurrence of the signal, computed for the case in which there are no false alarms before the change and the change occurs after the process has been running long enough for the control statistic to be in steady-state at the sample immediately before the change occurs. The mean of the steady-state run length distribution is called the steady-state average run length. This steady-state ARL has been used as a measure of detection time for process changes which occur after the control chart has been in operation for some time.

The theory of Markov chains has been used successfully to compute the ARL of the CUSUM charts. Brooks and Evans([11]) give a Markov chain representation of the one-sided CUSUM procedure based on an integer-valued CUSUM. This approach is used to obtain approximations in the continuous case, but a more accurate method using the recursive numerical integration is given by Woodall ([105]). Champ and Rigdon ([13]) showed that if the midpoint rule is used to approximate the integral in the integral equation, the integral equation and Markov chain approaches yield the same approximations for the ARL.

Chapter 3

Max-CUSUM Chart

3.1 Introduction

The CUSUM control chart has been developed in an effort to provide an alternative to the Shewhart chart. As discussed in Chapter 2, this chart is more sensitive to small but persistent shifts in the process mean and/or standard deviation. It is however very sensitive to large and instantaneous or temporary shifts in these parameter(s). Most of the CUSUM schemes for variables data discussed in the literature require running two CUSUM charts concurrently, one for monitoring the process location and another for monitoring the process spread. However recent studies propose simultaneous CUSUM charts which plot the two parameters on the same chart using different quantities.

This chapter proposes an alternative CUSUM chart that simultaneously monitor process mean and process standard deviation using one quality characteristic. This control chart is called the maximum cumulative sum control chart (Max-CUSUM chart). It is assumed that a special cause of variation may simultaneously cause a shift in either one or the process location and the spread. The proposed chart is based on the well-known standardization procedures of the normal distribution. Some important properties of this proposed procedure are (i) the chart is capable of quickly detecting both small and large shifts in the process mean and/or standard deviation, (ii) it is also capable of handling cases of varying sample sizes, and (iii) it shows the parameter that has shifted and the direction of the shift.

3.2 The New Control Chart

Let $X_i = X_{i1}, ..., X_{in_i}$, $i = 1, 2, ...$, denote a sequence of samples of size n_i taken on a quality characteristic X. It is assumed that, for each i, $X_{i1}, ..., X_{in_i}$ are independent and identically distributed observations following a normal distribution with means and standard deviations possibly depending on i, where i indicates the i^{th} group. Let μ_0 and σ_0 be the nominal process mean and standard deviation previously established. Assume that the process parameters μ and σ can be expressed as $\mu = \mu_0 + a\sigma_0$ and $\sigma = b\sigma_0$ for $b > 0$, where $a = 0$ and $b = 1$ when the process is in control, otherwise, the process has changed due to some assignable causes. The constants a and b represent shifts in the mean and standard deviation respectively.

Let $\bar{X}_i = (X_{i1} + ... + X_{in_i})/n_i$ and $S_i^2 = \sum_{j=1}^{n_i}(X_{ij} - \bar{X}_i)^2/(n_i - 1)$ be the mean and variance for the i^{th} sample respectively. The sample mean $\bar{X}_i$ and sample variance S_i^2 are the uniformly minimum variance unbiased estimators for the corresponding population parameters. These statistics are also independently distributed as are the sample values. These two statistics follow different distributions. The CUSUM charts for the mean and standard deviation are based on $\bar{X}_i$ and S_i respectively. To develop a single chart, we define the following transformed statistics:

$$Z_i = \sqrt{n_i}\frac{(\bar{X}_i - \mu_0)}{\sigma_0} \tag{3.1}$$

and

$$Y_i = \Phi^{-1}\left\{H\left[\frac{(n-1)S_i^2}{\sigma_0^2}; n-1\right]\right\}, \tag{3.2}$$

where

$$\Phi(z) = P(Z \leq z),$$

for $Z \sim N(0, 1)$, the standard normal distribution. The function $\Phi^{-1}(\cdot)$ is the inverse of the standard normal cumulative distribution function, and $H(w; p) = P(W \leq w|p)$ for $W \sim \chi_p^2$, the chi-square distribution with p degrees of freedom.

These new variables, Z_i and Y_i are independent and when $a = 0$ and $b = 1$, they both follow the standard normal distribution and do not depend on the sample size. The CUSUM statistics based on Z_i and Y_i are given by

$$C_i^+ = \max[0, Z_i - k + C_{i-1}^+], \tag{3.3}$$

$$C_i^- = \max[0, -k - Z_i + C_{i-1}^-], \tag{3.4}$$

and

$$S_i^+ = \max[0, Y_i - k + S_{i-1}^+], \tag{3.5}$$

$$S_i^- = \max[0, -k - Y_i + S_{i-1}^-], \tag{3.6}$$

respectively, where C_0 and S_0 are starting points and $max[a, b]$ denotes the maximum of a and b.

If either C_i^+ or C_i^- becomes greater than the decision interval, the process is said to be out of control due to changes in the process mean from the target value. In the same manner, if S_i^+ or S_i^- becomes greater than the decision interval, the process is deemed out of control due to changes in the process standard deviation from its target value. To detect shifts in the process mean and standard deviation, we usually run two control charts concurrently or combine the two charts by plotting two different quantities on the same chart, one for the process mean and another for the process standard deviation. If an out-of-control signal is issued, the process is stopped and a search for assignable cause(s) of variation is undertaken. If both statistics fall below the decision interval, it is assumed that the process is operating on target. If the process is operating on target, we do not stop monitoring the process, the monitoring is continued throughout the production process so that if the process goes out of control, the control chart can issue an out-of-control signal.

Because Z_i and Y_i follow the same distribution, a new statistic for a single control chart that can simultaneously monitor both process mean and standard deviation using a single variable is defined as:

$$M_i = \max[C_i^+, C_i^-, S_i^+, S_i^-] \tag{3.7}$$

The statistic M_i will be large when the process mean has drifted away from μ_0 and/or when the process standard deviation has drifted away from σ_0. Small values of M_i indicate that the process is in control. Since M_i's are non-negative, they are compared with the upper decision interval only.

The ARL of a control chart is often used as a measure of the performance of the chart. The ARL of the chart is the average number of points that must be plotted before a point plots above or below the control limits. If this happens, an out-of-control signal is issued indicating the possible presence of assignable cause(s) of variation and a search for the assignable cause(s) of variation must be taken. A chart is considered to be more efficient if its ARL is smaller than those of all other competing charts when the process is out of control and the largest when the process is in control.

The out-of-control signal is issued when either the mean or standard deviation or both have shifted from their target values. Therefore the plan (the sample size and control limits) is chosen so that the ARL is large, when the process is in control and small when the process is out of control. Cox ([25]) suggested that the criteria for a good chart are: (i) acceptable risks of incorrect actions, (ii) expected average quality levels reaching the customer and (iii) expected average inspection loads. Therefore the in control ARL should be chosen so as to minimize the frequency of false alarm and to ensure adequate response times to genuine shifts.

Recall that h is the decision interval and k is the reference value of the chart. For a predetermined in control ARL, for quickly detecting shifts in the mean and variability, an optimal combination of h and k is determined which will minimize the out-of-control ARL for a specified change in the mean and standard deviation. The proposed Max-CUSUM chart is sensitive to changes in both mean and standard deviation when there is an increase in the standard deviation and is less sensitive when the standard deviation shifts downwards. This phenomenon has been observed in other charts based on the standardized values (Domangue and Patch [31]).

3.3 Design of a Max-CUSUM Chart

We use the statistic M_i to construct a new control chart. Because M_i is the maximum of four statistics, we call this new chart the Max-CUSUM chart. We use theoretical results by Hawkins and Olwell ([40]) and the Markov chain approach developed by Brook and Evans ([11]) and successfully applied by Champ and Woodall ([14]) for the Shewhart chart, Lucus and Saccucci ([62]) for the EWMA chart and Lucus and Crosier ([60]) for the CUSUM chart, to compute the ARL for our Max-CUSUM chart.

The ARL's of the Max-CUSUM procedure is approximated using a discrete Markov chain. The possible values of M_i are represented by $t+1$ states. One state is an absorbing state representing $M_i > h$. The remaining t transient states are numbered 0, 1, 2, ..., (t-1) and represent values of M_i between 0 and h.

For a given in control ARL, and a shift for the mean and/or standard deviation intended to be detected by the chart, the reference value (k) is computed as half the shift we want to detect. For a given (ARL, k) combination, the value of the decision interval (h) is fixed. When the mean and standard deviation shift simultaneously, we can use the standard CUSUM chart procedures for standardized variables with decision interval $h^+ = h/b$ and reference value $k^+ = (k-a)/b$ to calculate the out-of-control ARL. This is equivalent to using the CUSUM chart with standard in control (h, k) values for a normal distribution with new mean $\mu = \mu_0 + a\sigma_0$ and standard deviation $\sigma = b\sigma_0$. We use the latter to calculate the ARL's in this thesis.

Table 3.1 gives the optimal combinations of h and k for an in control ARL fixed at 250. The smallest value of an out-of-control ARL is calculated with respect to specified shifts in the process mean alone, standard deviation alone and shifts in both mean and standard deviation using the optimal in control ARL CUSUM chart parameters. We assume that the process starts in an in control state and thus the initial value of the CUSUM statistic is set at zero. For example if one wants to have in control ARL of 250 and to guard against 3σ increase in the mean and 1.25σ increase in the standard deviation, i.e., $a = 3$ and $b = 1.25$, the optimal parameter values are $h = 1.025$ and $k = 1.500$. These shifts can on average be detected with the first sample i.e., the ARL is approximately one. The good feature about the Max-CUSUM chart is that smaller shifts in the mean and/or standard deviation are detected much faster than in single Shewhart chart (Max chart) and the single EWMA chart (Max-EWMA chart). The comparison of these charts is done in the next section.

Table 3.1 shows that small values of k with large values of h, result in quick detection of small shifts in mean and/or standard deviations. To keep the in control ARL at 250, a decrease in h results in an increase in the value of k for a given value of the standard deviation at different values of the mean. If one wants to guard against a 3σ increase in the mean and a 3σ increase in the standard deviation, the value of $h = 1.025$ and the value of $k = 1.500$. But for a 1σ increase in mean and 3σ increase in standard deviation, $h = 2.476$ and the value of k decreases to $k = 0.500$.

The Max-CUSUM scheme is sensitive to both small and large shifts in both process mean and standard deviation. A 0.25σ increase in the process mean reduces the ARL from 250 to 19 and a 1.25σ increase in the process standard deviation with a 0.25σ increase in the process mean reduces the ARL from 250 to 15 runs. If both parameters increased by large values, the ARL is reduced to 1. Thus the increase will on average be detected with the very first sample. For example, a 3σ increase in both parameters will be expected to be detected with the first sample.

Table 3.1: (k,h) combinations and the corresponding ARL for the Max-CUSUM chart.

$ARL_0 = 250$									
		a							
b	Parameter	0.00	0.25	0.50	1.00	1.50	2.00	2.50	3.00
1.00	h	2.476	5.234	3.733	2.476	1.877	1.511	1.245	1.025
	k	0.500	0.125	0.250	0.500	0.750	1.000	1.250	1.500
	ARL	250.02	18.52	7.66	3.19	2.04	1.59	1.38	1.26
1.25	h	1.980	5.234	3.733	2.476	1.877	1.511	1.245	1.025
	k	0.400	0.125	0.250	0.500	0.750	1.000	1.250	1.500
	ARL	12.60	14.35	6.23	2.72	1.88	1.40	1.11	1.10
1.50	h	1.650	5.234	3.733	2.476	1.877	1.511	1.245	1.025
	k	0.333	0.125	0.250	0.500	0.750	1.000	1.250	1.500
	ARL	9.61	11.66	5.28	2.41	1.65	1.35	1.11	1.10
2.00	h	1.238	5.234	3.733	2.476	1.877	1.511	1.245	1.025
	k	0.250	0.125	0.250	0.500	0.750	1.000	1.250	1.500
	ARL	6.60	8.46	4.12	2.04	1.47	1.24	1.11	1.10
2.50	h	0.990	5.234	3.733	2.476	1.877	1.511	1.245	1.025
	k	0.200	0.125	0.250	0.500	0.750	1.000	1.250	1.500
	ARL	5.34	6.66	3.45	1.83	1.37	1.18	1.10	1.10
3.00	h	0.825	5.234	3.733	2.476	1.877	1.511	1.245	1.025
	k	0.167	0.125	0.250	0.500	0.750	1.000	1.250	1.500
	ARL	4.51	5.54	3.02	1.69	1.30	1.15	1.07	1.04
4.00	h	0.619	5.234	3.733	2.476	1.877	1.511	1.245	1.025
	k	0.125	0.125	0.250	0.500	0.750	1.000	1.250	1.500
	ARL	3.73	4.25	2.53	1.54	1.23	1.11	1.05	1.02

Another alternative method of assessing the performance of the CUSUM chart is to fix the values of h and k and calculate the ARL's for various shifts in the mean and/or standard deviation. This is displayed in Table 3.2. The value of $k = 0.5$ and thus we want to detect a 1σ shift in the mean and $h = 2.476$. This combination gives an in control ARL = 250. From the table it can be concluded that, even though the chart is designed to detect a 1σ shift in the process, it is sensitive to both small and large shifts in the mean and/or standard deviation.

Table 3.2: ARL's for the Max-CUSUM chart with $h = 2.476$ and $k = 0.500$.

$ARL_0 = 250$								
	a							
b	0.00	0.25	0.50	1.00	1.50	2.00	2.50	3.00
1.00	250.77	6.15	4.75	3.19	2.39	1.92	1.62	1.41
1.25	12.63	5.15	4.01	2.72	2.05	1.66	1.42	1.25
1.50	9.60	4.48	3.52	2.41	1.83	1.50	1.29	1.16
2.00	6.64	3.67	2.92	2.04	1.58	1.32	1.17	1.08
2.50	5.33	3.20	2.57	1.83	1.44	1.23	1.11	1.05
3.00	4.51	2.90	2.35	1.69	1.36	1.18	1.08	1.03
4.00	3.73	2.55	2.09	1.54	1.26	1.12	1.05	1.02

3.4 Comparison with Other Procedures

In this section, we compare the Max-CUSUM chart with other recently proposed single charts used for quality monitoring. Most of the CUSUM charts developed are designed to monitor the mean and standard deviation separately, even the combined CUSUM charts monitor these parameters separately in the same plots. This is done by plotting the charts using different plotting variables for the means and standard deviations, and then calculating ARLs separately for each parameter. The ARL for the chart will be taken as the minimum of the two ARL's. The Max-CUSUM is compared with the omnibus CUSUM chart proposed by Domanque and

Patch ([31]), the Max chart by Chen and Cheng ([21]), the Max-EWMA chart by Chen, Cheng and Xie ([23]) and the Combined Shewhart-CUSUM chart by Lucus ([58]).

Table 3.4 shows the ARL's for the Max-CUSUM chart and the omnibus CUSUM chart developed by Domangue and Patch ([31]) for shifts shown in Table 3.3. For various changes in the mean and/or standard deviation, we have calculated the ARL's for the Max-CUSUM chart and compared them with those given by Domangue and Patch ([31]) in Table 4. The Max-CUSUM chart performs better than the omnibus CUSUM chart for all shifts since its ARL's are smaller than those of the omnibus chart. The Max-CUSUM chart is also easy to plot and read as compared to the omnibus CUSUM chart since it uses only one plotting variable for each sample.

Table 3.3: Level of shifts in mean and standard deviation considered.

Label	μ	σ
S_1	0.75	1.0
S_2	1.5	1.0
S_3	0	1.2
S_4	0	1.4
S_5	0.75	1.3
S_6	1.0	1.2

Table 3.4: ARL's for the Max-CUSUM and the omnibus CUSUM charts.

$k = 1$	$h = 1.279$		$\alpha = 0.5$		$n = 1$	
Scheme	S_1	S_2	S_3	S_4	S_5	S_6
Omnibus	37.0	7.0	50.4	21.5	15.7	13.0
Max-CUSUM	2.5	1.5	30.7	16.9	2.4	2.1

In Table 3.5 we compare the Max-CUSUM chart with the Max chart (Chen and Cheng [21]). The Max chart is less sensitive to small shifts in the mean and/or standard deviation as compared to the Max-CUSUM chart. For large shifts in these parameters, there is no significant difference in the performance of these two charts. However, the Max chart performs better than the Max-CUSUM chart when the standard deviation shifts by large amount at low shifts in the mean.

Table 3.5: ARL's for Max-CUSUM chart and the Max chart.

$ARL_0 = 250$												
	Max-CUSUM						Max chart n=4					
	a						a					
b	0.00	0.25	0.50	1.00	2.00	3.00	0.00	0.25	0.50	1.00	2.00	3.00
1.00	250.0	18.5	7.7	3.2	1.6	1.3	250	143.8	49.3	7.2	1.2	1.0
1.25	12.6	14.4	6.2	2.7	1.4	1.1	34.3	27.2	15.9	4.9	1.3	1.0
1.50	9.6	11.7	5.2	2.4	1.4	1.1	9.8	8.9	6.9	3.5	1.3	1.0
2.00	6.6	8.5	4.1	2.0	1.2	1.1	2.9	2.8	2.6	2.1	1.3	1.1
3.00	4.5	5.5	3.0	1.7	1.2	1.1	1.4	1.4	1.4	1.3	1.2	1.1

Lucas ([58]) developed a combined Shewhart-CUSUM chart. Table 3.6 gives the ARLs for this chart in comparison with those of our Max-CUSUM chart. The Max-CUSUM chart is superior to the combined Shewhart-CUSUM chart for small shifts in the mean while the two charts' performance is comparable for larger shifts in the process mean. The advantage of the Max-CUSUM chart over the combined Shewhart-CUSUM chart is the fact that, Max-CUSUM is capable of simultaneously detecting shifts in mean and standard deviation of the process.

Table 3.6: ARL's for the combined Shewhart-CUSUM and Max-CUSUM schemes, with $ARL_0 = 303$.

Shifts in mean	0.00	0.25	0.50	1.00	1.50	2.00	2.50	3.00	4.00	5.00
Combined Shewhart-CUSUM	303.2	65.6	20.2	5.3	2.9	2.0	1.6	1.3	1.1	1.0
Max-CUSUM	303.2	38.8	15.3	5.0	3.2	2.4	1.8	1.5	1.2	1.0

Table 3.7 shows the performance of the Max-CUSUM chart and Max-EWMA

chart for in control ARL = 250. Both charts are sensitive to small and large shifts in the mean and/or standard deviation with the Max-CUSUM chart performing better than the Max-EWMA chart for small shifts in the process mean and/or standard deviation while the Max-EWMA chart performs better than the Max-CUSUM chart for large shifts, particularly for large shifts in the standard deviation. These two charts use only one plotting variable for each sample and have good procedures of indicating the source as well as the direction of shifts in the process parameters.

Table 3.7: ARL's for Max-CUSUM chart and the Max-EWMA chart.

$ARL_0 = 250$												
	Max-CUSUM						Max-EWMA					
	a						a					
b	0.00	0.25	0.50	1.00	2.00	3.00	0.00	0.25	0.50	1.00	2.00	3.00
1.00	250.0	18.5	7.7	3.2	1.6	1.3	250.0	24.6	8.6	2.9	1.1	1.0
1.25	12.6	14.4	6.2	2.7	1.4	1.1	17.8	12.3	7.1	2.9	1.2	1.0
1.50	9.6	11.7	5.3	2.4	1.4	1.1	6.3	5.7	4.5	2.5	1.2	1.0
2.00	6.6	8.5	4.1	2.0	1.2	1.1	2.5	2.5	2.3	1.8	1.2	1.0
3.00	4.5	5.5	3.0	1.7	1.2	1.1	1.7	1.6	1.6	1.5	1.2	1.1

3.5 Charting Procedures

The charting procedure of a Max-CUSUM chart is similar to that of the standard upper CUSUM chart. The successive CUSUM values, M_i's are plotted against the sample numbers. If a point plots below the decision interval, the process is said to be in control and the point is plotted using a symbol such as a dot. An out-of-control signal is given if any point plots above the decision interval and is plotted using one of the characters defined below. The following procedure is used in building the CUSUM chart:

1. Specify the following parameters: the in control or target value of the mean μ_0 and the in control or target value of the standard deviation σ_0.

2. If μ_0 is not known, use the sample grand average $\bar{\bar{X}}$ of the data to estimate it, where $\bar{\bar{X}} = (\bar{X}_1 + ... + \bar{X}_m)/m$. If σ_0 is unknown, use $\bar{R}/d_2$ or $\bar{S}/c_4$ to estimate it, where $\bar{R} = (R_1 + ... + R_m)/m$ is the average of the sample ranges and $\bar{S} = (S_1 + ... + S_m)/m$ is the average of the sample standard deviations, and $d_2 = d_2(\bar{n})$ and $c_4 = c_4(\bar{n})$ are statistically determined constants with $\bar{n} = (n_1 + ... + n_m)/m$. When the sample sizes vary, we use a weighted average approach to calculate $\bar{\bar{X}}$ and $\bar{S}$. If n_i is the number of observations in the i^{th} sample, then use

$$\bar{\bar{x}} = \frac{\sum_{i=1}^{m} n_i \bar{x}_i}{\sum_{i=1}^{m} n_i}$$

and

$$\bar{S} = \left[\frac{\sum_{i=1}^{m}(n_i - 1)S_i^2}{\sum_{i=1}^{m} n_i - m}\right]^{1/2}$$

3. For each sample compute Z_i and Y_i.

4. To detect specified changes in the process mean and standard deviation for a specified in control ARL, choose an optimal (h, k) combination and calculate C_i^+, C_i^-, S_i^+ and S_i^-.

5. Compute the M_i's and compare them with h, the decision interval.

6. Denote the sample points with a dot and plot them against the sample number if $M_i \leq h$.

7. If any of the M_i's is greater than the decision interval, h, the following plotting characters should be used to show the direction as well as the statistic that is plotting above the decision interval.

   (i) If $C_i^+ > h$, plot $C+$. This shows an increase in the process mean.

(ii) If $C_i^- > h$, plot $C-$. This indicates a decrease in the process mean.

(iii) If $S_i^+ > h$, plot $S+$. This shows an increase in the process standard deviation.

(iv) If $S_i^- > h$, plot $S-$. This shows a decrease in the process standard deviation.

(v) If both $C_i^+ > h$, and $S_i^+ > h$, plot $B++$. This indicates an increase in both the mean and the standard deviation of the process.

(vi) If $C_i^+ > h$ and $S_i^- > h$, plot $B+-$. This indicates an increase in the mean and a decrease in the standard deviation of the process.

(vii) If $C_i^- > h$ and $S_i^+ > h$, plot $B-+$. This indicates a decrease in the mean and an increase in the standard deviation of the process.

(viii) If $C_i^- > h$ and $S_i^- > h$, plot $B--$. This shows a decrease in both the mean and the standard deviation of the process.

8. Investigate the cause(s) of shift for each out-of-control point in the chart and carry out the remedial measures needed to bring the process back into an in control state.

3.6 An Example

We show the application of the Max-CUSUM chart to real data. The data is used to set up a control chart for both *phase I*. A Max-CUSUM chart is applied to real data obtained from DeVor, Chang and Sutherland ([30]). The data are measurements of the inside diameter of the cylinder bores in an engine block. The measurements are made to $1/10,000$ of an inch. Samples of size $n = 5$ are taken roughly every half hour, and the first 35 samples are given in Table 3.8. The actual measurements are of the form 3.5205, 3.5202, 3.5204 and so on. The entries given in Table 7 provide the last three digits in the measurements.

Table 3.8: Cylinder diameter data

Sample i	X_{i1}	X_{i2}	X_{i3}	X_{i4}	X_{i5}	Sample i	X_{i1}	X_{i2}	X_{i3}	X_{i4}	X_{i5}
1	205	202	204	207	205	19	207	206	194	197	201
2	202	196	201	198	202	20	200	204	198	199	199
3	201	202	199	197	196	21	203	200	204	199	200
4	205	203	196	201	197	22	196	203	197	201	194
5	199	196	201	200	195	23	197	199	203	200	196
6	203	198	192	217	196	24	201	197	196	199	207
7	202	202	198	203	202	25	204	196	201	199	197
8	197	196	196	200	204	26	206	206	199	200	203
9	199	200	204	196	202	27	204	203	199	199	197
10	202	196	204	195	197	28	199	201	201	194	200
11	205	204	202	208	205	29	201	196	197	204	200
12	200	201	199	200	201	30	203	206	201	196	201
13	205	196	201	197	198	31	203	197	199	197	201
14	202	199	200	198	200	32	197	194	199	200	199
15	200	200	201	205	201	33	200	201	200	197	200
16	201	187	209	202	200	34	199	199	201	201	201
17	202	202	204	198	203	35	200	204	197	197	199
18	201	198	204	201	201						

Suppose, based on past experience, an operator wants to detect a shift in the mean of 1σ, that is $a = 1$ and a shift in the standard deviation of 2σ; that is $b = 2$ with an in control ARL = 250, the corresponding decision interval from Table 3.1 is $h = 2.475$ and the reference value is $k = 0.500$. The chart is developed as follows: The nominal mean μ_0 is estimated by $\bar{\bar{X}}$, the average of sample averages and σ_0 is estimated by $\bar{S}/c_4$. The sample produced the following estimates $\bar{\bar{X}} = 200.25$ and $\bar{S}/c_4 = 3.31$

The Max-CUSUM chart in Figure 3.1 which plots all the 35 observations shows that several points plot above the decision interval. Sample number 6 shows an increase in the standard deviation as the plotting symbol is $S+$. After this sample, CUSUM values corresponding to samples 7 and 8 also plot above the decision interval. However these points shows that the standard deviation is decreasing towards the in control values. Due to very high value of the CUSUM statistic for the standard deviation in sample 6, the successive cumulative values of samples 7 and 8 plot above the decision interval even though the standard deviation values corresponding to these samples are in control. We therefore investigate the cause of higher variability at sample number 6. According to DeVor, Chang and Sutherland ([30]), this sample was taken when the regular operator was absent, and a relief, inexperienced operator was in charge of the production line and the operator effect could have affected the process.

The CUSUM statistic corresponding to sample number 11 also plots above the decision interval. Because now the plotting symbols is $C+$, this point corresponds to an increase in the process mean. This corresponds to a sample taken at 1:00 P.M. when production had just resumed after lunch break. The machines were shut down at lunch time for tool changing and thus these items were produced when the machines were still cold. Once the machines warmed up, the process settled to an in control state. This shows that the shift in the mean was caused by the machine tune-up problem.

The statistic for sample 16 also plots above the decision interval, and with the symbol $S+$ this indicates an increase in the standard deviation. According to DeVor, Chang and Sutherland ([30]), this sample corresponds to a time when an inexperienced operator was in control of the process and could have affected the process operation. In addition to the above mentioned points which also plotted above the control limit in the Shewhart chart, Max chart and EWMA chart, the statistic for sample 34 plots above the decision interval. This point corresponds to a decrease in the standard deviation. The Shewhart S-chart plotted this value close to the lower control limit but within the acceptable area. Table 3.1 shows that the Max-CUSUM chart is very sensitive to small shift and thus signals for this small decrease in the standard deviation. A decrease in the standard deviation is associated with an improvement in the process since it produces products that are closer to the targeted value.

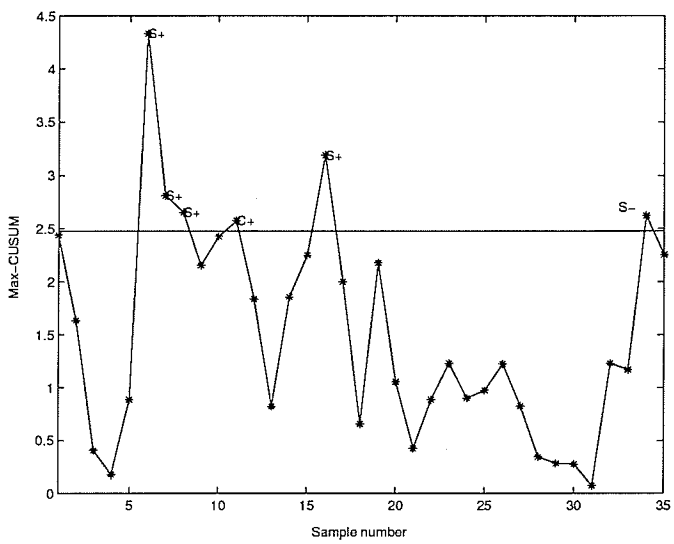

Figure 3.1: The first Max-CUSUM control chart for the cylinder diameter data

When these four samples are removed from the data, new estimates for the mean and standard deviation were computed, giving the following values: $\bar{\bar{X}} = 200.08$ and $\bar{S}/c_4 = 3.02$. The revised chart is shown in Figure 3.2. The chart plots only one point above the decision interval. This point corresponding to sample 1, shows an increase in the mean. This point corresponds to a sample that was taken at 8:00 A.M. This corresponds roughly to the start up of the production line in the morning, when the machine was cold. Once the machine warmed up, the production returns to an in control state.

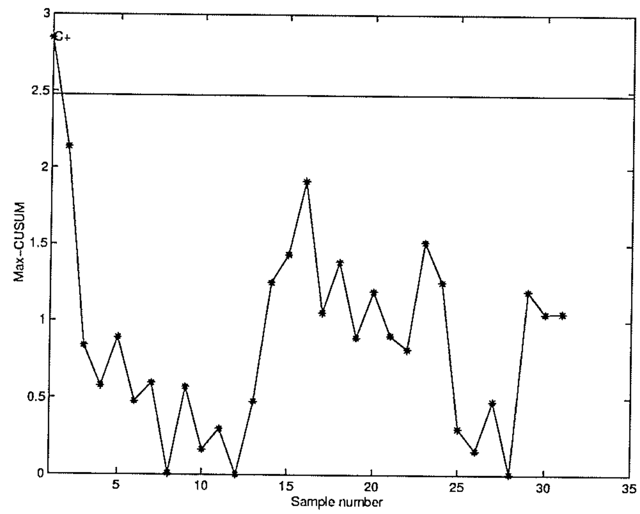

Figure 3.2: The second Max-CUSUM control chart for the cylinder diameter data

When sample 1 is removed from the data, we re-calculate the process mean and the process standard deviation estimates and obtain $\bar{\bar{X}} = 199.93$ and $\bar{S}/c_4 = 3.06$. The Max-CUSUM chart for this new data is shown in Figure 3.3. All the points plot within the decision interval showing that the process is in control. This chart can now be used to monitor the current process.

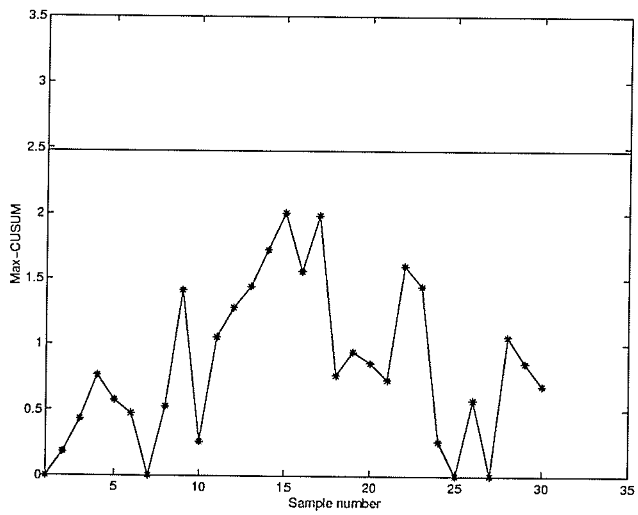

Figure 3.3: The third Max-CUSUM control chart for the cylinder diameter data

3.7 Conclusions and Recommendations

One disadvantage of the standard CUSUM chart is that it does not quickly detect a large and temporary increase in the process mean and/or standard deviation and thus is not recommended for monitoring processes experiencing large increases in both mean and variability.

A good feature of the Max-CUSUM chart is its ability to quickly detect both small and large changes in the mean and/or standard deviation. Another advantage of the Max-CUSUM is that we are able to monitor both the process center and spread using one chart. The performance of the proposed Max-CUSUM is very competitive in comparison with the Max chart and the Max-EWMA chart. The Max-CUSUM chart is easy to chart and also performs better than its competitors for detecting small shifts in the process parameters.

Chapter 4

SS-CUSUM Chart

4.1 Introduction

In this chapter, we propose a new CUSUM chart capable of simultaneously monitoring the process mean and process standard deviation. This chart is an extension of the Shewhart based semicircle chart proposed by Chao and Cheng ([19]) and the SS-EWMA chart proposed by Xie ([108]).

To simplify the CUSUM chart, we propose a new single CUSUM chart and call it the Sum of Square Cumulative Sum (SS-CUSUM) control chart. This chart is based on the sum of squares of the maximum standard CUSUM values. The properties of this chart are similar to those of the Max-CUSUM chart proposed in chapter 3. However, the SS-CUSUM chart has an added advantage of being easy to implement, and if a trend develops in either the mean and/or standard deviation, it can be quickly detected by examining whether the points plot far from the axes. An out-of-control signal also immediately identifies the parameter that has shifted, the direction of the shift as well as the time at which the process went out of control. We investigate the sampling behavior of the proposed statistic and procedures for constructing a new single chart, the SS-CUSUM chart, which to a large extent, satisfies the criteria discussed for the development of the Max-CUSUM chart.

4.2 The New Control Chart

This new chart is developed under the same normality and independence assumptions used for the development of the Max-CUSUM chart. We also consider the case of a step change in the process mean and/or standard deviation. The design procedures are summarized as follows: Let $X_i = X_{i1}, ..., X_{in_i}$, $i = 1, 2, ...$, denote a sequence of samples of size n_i taken on a quality characteristic X. It is assumed that, for each i, $X_{i1}, ..., X_{in_i}$ are independent and identically distributed observations following a normal distribution with means and standard deviations possibly depending on i, where i indicates the i^{th} group. Let μ_0 and σ_0 be the nominal process mean and standard deviation previously established. Assume that the process parameters μ and σ can be expressed as $\mu = \mu_0 + a\sigma_0$ and $\sigma = b\sigma_0$, where $a = 0$ and $b = 1$ when the process is in control, otherwise, the process has changed due to some assignable causes. Then a represents a shift in the process mean and b a shift in the process standard deviation and $b > 0$.

Let $\bar{X}_i$ and S_i^2 be the mean and variance for the i^{th} sample respectively as before. The CUSUM charts for the mean and standard deviation are based on $\bar{X}_i$ and S_i respectively. In developing the SS-CUSUM chart, we carry out the same transformation as for the Max-CUSUM chart. Formulae for Z_i and Y_i are given in equations (3.1) and (3.2) of chapter 3.

In the same manner, the CUSUM statistics based on Z_i and Y_i are given by

$$C_i^+ = \max[0, Z_i - k + C_{i-1}^+], \tag{4.1}$$

$$C_i^- = \max[0, -k - Z_i + C_{i-1}^-], \tag{4.2}$$

$$S_i^+ = \max[0, Y_i - k + S_{i-1}^+], \tag{4.3}$$

$$S_i^- = \max[0, -k - Y_i + S_{i-1}^-]. \tag{4.4}$$

We define the following new statistics to construct the new chart:

$$M_i = \max[C_i^+, C_i^-], \tag{4.5}$$

$$V_i = \max[S_i^+, S_i^-] \tag{4.6}$$

and

$$SS_i = M_i^2 + V_i^2 \tag{4.7}$$

The statistic in equation (4.7) defines a circle. But since both M_i and V_i are nonnegative, and we plot (V_i, M_i) for each sample, the first quadrant of a circle centered at (0, 0) is sufficient for plotting the SS-CUSUM chart. The statistic for the process mean (M_i) will be plotted on the ordinate (Y-axis) and the statistic for the standard deviation (V_i) on the abscissa (X-axis). A point falling outside the circle indicates an out-of-control situation, the process is said to be in control if all points, (V_i, M_i) fall within the circle.

4.3 Design of the SS-CUSUM Chart

The performance of a control chart can be assessed by looking at its ARL. We have studied the ARL with respect to shifts in the process mean alone, shift in the process standard deviation alone and shifts in both process mean and standard deviation. For the SS-CUSUM chart, there is no direct way to compute the ARL, so each ARL value is obtained using 10,000 simulations. In Table 4.1, we find the optimal combination of h and k for a given in-control ARL, where h and k are known as the decision interval and reference value respectively. The shift in the standard deviation is denoted by b and the shift in the mean is denoted by a as stated before.

Table 4.1 gives the optimal combinations of h and k for an in-control ARL fixed at 250. The smallest value of an out-of-control ARL is calculated with respect to a pair of specified shifts in both mean and standard deviation using the optimal in-control ARL parameters. We assume that the process starts in an in-control state and thus the initial value of the CUSUM statistic is set at zero. The results suggest that the chart is sensitive to both small and large shifts in the mean and/or standard deviation.

An out-of-control ARL is calculated for each pair of means and standard deviation using a transformed noncentral chi-square distribution and the optimal values of h and k. The SS-CUSUM chart is developed by drawing a circle with radius $r = h$, and plotting the $(V_i,\ M_i)$ points in the chart.

We study the ARL with respect to mean shift (i.e. $\mu = \mu_0 + a\sigma$,) and/or standard deviation shift (i.e. $\sigma = b\sigma_0$). The SS-CUSUM chart detects the shift in mean and/or standard deviation very well. It quickly detects both small and large shifts in both parameters for given in-control ARL. For example a 0.25σ shifts in the mean can be detected on average on the 11^{th} sample and a 2σ shift in the mean with any level of shift in the process standard deviation can be expected to be detected on the second sample.

In Table 4.2, we show the performance of the SS-CUSUM chart when a chart is designed to detect a 1σ shift in the mean and/or standard deviation of the process. This is accomplished by fixing the reference value and decision interval to $k = 0.500$ and $h = 3.841$ respectively. The ARL values in the table shows that this scheme is sensitive to both small and large shifts in the process mean and/or standard deviation. The CUSUM charts discussed in the literature that are designed to detect a 1σ shift in the mean are only sensitive to small shift and less sensitive to large shifts.

Table 4.1: (k,h) combinations and the corresponding ARL for the SS-CUSUM chart with $ARL_0 = 250$

$ARL_0 = 250$									
		a							
b	Parameter	0.00	0.25	0.50	1.00	1.50	2.00	2.50	3.00
1.00	h	3.841	5.247	4.035	3.841	2.535	2.017	1.745	1.514
	k	0.500	0.125	0.250	0.500	0.750	1.000	1.250	1.500
	ARL	250.00	11.37	6.93	3.12	2.47	1.88	1.42	1.31
1.25	h	3.625	8.800	6.087	3.625	2.630	1.986	1.547	1.215
	k	0.500	0.125	0.250	0.500	0.750	1.000	1.250	1.500
	ARL	9.72	9.00	5.23	2.86	2.34	1.44	1.22	1.18
1.50	h	3.625	8.800	6.087	3.625	2.630	1.986	1.547	1.215
	k	0.500	0.125	0.250	0.500	0.750	1.000	1.250	1.500
	ARL	7.01	6.49	4.48	2.23	2.00	1.36	1.11	1.10
2.00	h	3.625	8.800	6.087	3.625	2.630	1.986	1.547	1.215
	k	0.500	0.125	0.250	0.500	0.750	1.000	1.250	1.500
	ARL	5.25	5.00	3.18	2.05	1.86	1.31	1.10	1.08
2.50	h	3.625	8.800	6.087	3.625	2.630	1.986	1.547	1.215
	k	0.500	0.125	0.250	0.500	0.750	1.000	1.250	1.500
	ARL	3.74	3.49	2.78	1.91	1.62	1.22	1.04	1.00
3.00	h	3.625	8.800	6.087	3.625	2.630	1.986	1.547	1.215
	k	0.500	0.125	0.250	0.500	0.750	1.000	1.250	1.500
	ARL	2.98	2.94	2.43	1.68	1.47	1.18	1.00	1.00
4.00	h	3.625	8.800	6.087	3.625	2.630	1.986	1.547	1.215
	k	0.500	0.125	0.250	0.500	0.750	1.000	1.250	1.500
	ARL	2.46	2.09	1.99	1.59	1.33	1.10	1.00	1.00

Table 4.2: ARL's for the SS-CUSUM chart with $h = 3.841$ and $k = 0.500$.

	a							
b	0.00	0.25	0.50	1.00	1.50	2.00	2.50	3.00
1.00	250.00	9.05	6.21	3.12	2.52	1.92	1.47	1.34
1.25	9.72	8.88	5.02	2.86	2.41	1.49	1.26	1.21
1.50	7.01	6.38	4.23	2.23	2.11	1.41	1.18	1.14
2.00	5.25	4.81	2.97	2.05	1.93	1.35	1.12	1.10
2.50	3.74	3.21	2.63	1.91	1.65	1.27	1.10	1.06
3.00	2.98	2.87	2.38	1.68	1.52	1.21	1.00	1.00
4.00	2.46	2.00	1.87	1.59	1.34	1.10	1.00	1.00

4.4 Comparison with Other Procedures

We compare the SS-CUSUM chart with other proposed single charts namely, Semicircle chart developed by Chao and Cheng ([19]), the SS-EWMA chart proposed by and Xie ([108]), the Max-CUSUM chart proposed in chapter 3 and the Max chart proposed by Chen and Cheng ([21]). It can be concluded by examining Tables 4.3 through 4.6 that, the proposed SS-CUSUM chart performs better than the SS-EWMA chart for shifts of order 0.5σ and smaller in the mean and 1.25σ and smaller in the standard deviation. It outperforms the Max-CUSUM chart, Semicircle chart and the Max chart for shifts of order up to 1.5σ. For large shifts in the mean and/or standard deviation, these charts are the same with the max chart performing slightly better for shifts of order 3σ and above. Therefore the SS-CUSUM chart is the best chart for detecting small shifts in the mean and/or standard deviation among its competitors.

Table 4.3: Comparison of SS-CUSUM chart with the Semicircle chart with ARL_0 = 185.

	a/b							
	1.0/0.75	1.5/0.75	1.5/0.5	1.5/1.0	0.5/1.5	1.5/1.5	1.0/2.0	1.5/2.0
SS-CUSM	4.83	3.54	5.85	2.67	3.18	1.94	1.88	1.65
Semicircle	88.86	11.41	62.08	5.69	8.26	3.01	2.79	2.18

Table 4.4: Comparison of SS-CUSUM chart with the Max-CUSUM chart.

	$ARL_0 = 250$											
	SS-CUSUM						Max-CUSUM					
	a						a					
b	0.25	0.50	1.00	1.50	2.00	2.50	0.25	0.50	1.00	1.50	2.00	2.50
1.00	11.4	6.9	3.1	2.5	1.9	1.4	18.5	7.7	3.2	2.0	1.6	1.4
1.25	9.0	5.2	2.9	2.3	1.4	1.2	14.4	6.2	2.7	1.9	1.4	1.1
1.50	6.5	4.5	2.2	2.0	1.4	1.1	11.7	5.3	2.4	1.7	1.4	1.1
2.00	5.0	3.2	2.1	1.9	1.3	1.1	8.5	4.1	2.0	1.5	1.2	1.1
2.50	3.5	2.8	1.9	1.6	1.2	1.0	6.7	3.5	1.8	1.4	1.2	1.1
3.00	2.9	2.4	1.7	1.5	1.2	1.0	5.5	3.0	1.7	1.3	1.2	1.1
4.00	2.1	2.0	1.6	1.3	1.1	1.0	4.3	2.5	1.5	1.2	1.1	1.1

Table 4.5: Comparison of SS-CUSUM chart with the SS-EWMA chart.

	$ARL_0 = 250$											
	SS-CUSUM						SS-EWMA					
	a						a					
b	0.25	0.50	1.00	1.50	2.00	2.50	0.25	0.50	1.00	1.50	2.00	2.50
1.00	11.4	6.9	3.1	2.5	1.9	1.4	24.4	8.8	3.1	1.6	1.1	1.0
1.25	9.0	5.2	2.9	2.3	1.4	1.2	11.7	6.6	2.8	1.6	1.2	1.0
1.50	6.5	4.5	2.2	2.0	1.4	1.1	5.3	4.1	2.3	1.5	1.2	1.0
2.00	5.0	3.2	2.1	1.9	1.3	1.1	2.1	2.0	1.6	1.3	1.2	1.1
2.50	3.5	2.8	1.9	1.6	1.2	1.0	1.4	1.4	1.3	1.2	1.1	1.1
3.00	2.9	2.4	1.7	1.5	1.2	1.0	1.2	1.2	1.2	1.1	1.1	1.1

Table 4.6: Comparison of SS-CUSUM chart with the Max chart.

$ARL_0 = 185$												
	SS-CUSUM						Max Chart					
	a						a					
b	0.00	0.25	0.50	1.00	2.00	3.00	0.00	0.25	0.50	1.00	2.00	3.00
1.00	250.0	11.4	6.9	3.1	1.9	1.3	250	143.8	49.3	7.2	1.2	1.0
1.25	9.7	9.0	5.2	2.9	1.4	1.2	34.3	27.2	15.9	4.9	1.3	1.0
1.50	7.0	6.5	4.5	2.2	1.4	1.1	9.8	8.9	6.9	3.5	1.3	1.0
2.00	5.3	5.0	3.2	2.0	1.3	1.1	2.9	2.8	2.6	2.1	1.3	1.1
3.00	3.0	2.9	2.4	1.7	1.2	1.0	1.4	1.4	1.4	1.3	1.2	1.1

4.5 Charting Procedures

The charting procedure of the SS-CUSUM chart is different from those of other CUSUM charts. Instead of plotting the CUSUM statistics against the sample numbers, successive pairs of (V_i, M_i)'s are plotted on the chart. The position of a point on the plane directly indicates the source of an assignable cause of variation. When a point shows deviation from the M (Mean) axis, this shows a shift in the process standard deviation and a point that shifts away from the V (Standard deviation) axis shows a shift in the process mean. An increase in either of these parameters is indicated by positive signs and a decrease by negative signs. A shift in both mean and standard deviation is shown by a point plotting along or near the line $M_i = V_i$.

The following procedures are followed in drawing the chart:

1. Specify the following parameters: the in-control or target value of the mean μ_0 as well as the in-control or target value of the standard deviation σ_0.

2. If μ_0 is unknown, use the grand average $\bar{\bar{X}}$ of the data to estimate it. If σ_0 is unknown, use $\bar{R}/d_2$ or $\bar{S}/c_4$ to estimate it.

3. For each sample compute Z_i and Y_i.

4. To detect specified changes in the process mean and standard deviation, choose an optimal $(h,\, k)$ combination and calculate C_i^+, C_i^-, S_i^+ and S_i^-.

5. Compute the M_i's and V_i's.

6. Find the radius $r = h$.

7. Draw a first quadrant of a circle centered at (0, 0) with radius r.

8. Plot the data points (V_i, M_i).

9. If any point is greater than the decision interval r, the sample number at which the shift occurred is indicated.

10. If any pair of the $(V_i, M_i\ )$ points is greater than the decision interval r, the following plotting characters should be used to show the direction as well as the statistic that is plotting above the interval.

If $M_i > r$, then

(i) If $C_i^+ > r$, plot $C+$. This shows an increase in the process mean.

(ii) If $C_i^- > r$, plot $C-$. This indicates a decrease in the process mean.

If $V_i > r$, then

(iii) If $S_i^+ > r$, plot $S+$. This shows an increase in the process standard deviation.

(iv) If $S_i^- > r$, plot $S-$. This shows a decrease in the process standard deviation.

If $M_i > r$ and $V_i > r$, then

(v) If both $C_i^+ > r$, and $S_i^+ > r$, plot $B++$. This indicates an increase in both the mean and standard deviation of the process.

(vi) If $C_i^+ > r$ and $S_i^- > r$, plot $B+-$. This indicates an increase in the mean and a decrease in the standard deviation of the process.

(vii) If $C_i^- > r$ and $S_i^+ > r$, plot $B-+$. This indicates a decrease in the mean and an increase in the standard deviation of the process.

(viii) If $C_i^- > r$ and $S_i^- > r$, plot $B--$. This shows a decrease in both mean and standard deviation of the process.

11. Investigate the cause(s) of shift for each out-of-control point in the chart and carry out the remedial measures needed to bring the process back into an in-control state.

4.6 An Example

To demonstrate the implementation of the proposed SS-CUSUM chart, we will as before use DeVor, Chang and Sutherland ([30]) data from their example on the measurements of the inside diameter of the cylinder bores in an engine block. These data are displayed in Table 3.8. Suppose based on past experience, an operator wanted to guard against a 1σ shift in the mean and various shifts in the standard deviation with an in-control ARL = 250. The corresponding chart parameters from Table 4.1 are $k = 0.5$ and $h = 3.625$. Therefore the chart will be drawn as a circle with radius $r = 3.625$.

The chart is developed as follows: The nominal mean μ_0 is estimated by $\bar{\bar{X}}$, and the nominal standard deviation σ_0 is estimated by $\bar{S}/c_4$. The sample produced the following estimates $\bar{\bar{X}} = 200.25$ and $\bar{S}/c_4 = 3.31$

The SS-CUSUM chart in Figure 4.1 which includes all 35 observations shows that one point plots above the decision interval indicating the possible presence of an assignable cause of variation. This point corresponds to the CUSUM statistic for sample number 6. The symbol $S+$ shows an increase in the process standard deviation. As discussed in chapter 3, this sample was taken when the regular experienced operator was not present, and a relief operator, who was inexperienced was in charge of the production line and thus the operator inexperience could have resulted in a change in the process performance.

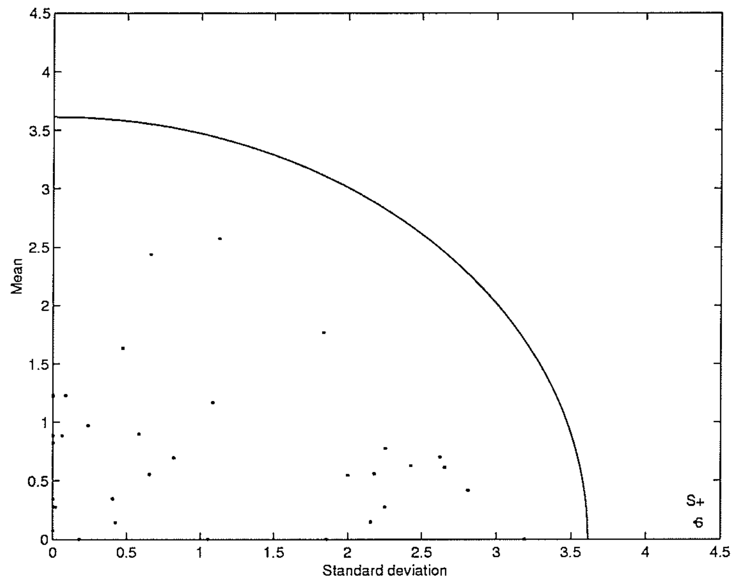

Figure 4.1: The first SS-CUSUM chart for the cylinder diameter data

Since we have knowledge of the reason for this change, this sample can be removed from the data set and new estimates computed as $\bar{\bar{X}} = 200.21$ and $\bar{S}/c_4 = 3.06$. The revised chart is shown in Figure 4.2. The chart shows that one point plots above the decision interval. This point corresponds to the sample number 15, this is number 16 in the original data. The plotting symbol shows an increase in the process standard deviation. According to DeVor, Chang and Sutherland ([30]), this corresponds to the time when an inexperienced operator was again in charge of the production line and this could have had an impact on the production process.

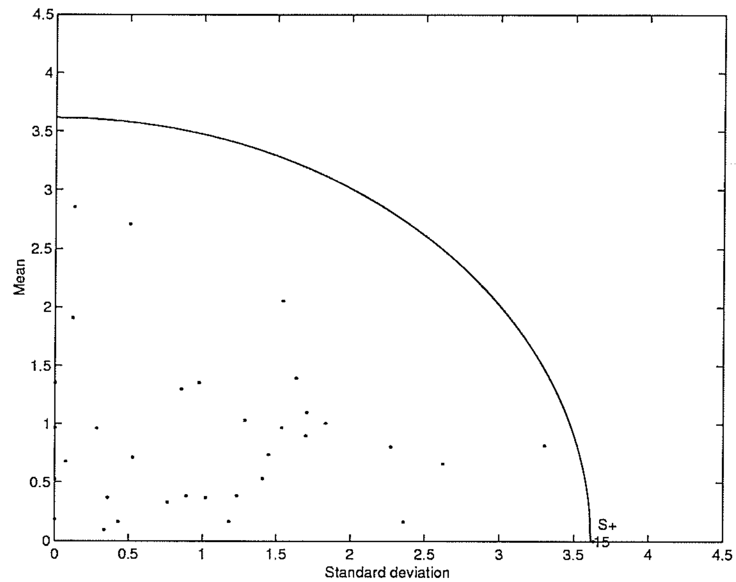

Figure 4.2: The second SS-CUSUM chart for the cylinder diameter data

When this sample is removed from the data set, new estimates are obtained as $\bar{\bar{X}} = 200.22$ and $\bar{S}/c_4 = 2.9$. The revised chart is shown in Figure 4.3. The chart shows that two samples, sample 10 and 11 in the new data set which correspond to samples 11 and 12 in the original data, show a shift in the production process. Sample 10 shows an increase in the process mean. According to DeVor, Chang and Sutherland ([30]), this sample was taken at 1:00 P.M. This is the first batch of production after the lunch break. The machines were shut down at lunch time for tool change and thus had not yet warmed up when these items were produced.

The next sample, sample 11 shows a shift in both the process mean and standard deviation because it is close to the line $M_i = V_i$. The chart shows that the mean had increased while the standard deviation had decreased below the nominal value. As can be seen these shifts follow immediately after a shift in the mean implying that the machine had not yet warmed up and possibly an interference by the operator in an effort to bring the process back to an in-control state resulted in an increase in the mean and a decrease in the standard deviation.

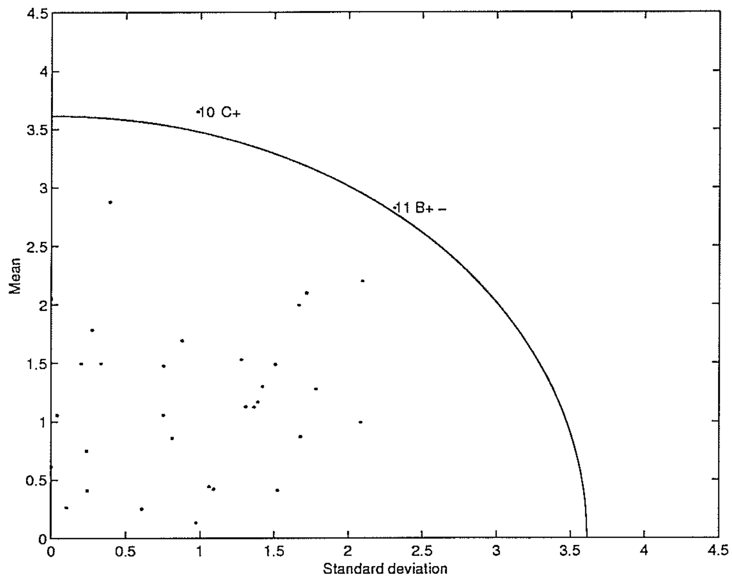

Figure 4.3: The third SS-CUSUM chart for the cylinder diameter data

When these two points are removed, the two estimates are recalculated as $\bar{\bar{X}} = 200.09$ and $\bar{S}/c_4 = 3.02$. The new chart is shown Figure 4.4. All points plotted within the decision interval indicating that the process is in control.

This chart gives results that are different from the Max-CUSUM for samples 1 and 12 only. Max-CUSUM showed that sample 1 was above the decision interval thus out of control while for SS-CUSUM it shows an in-control state. Sample 12 for the SS-CUSUM plots outside the decision interval indicating that both mean and standard deviation shifted while Max-CUSUM did not pick up this shift but showed that it was close to the decision interval.

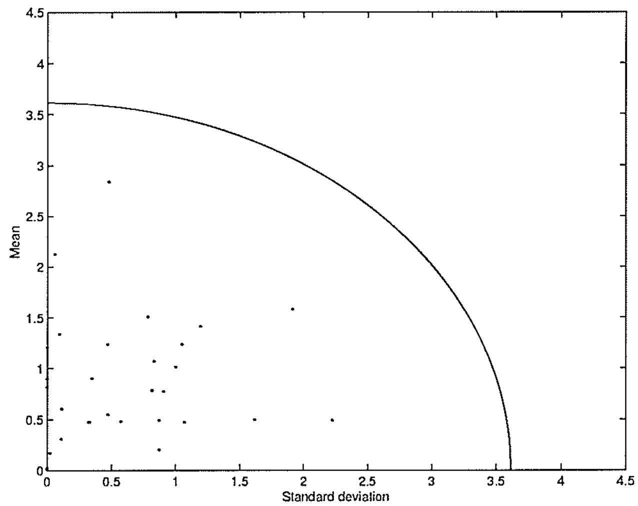

Figure 4.4: The fourth Max-CUSUM chart for the cylinder diameter data

4.7 Conclusions and Recommendations

We have proposed and studied a new control charting scheme, the SS-CUSUM chart, to provide a new alternative to the commonly used control charts for simultaneously monitoring and detecting possible changes in the process mean and standard deviation. This chart is very easy to use and it quickly detects both small and large shifts in the process mean and standard deviation. This new control chart has an added advantage over other charts because it is also sensitive to decreases in the process standard deviation. Most of the charts proposed in the literature that are based on standardized values do not quickly detect shifts in the process standard deviation (Domangue and Patch [31]).

We strongly recommend the use of the SS-CUSUM scheme in particular in the production plant where quality control is mostly the responsibility of workforce not well trained in statistical tools. This is due to the fact that this chart is easy to construct and interpret when an out of control signal is issued.

Chapter 5

Multivariate Max-CUSUM Chart

5.1 Introduction

In chapters 3 and 4, we discussed control charts for the case where the quality of an item is determined by a single quality characteristic. There are many situations in which the overall quality of an item is determined by several (say p) correlated quality characteristics. Examples of such processes include the following: in a lumber manufacturing plant the quality of lumber may be monitored by measuring the stiffness and bending strength of the lumber, in a chemical industry, the process may be a function of temperature, pressure as well as viscosity and in an automobile plant, the usefulness of an automobile part may depend on an inner diameter and an outer diameter. The product is considered to be in statistical control if all critical product quality characteristics are simultaneously in control. Therefore it is necessary to use a scheme that can simultaneously monitor these correlated quality characteristics. We propose new control charts for monitoring such processes in chapters 5 and 6.

In this chapter, we propose a multivariate CUSUM control chart that can simultaneously monitor both process location and variability using a single plotting variable. We show that procedures used for univariate variables control charts can be applied to monitor the multivariate processes. We consider only the upper control limits for monitoring the multivariate processes. This is because in multivariate procedures, we are monitoring the significance of the magnitude of the shift for the mean vector and/or covariance matrix from their target or nominal values and thus the direction of the shift does not play an important role.

At each sample period i, a $p\times 1$ vector of observations denoted as $\boldsymbol{X}_i$, is obtained from the process and the information in these vectors is used to judge the quality of the process. The underlying probability distribution of these p quality characteristics is assumed to be multivariate normal with mean vector $\boldsymbol{\mu}$ and covariance matrix $\boldsymbol{\Sigma}$. The unknown mean vector and unknown covariance matrix are respectively written as:

$$\boldsymbol{\mu} = \begin{bmatrix} \mu_1 \\ \mu_2 \\ \cdot \\ \cdot \\ \cdot \\ \mu_p \end{bmatrix}$$

and

$$\boldsymbol{\Sigma} = \begin{bmatrix} \sigma_{11} & \sigma_{12} & \cdot & \cdot & \cdot & \sigma_{1p} \\ \sigma_{21} & \sigma_{22} & \cdot & \cdot & \cdot & \sigma_{2p} \\ \cdot & \cdot & \cdot & & & \cdot \\ \cdot & \cdot & & \cdot & & \cdot \\ \cdot & \cdot & & & \cdot & \cdot \\ \sigma_{p1} & \sigma_{p2} & \cdot & \cdot & \cdot & \sigma_{pp} \end{bmatrix}$$

where μ_i is the mean of the i^{th} (for $i = 1, 2, ..., p$) characteristic and σ_{ii} is the variance of the i^{th} characteristic. The covariance between the i^{th} and j^{th} characteristics is denoted by the off-diagonal element σ_{ij}, $(i, j = 1, 2, ..., p, i \neq j)$.

We use the Markov chain approach to compute the chart's ARL. The multivariate control chart proposed in this chapter is called the Maximum Multivariate Cumulative Sum (Max-MCUSUM) control chart as it is developed using maximum values of the computed CUSUM values. If the process mean vector and/or covariance matrix have substantially shifted from their target values, the points will plot above the upper control limit and when the magnitude of the shift is small all points will plot below the upper control limit.

We show that when testing for shifts in the process mean vector and/or covariance matrix, of a multivariate normal process, the multivariate CUSUM procedure, which is related to the sequential probability ratio test, reduces to a univariate normal CUSUM chart procedure. This scheme is based on the derivations and assumptions discussed by Healy ([41]). The procedure is straightforward and can be carried out by employees with little training in the use of control charts and elementary knowledge of statistics. The performance of the proposed control chart is determined by the distance of the off-target parameter (known) from the on-target value and not by the direction of the off-target parameter.

5.2 The New Control Chart

5.2.1 Control Chart for the Mean Vector

Assume that we have a sequence of independent and identically distributed multivariate normal random variables $\boldsymbol{X}_1$, $\boldsymbol{X}_2$, ..., where $\boldsymbol{X}_1 = (X_{11}, ..., X_{1p})'$, a $p \times 1$ vector of observations. The first $\boldsymbol{X}_1$, $\boldsymbol{X}_2$, ... , $\boldsymbol{X}_{m-1}$ vectors, have a good distribution function F_G when the process is in control, but the next $\boldsymbol{X}_m$, $\boldsymbol{X}_{m+1}$, ... have a different distribution, F_B indicating a shift in the mean vector. We assume that the production process shifts at an unknown time m. The objective is to detect that the shift has happened and when the shift in the process mean vector occurs.

It will be shown later that the CUSUM procedure signals that the shift in the mean vector has occurred as soon as:

$$S_i = \sum_{i=1}^{n} log\frac{f_B(x_i)}{f_G(x_i)} - min \sum_{i=1}^{k} log\frac{f_B(x_i)}{f_G(x_i)} > L,$$

where f_G and f_B are densities corresponding to F_G and F_B, respectively and L is a constant that determines the operating characteristics of the procedures (Healy [41]).

The statistic S_i can be calculated recursively in the following way:

$$S_i = max\left(0, S_{i-1} + log\frac{f_B(x_i)}{f_G(x_i)}\right) > L. \tag{5.1}$$

As will be shown, rescaling equation (5.1) by dividing the $log\frac{f_B(x_i)}{f_G(x_i)}$ and L by the same constant results in an easy to use equation (5.5). The initial value of our CUSUM chart is set to $S_0 = 0$. At every time period, the CUSUM statistic is compared with a fixed decision interval L and if it is more than this L, a shift is signalled. After detection of the shift, and corrective action taken, the CUSUM statistic is reset to the initial value S_0.

We assume that $\boldsymbol{X}_i$ comes from a multivariate normal distribution with either a mean $\boldsymbol{\mu}_G$, when the process is in control, or mean $\boldsymbol{\mu}_B$, when the process is out of control where $\boldsymbol{\mu}_B = \boldsymbol{\mu}_G + \boldsymbol{\delta}$, and a known common covariance matrix $\boldsymbol{\Sigma}$. If for each independent normal random variable $\boldsymbol{X}_i$, we measure p quality characteristics, a vector of size $p \times 1$ is formed and a covariance matrix of order $p \times p$ is also formed. For the multivariate normal distribution, the CUSUM chart is developed through the likelihood ratio given as:

$$\frac{f_B(x_i)}{f_G(x_i)} = \frac{(2\pi)^{-p/2}|\boldsymbol{\Sigma}|^{-1/2}exp(-0.5(\boldsymbol{X}_i - \boldsymbol{\mu}_B)'\boldsymbol{\Sigma}^{-1}(\boldsymbol{X}_i - \boldsymbol{\mu}_B))}{(2\pi)^{-p/2}|\boldsymbol{\Sigma}|^{-1/2}exp(-0.5(\boldsymbol{X}_i - \boldsymbol{\mu}_G)'\boldsymbol{\Sigma}^{-1}(\boldsymbol{X}_i - \boldsymbol{\mu}_G))} \tag{5.2}$$

$$= \frac{exp(-0.5(\boldsymbol{X}_i - \boldsymbol{\mu}_B)'\boldsymbol{\Sigma}^{-1}(\boldsymbol{X}_i - \boldsymbol{\mu}_B))}{exp(-0.5(\boldsymbol{X}_i - \boldsymbol{\mu}_G)'\boldsymbol{\Sigma}^{-1}(\boldsymbol{X}_i - \boldsymbol{\mu}_G))} \tag{5.3}$$

Taking natural logarithms, we obtain

$$log\frac{f_B(x_i)}{f_G(x_i)} = (\boldsymbol{\mu}_B - \boldsymbol{\mu}_G)'\boldsymbol{\Sigma}^{-1}\boldsymbol{X}_i - 0.5(\boldsymbol{\mu}_B + \boldsymbol{\mu}_G)'\boldsymbol{\Sigma}^{-1}(\boldsymbol{\mu}_B - \boldsymbol{\mu}_G) \tag{5.4}$$

The CUSUM for the multivariate process is computed by substituting equation (5.4) into equation (5.1) and the rescaling to obtain an easy to use equation (5.5) as:

$$S_i = max(S_{i-1} + a'\boldsymbol{X}_i - k, 0) > h, \tag{5.5}$$

where

$$a' = \frac{(\boldsymbol{\mu}_B - \boldsymbol{\mu}_G)'\boldsymbol{\Sigma}^{-1}}{[(\boldsymbol{\mu}_B - \boldsymbol{\mu}_G)'\boldsymbol{\Sigma}^{-1}(\boldsymbol{\mu}_B - \boldsymbol{\mu}_G)]^{1/2}}$$

and

$$k = 0.5\frac{(\boldsymbol{\mu}_B + \boldsymbol{\mu}_G)'\boldsymbol{\Sigma}^{-1}(\boldsymbol{\mu}_B - \boldsymbol{\mu}_G)}{[(\boldsymbol{\mu}_B - \boldsymbol{\mu}_G)'\boldsymbol{\Sigma}^{-1}(\boldsymbol{\mu}_B - \boldsymbol{\mu}_G)]^{1/2}}.$$

Now the random variable $a'\mathbf{X}_i$ has a univariate normal distribution.

Define the noncentrality parameter as:

$$D = \sqrt{(\boldsymbol{\mu}_B - \boldsymbol{\mu}_G)'\boldsymbol{\Sigma}^{-1}(\boldsymbol{\mu}_B - \boldsymbol{\mu}_G)} \tag{5.6}$$

and

$$Z_i = a'(\boldsymbol{X}_i - \boldsymbol{\mu}_G). \tag{5.7}$$

The CUSUM chart for detecting a shift in the mean vector of a multivariate normal may be written as:

$$C_i = max(0, C_{i-1} + Z_i - 0.5D) > h. \tag{5.8}$$

The function Z_i therefore has a standard univariate normal distribution when $\boldsymbol{X}_i$ has mean equal to $\boldsymbol{\mu}_G$. If the mean shift to $\boldsymbol{\mu}_B$, then $a'(\boldsymbol{X}_i - \boldsymbol{\mu}_G)$ has a univariate normal distribution with mean D and variance 1. Therefore, for detecting a shift in the mean of a multivariate normal random variable, the CUSUM procedure reduces to a univariate normal CUSUM procedure.

5.2.2 Control Chart for the Covariance Matrix

Like the process mean, the process variability, usually summarized by a covariance matrix in the multivariate case, is important for assessing whether the process is in control or not. Several CUSUM control schemes for detecting shifts in the process variability for multivariate processes have been studied including charts by Healy ([41]) and Chan and Zhang ([15]). These schemes use a chart that only shows changes in the process covariance matrix assuming that the process mean vector remains constant throughout the production process.

Using the likelihood ratio test technique as above and assuming the two states of production, that is steady state and non-steady state, Healy ([41]) developed a CUSUM chart for the process standard deviation. When the process is in a good state, it is distributed as multivariate normal with mean $\boldsymbol{\mu}$ and covariance matrix $\boldsymbol{\Sigma}$. If the process variability has shifted, the mean remains at $\boldsymbol{\mu}$ but the covariance matrix shift to $b\boldsymbol{\Sigma}$, for $b > 0$. This assumes that when a shift occurs, all variances shift proportionally and the correlations between the variables remain the same. This type of shift could occur when something happens in a manufacturing process that affects all of the variables in the process. For example, if one were taking measurements on a transmission system at several frequencies, an increase in the variability at one frequency would often be accompanied by a proportional increase in the variability at another frequency. The likelihood ratio is given as:

$$\frac{f_B(x_i)}{f_G(x_i)} = \frac{(2\pi)^{-p/2}(|b\boldsymbol{\Sigma}|)^{-1/2}exp(-0.5(\boldsymbol{X}_i - \boldsymbol{\mu})'(b\boldsymbol{\Sigma})^{-1}(\boldsymbol{X}_i - \boldsymbol{\mu}))}{(2\pi)^{-p/2}|\boldsymbol{\Sigma}|^{-1/2}exp(-0.5(\boldsymbol{X}_i - \boldsymbol{\mu})'\boldsymbol{\Sigma}^{-1}(\boldsymbol{X}_i - \boldsymbol{\mu}))} \tag{5.9}$$

$$= b^{-1/2}exp[-0.5(\boldsymbol{X}_i - \boldsymbol{\mu})'\boldsymbol{\Sigma}^{-1}(\boldsymbol{X}_i - \boldsymbol{\mu})(\frac{1}{b} - 1)] \tag{5.10}$$

Taking the natural logarithms of the likelihood, we get

$$log\frac{f_B(x_i)}{f_G(x_i)} = \frac{-1}{2}logb + 0.5(\boldsymbol{X}_i - \boldsymbol{\mu})'\boldsymbol{\Sigma}^{-1}(\boldsymbol{X}_i - \boldsymbol{\mu})(1 - \frac{1}{b}). \tag{5.11}$$

The CUSUM statistic for detecting a shift in the covariance matrix of a multivariate process is obtained by substituting equation (5.11) into equation (5.1) and the rescaling. This gives the S_i as:

$$S_i = \max(S_{i-1} + (\boldsymbol{X}_i - \boldsymbol{\mu})'\Sigma^{-1}(\boldsymbol{X}_i - \boldsymbol{\mu}) - k, 0) > h, \tag{5.12}$$

where

$$k = \ log(b) \left(\frac{b}{b-1}\right)$$

.

When the process experiences a shift in the mean vector and covariance matrix, the noncentrality parameter is defined as:

$$D^* = \sqrt{(\boldsymbol{\mu}_B - \boldsymbol{\mu}_G)'(b\boldsymbol{\Sigma})^{-1}(\boldsymbol{\mu}_B - \boldsymbol{\mu}_G)}. \tag{5.13}$$

It has been shown by Muirhead ([73]) that $(\boldsymbol{X}_i - \boldsymbol{\mu})'\Sigma^{-1}(\boldsymbol{X}_i - \boldsymbol{\mu})$ follows a chi-square distribution with p degrees of freedom. If the population covariance matrix is unknown, it is estimated with the sample covariance matrix $\boldsymbol{S}$. Then $(\boldsymbol{X}_i - \boldsymbol{\mu})'\boldsymbol{S}^{-1}(\boldsymbol{X}_i - \boldsymbol{\mu})$ will follow an F-distribution; $F_{p,n-p}$, with p and $n-p$ degrees of freedom.

To develop a single multivariate CUSUM chart that is capable of simultaneously monitoring the process mean vector and covariance matrix, we carry out the following transformation;

$$Y_i = \Phi^{-1}\left\{H(\boldsymbol{X}_i - \boldsymbol{\mu})'\Sigma^{-1}(\boldsymbol{X}_{\ i} - \boldsymbol{\mu}); p\right\}, \tag{5.14}$$

where

$$\Phi(z) = P(Z \leq z),$$

for $Z \sim N(0, 1)$, the standard normal distribution. The function $\Phi^{-1}(\cdot)$ is the inverse of the standard normal cumulative distribution function, and $H(w;p) = P(W \leq w|p)$ for $W \sim \chi^2_p$, the chi-square distribution with p degrees of freedom.

In equations (5.7) and (5.14), Z_i and Y_i are independent and when both process location and variability are in control, that is $\boldsymbol{\delta} = \mathbf{0}$ and $b = 1$, they both follow the standard univariate normal distribution and their distributions do not depend on the sample size. Since Z_i and Y_i have the same distribution, we can construct a single CUSUM control chart that will simultaneously monitor both the process location and the process variability.

The CUSUM statistics based on these independent and identically distributed standard univariate normal random variables, Z_i and Y_i are given as:

$$\begin{aligned} C_i^+ &= \max[0, Z_i - 0.5D + C_{i-1}^+], \\ C_i^- &= \max[0, -0.5D - Z_i + C_{i-1}^-], \end{aligned} \tag{5.15}$$

for monitoring the process location and

$$\begin{aligned} S_i^+ &= \max[0, Y_i - k + S_{i-1}^+], \\ S_i^- &= \max[0, -k - Y_i + S_{i-1}^-], \end{aligned} \tag{5.16}$$

for monitoring the process variability, with C_0 and S_0 as starting points. Because in multivariate quality control procedures, we are monitoring the significance of the magnitude of the shift and not the direction, the CUSUM statistics above are transformed to the following statistics

$$\begin{aligned} C_i &= \max[C_i^+, C_i^-] \\ S_i &= \max[S_i^+, S_i^-] \end{aligned}$$

Because Z_i and Y_i follows the same distribution, a new statistic for the multivariate control chart can be developed by defining the following:

$$M_i = \max[C_i, S_i] \tag{5.17}$$

Since we use the maximum of the CUSUM statistics to develop our chart, it is called the Maximum Multivariate Cumulative Sum (Max-MCUSUM) control chart.

The statistic M_i will be large when the process mean vector is drifted away from the nominal value $\boldsymbol{\mu}_G$ and/or when the process covariance matrix has drifted away from the nominal value $\boldsymbol{\Sigma}$. Small values of M_i show that the process is in statistical control. Since $M_i \geq 0$, it is only compared with the upper control limit.

5.3 Design of a Max-MCUSUM Chart

This multivariate control chart is constructed by transforming the multivariate normal random variables to univariate normal random variables. The design procedure developed for the Max-CUSUM chart in chapter 3 can then be used to find the decision interval, the reference value and the ARL for this multivariate CUSUM chart. The Max-MCUSUM chart procedure is represented by a Markov chain and the results of Brook and Evans ([11]) are extended to obtain the ARL for this multivariate CUSUM chart.

The ARL depends on the standard univariate CUSUM chart parameters; the reference value k and decision interval h together with the multivariate noncentrality parameter D^* defined in equation (5.13). At a given value of h, the decision interval, we calculate the value of k for the given level of the shift in the mean vector and/or covariance matrix intended to be quickly detected and use the $(h,\ k)$ combination to calculate the ARL. To guard against a particular shift in the mean vector and/or covariance matrix, the reference value is computed as $k = 0.5D^*$. The shift in the covariance matrix is denoted by b as specified earlier and the shift in the mean vector is denoted by $\boldsymbol{\delta}$. Here we assume the mean vector shifts by the same amount for all components in a unit and that all variances shift proportionally, therefore the correlations between variables remain the same.

Table 5.1 and Table 5.2 give the optimal combinations of k and h used to detect various changes in the mean vector and/or covariance matrix with an in-control ARL set at 250 and the correlation coefficient $\rho = 0.1$, for values of p set at 2 and 5. The smallest value of an out-of-control ARL is determined for a pair of changes in process mean and process variability using the optimal in-control ARL parameters. We assume that the process starts in an in-control state and then determine the ARL for a specified change in the process parameters. The CUSUM statistic is set to zero at the start of the process assuming the process starts in an in-control state. When the process shifts from an in-control state, we expect the CUSUM statistic to increase until crossing the decision interval. When this happens, the process issues the out-of-control signal, and a search for the assignable cause(s) of variation should be undertaken.

From Table 5.1 and Table 5.2, we can see that the Max-MCUSUM quickly detects both small and large changes in the process mean vector and/or covariance matrix. For example to detect a change in the mean vector from $\mathbf{0}$ to $\mathbf{0.5}$ when the covariance matrix has shifted by a multiple of 1.5, the ARL reduces from 250 to about 5 samples when we monitor two quality characteristics per item produced. This is detected on average by the 4th sample when we are monitoring five quality characteristics per item produced. To detect a large change in both parameters, we only need about 2 samples. For example if the mean vector shift to $\mathbf{2.5}$ and the covariance matrix also shifts by a multiple of 4, the ARL $= 1.5$. Note that these results are for the case where $\rho = 0.1$.

Table 5.1: (k,h) combinations and the corresponding ARL's for the Max-MCUSUM Chart with $p = 2$.

$\rho = 0.1$								
		δ						
b	Parameter	0.00	0.25	0.50	1.00	1.50	2.00	2.50
	h	2.024	4.561	3.157	2.024	1.497	1.155	0.868
1.00	k	0.674	0.168	0.337	0.674	1.011	1.348	1.685
	ARL	250.13	15.33	6.33	2.73	1.86	1.53	1.36
	h	2.024	4.561	3.157	2.024	1.497	1.155	0.868
1.25	k	0.674	0.168	0.337	0.674	1.011	1.348	1.685
	ARL	9.43	12.02	5.24	2.38	1.66	1.30	1.26
	h	2.024	4.561	3.157	2.024	1.497	1.155	0.868
1.50	k	0.674	0.168	0.337	0.674	1.011	1.348	1.685
	ARL	7.48	9.87	4.51	2.13	1.54	1.30	1.18
	h	2.024	4.561	3.157	2.024	1.497	1.155	0.868
2.00	k	0.674	0.168	0.337	0.674	1.011	1.348	1.685
	ARL	5.46	7.27	3.59	1.82	1.38	1.19	1.11
	h	2.024	4.561	3.157	2.024	1.497	1.155	0.868
2.50	k	0.674	0.168	0.337	0.674	1.011	1.348	1.685
	ARL	4.47	5.79	3.05	1.66	1.30	1.14	1.07
	h	2.024	4.561	3.157	2.024	1.497	1.155	0.868
3.00	k	0.674	0.168	0.337	0.674	1.011	1.348	1.685
	ARL	3.90	4.87	2.71	1.56	1.24	1.10	1.05
	h	2.024	4.561	3.157	2.024	1.497	1.155	0.868
4.00	k	0.674	0.168	0.337	0.674	1.011	1.348	1.685
	ARL	3.28	3.81	2.32	1.44	1.18	1.08	1.03

Table 5.2: (k,h) combinations and the corresponding ARL's for the Max-MCUSUM chart with $p = 5$.

$\rho = 0.1$								
		δ						
b	Parameter	0.00	0.25	0.50	1.00	1.50	2.00	2.50
1.00	h	1.580	3.848	2.567	1.580	1.094	0.696	0.276
	k	0.945	0.236	0.472	0.945	1.417	1.890	2.362
	ARL	250.10	11.97	4.96	2.33	1.72	1.48	1.34
1.25	h	1.580	3.848	2.567	1.580	1.094	0.696	0.276
	k	0.945	0.236	0.472	0.945	1.417	1.890	2.362
	ARL	7.17	9.54	4.21	2.09	1.58	1.36	1.25
1.50	h	1.580	3.848	2.567	1.580	1.094	0.696	0.276
	k	0.945	0.236	0.472	0.945	1.417	1.890	2.362
	ARL	6.00	7.93	3.69	1.92	1.48	1.29	1.18
2.00	h	1.580	3.848	2.567	1.580	1.094	0.696	0.276
	k	0.945	0.236	0.472	0.945	1.417	1.890	2.362
	ARL	4.66	5.97	3.04	1.71	1.35	1.19	1.11
2.50	h	1.580	3.848	2.567	1.580	1.094	0.696	0.276
	k	0.945	0.236	0.472	0.945	1.417	1.890	2.362
	ARL	3.94	4.85	2.65	1.58	1.27	1.14	1.07
3.00	h	1.580	3.848	2.567	1.580	1.094	0.696	0.276
	k	0.945	0.236	0.472	0.945	1.417	1.890	2.362
	ARL	3.51	4.15	2.40	1.50	1.23	1.11	1.05
4.00	h	1.580	3.848	2.567	1.580	1.094	0.696	0.276
	k	0.945	0.236	0.472	0.945	1.417	1.890	2.362
	ARL	3.03	3.34	2.11	1.41	1.17	1.07	1.03

The Max-MCUSUM scheme is slightly more sensitive in detecting shifts in the mean and/or standard deviation when there are more quality characteristics being monitored in each product. This makes it more applicable in monitoring many chemical processes where a large number of attributes of a process are being monitored. Most of the CUSUM charts discussed in the literature are only effective in detecting small shifts in the process. Tables 5.3 and 5.4 show the performance of the Max-MCUSUM chart that is designed to detect a 1σ shift in the process mean vector and/or covariance matrix. These tables show that the Max-MCUSUM chart is sensitive to both small and large shifts in the process location and spread.

Table 5.3: ARL's for the Max-MCUSUM chart with $h = 2.554$ and $k = 0.500$ when $p = 2$

$\rho = 0.1$ δ								
b	0.00	0.25	0.50	1.00	1.50	2.00	2.50	3.00
1.00	250.35	4.64	3.74	2.73	2.12	1.74	1.49	1.32
1.25	13.28	4.13	3.35	2.38	1.85	1.53	1.32	1.19
1.50	9.95	3.74	3.02	2.14	1.67	1.39	1.22	1.12
2.00	6.84	3.21	2.59	1.85	1.46	1.25	1.12	1.06
2.50	5.41	2.87	2.33	1.68	1.35	1.17	1.08	1.03
3.00	4.61	2.65	2.16	1.58	1.28	1.13	1.05	1.02
4.00	3.75	2.37	1.95	1.46	1.21	1.09	1.03	1.00

Table 5.4: ARL's for the Max-MCUSUM chart with $h = 2.037$ and $k = 0.500$ when $p = 5$

$\rho = 0.1$								
	δ							
b	0.00	0.25	0.50	1.00	1.50	2.00	2.50	3.00
1.00	250.47	3.48	3.00	2.33	1.89	1.69	1.41	1.27
1.25	9.52	3.24	2.75	2.09	1.69	1.44	1.27	1.17
1.50	7.60	3.04	2.56	1.93	1.56	1.33	1.19	1.11
2.00	5.64	2.73	2.28	1.71	1.39	1.21	1.11	1.05
2.50	4.65	2.52	2.10	1.58	1.30	1.15	1.07	1.03
3.00	4.08	2.38	1.98	1.50	1.25	1.12	1.05	1.02
4.00	3.44	2.19	1.83	1.41	1.19	1.08	1.03	1.01

5.4 The Power of a Max-MCUSUM Chart

The power function of a statistical test describes the probability of rejecting the null hypothesis at various values of the underlying parameters. In this section, we present the power function of the Max-MCUSUM chart for monitoring the process mean vector and/or covariance matrix of a multivariate process. We present the power curve for increases in the mean vector and /or covariance matrix. This power is computed as the reciprocal of the ARL of the scheme. We investigate the power of the chart as a function of the correlation coefficient between two variables.

From Figure 5.1, we can see that the power of the Max-MCUSUM chart, depends not on the magnitude of the correlation coefficient, but on the direction. When there is a negative relationship between variates, an increase in the process mean and/or standard deviation results in an increase in the power as the relationship becomes stronger. When there is a positive relationship, as the correlation increases, an increase in the parameters will not be quickly detected. Therefore like the T^2 control chart, investigated by Wierda ([101]), the power of Max-MCUSUM chart is low if the shift structure is in accordance with the correlation structure and high if the shift structure is opposite to the correlation structure.

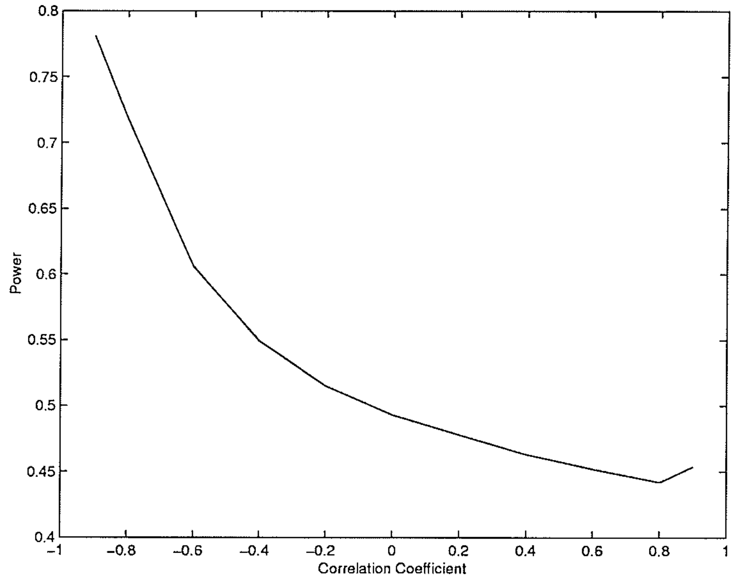

Figure 5.1: Plot of the power for the Max-MCUSUM chart against correlation coefficients between variables

5.5 Comparison with Other Procedures

The multivariate CUSUM control charts developed in the literature are designed to monitor the process mean and variability using separate charts or different plotting variables in case of simultaneous charts. Therefore it is impossible to compare the Max-MCUSUM chart with those existing charts on an equal footing. This chart will be compared with a single multivariate Max-MEWMA chart developed by Xie ([108]). These two charts are compared at an in-control ARL = 200 and the correlation between observations fixed at $\rho = 0.6$. Comparison of these charts is displayed in Table 5.5. The Max-MCUSUM chart performs better than the Max-MEWMA chart when detecting shifts in the process mean vector alone, and when both process mean vector and covariance matrix experience smaller shifts. However, when only the covariance matrix shifts, the Max-MEWMA chart out performs the Max-MCUSUM chart. These charts are sensitive to large shifts in the process mean and/or standard deviation. The standard CUSUM chart is specifically designed to detect small shifts in the process and it is not effective in detecting large shifts. However our proposed chart has, in addition to being easy to chart than the traditional multivariate CUSUM charts, a good ability to simultaneously detect both small and large shifts in the mean vector and covariance matrix.

Table 5.5: ARL's for Max-MCUSUM chart and the Max-MEWMA chart.

$ARL_0 = 200$ with $\rho = 0.6$							
	Max-MCUSUM						
	a						
b	0.00	0.50	1.00	1.50	2.00	2.50	3.00
1.00	200.4	4.3	2.9	2.2	1.8	1.5	1.4
1.50	8.4	3.3	2.3	1.7	1.4	1.2	1.1
2.00	5.9	2.8	1.9	1.5	1.3	1.1	1.1
2.50	4.8	2.5	1.7	1.4	1.2	1.1	1.0
3.00	4.1	2.3	1.6	1.3	1.1	1.1	1.0
	Max-MEWMA						
	a						
b	0.00	0.50	1.00	1.50	2.00	2.50	3.00
1.00	200.1	18.2	5.3	3.2	2.3	2.0	1.7
1.50	7.5	6.1	4.1	3.0	2.3	1.7	1.5
2.00	3.4	3.2	2.9	2.4	2.1	1.7	1.5
2.50	2.4	2.4	2.2	2.1	1.9	1.7	1.3
3.00	2.0	2.0	1.9	1.8	1.7	1.1	1.0

5.6 Charting Procedures

The charting procedure of a Max-MCUSUM chart is similar to that of the Max-CUSUM chart. The successive CUSUM values, M_i's are plotted against the sample numbers. If a point plots below the decision interval, the process is said to be in statistical control and the point is plotted as a dot point. An out-of-control signal is issued if any point plots above the decision interval and is plotted as one of the characters defined below. The following procedure is followed in building the Max-MCUSUM chart:

1. Specify the following parameters; p and the in-control or target value of the mean vector $\boldsymbol{\mu}_G$, $\boldsymbol{\mu}_B$ and the in-control or target value of the covariance matrix $\boldsymbol{\Sigma}$.

2. If $\boldsymbol{\mu}_B$ is not known, use the sample mean vector $\bar{\bar{\boldsymbol{X}}}$ which is a p-dimensional vector of sample means. In the same manner, if the population covariance matrix is unknown, we use the sample covariance matrix $\boldsymbol{S}$ to estimate the population covariance matrix.

3. For each sample compute Z_i and Y_i.

4. To detect specified changes in the process mean vector and covariance matrix, choose an optimal $(h,\ k)$ combination and calculate the cumulative sums, C_i^+, C_i^-, S_i^+ and S_i^- and transform them to C_i and S_i.

5. Compute the M_i's and compare them with h; the decision interval.

6. Denote the sample points with a dot and plot them against the sample number if $M_i \leq h$.

7. If any of the M_i's are greater than the decision interval; h, the following plotting characters should be used to show the statistic that is plotting above the interval.

   (i) If $C_i \geq h$, plot $C+$. This shows a shift in the process mean vector.

   (ii) If $S_i \geq h$, plot $V+$. This shows a shift in the process covariance matrix.

   (iii) If both $C_i \geq h$ and $S_i \geq h$, plot $B++$. This indicates a shift in both the mean vector and covariance matrix of the process.

8. Investigate the cause(s) of the shift for each out-of-control point in the chart and carry out the remedial measures needed to bring the process back into an in-control state.

5.7 Illustrative Example

Max-MCUSUM chart is applied to real data obtained from Sultan ([92]) which was also used by Spiring and Cheng ([91]) for their simultaneous multivariate control chart. The data are from a steel manufacturing process that measured the Brinnel hardness (x) and the tensile strength (y) for 30 samples. To illustrate the multivariate control chart procedure the samples of the form $(x, y)'$ were aligned in subgroups of five using the sequential sample numbers as shown in Table 5.6.

Table 5.6: Brinnel hardness and tensile strength data

Subgroup											
samples	1		2		3		4		5		6
1	143 34.2	6	178 51.5	11	175 57.3	16	182 57.2	21	160 45.5	26	195 58.0
2	200 57.0	7	162 45.9	12	187 58.5	17	177 50.6	22	183 53.6	27	134 45.7
3	160 47.5	8	215 59.1	13	187 58.2	18	204 55.1	23	179 51.2	28	187 42.0
4	181 53.4	9	161 48.4	14	186 57.0	19	178 50.9	24	194 57.7	29	135 40.5
5	148 47.8	10	141 47.3	15	172 49.4	20	196 57.9	25	181 55.6	30	159 58.0

The Max-MCUSUM chart requires knowledge of the in-control or target value of the mean vector, Spiring and Cheng ([91]) gave this as:

$$\boldsymbol{\mu}_G = \begin{bmatrix} 175 \\ 55 \end{bmatrix},$$

the covariance matrix $\boldsymbol{\Sigma}$ is not given and is thus estimated by $\boldsymbol{S} = \frac{\sum_{j=1}^{k} \mathbf{S_j}}{k}$, where $\boldsymbol{S}_j = n^{-1} \sum_{j=1}^{n} (\boldsymbol{X}_i - \bar{X}_n)(\boldsymbol{X}_i - \bar{X}_n)'$. From the subgroup information,

$$\boldsymbol{S} = \begin{bmatrix} 332.13 & 69.26 \\ 69.26 & 29.97 \end{bmatrix}.$$

The sample grand mean is

$$\bar{\bar{\boldsymbol{X}}} = \begin{bmatrix} 174.67 \\ 51.67 \end{bmatrix}.$$

To construct the Max-MCUSUM chart for detecting a shift in the process mean vector and covariance matrix, we estimate $\boldsymbol{\mu}_B$ with $\bar{\bar{\boldsymbol{X}}}$ and $\boldsymbol{\Sigma}$ with $\boldsymbol{S}$ and substitute these estimators into equation (5.13). This gives $D^* = 0.827$. The reference value

$k = D^*/2 = 0.414$. If we want an in-control ARL to be equal to 250, the decision interval is determined using the procedure used to derive Tables 5.1 and 5.2. This gives a decision interval $h = 3.97$.

From Figure 5.2, the Max-MCUSUM chart shows that none of the subgroup means are different from the target values. The chart however shows that there was a shift in variability for subgroup 6. Thus the covariance matrix for this subgroup should be investigated to identify the cause(s) of variation. Spiring and Cheng ([91])'s simultaneous chart gave the same results but their chart is complicated since they plotted two plotting quantities in the same chart. One quantity for detecting shifts in the mean vector and another for detecting shifts in the covariance matrix.

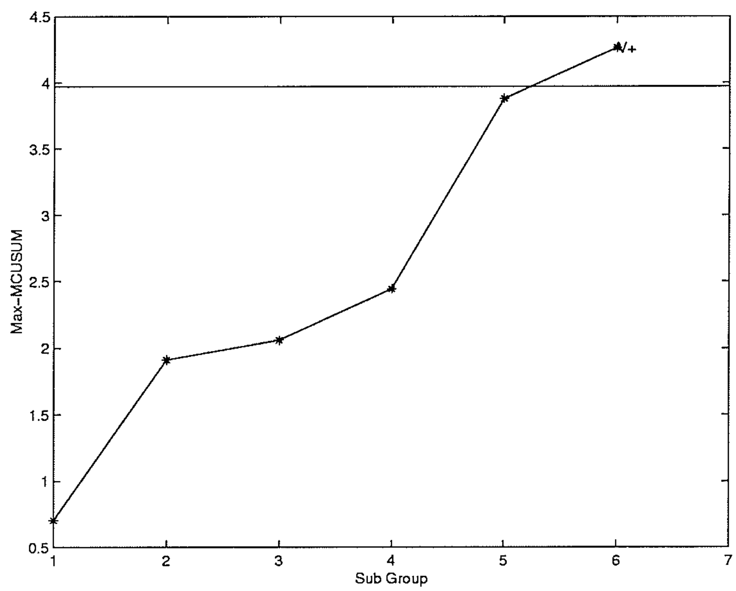

Figure 5.2: The Max-MCUSUM chart for the Brinnel hardness and tensile strength data.

5.8 Conclusions and Recommendations

We have proposed the Max-MCUSUM chart for monitoring changes in the process mean vector and/or covariance matrix of a multivariate normal process. The Max-MCUSUM chart is a natural extension of the univariate Max-CUSUM chart proposed in chapter 3.

The main advantage of using this proposed chart over other existing multivariate control charts is that one can monitor both the process location and the process spread simultaneously using one chart. This chart is also easy to construct as it is based on transforming the multivariate normal random variables into standard univariate normal random variables.

If an out of control signal is issued we recommend using individual CUSUM charts suggested by Woodall and Ncube ([106]), to identify the component(s) that has shifted for the mean vector, covariance matrix or both if any of the charts indicates that both parameters have shifted.

Chapter 6

Multivariate Max-Chart

6.1 Introduction

In this chapter, we investigate a Shewhart-type multivariate chart. By Shewhart-type chart, we mean that the statistics that are plotted on the control chart are not smoothed as in the EWMA chart, or summed as in the CUSUM chart. The Shewhart-type chart has no memory. That is, previous observations do not influence the probability of future out-of-control signals. Hotelling ([42]), introduced a statistic which can be used to assess the quality characteristics of multivariate processes by plotting this statistic (T^2) against time. Several charts based on this statistic have been proposed to monitor both the process mean and the variability. These include charts proposed by Tracy, Young and Mason ([95]), Mason, Tracy and Young ([67]), Spiring and Cheng ([91]) and many more.

A single Shewhart-type multivariate scheme is proposed in this chapter in an effort to develop a simple scheme that monitors both mean and variability of the process simultaneously. We show that when testing for shifts in the mean and/or standard deviation, of a multivariate normal random variable, the T^2 chart, reduces to a univariate normal Shewhart chart. The T^2 statistic is transformed into a standard normal variable under the assumption that the process is in-control. The procedure is straightforward and can be carried out by employees with little training in the use of control chart and an elementary knowledge of statistics. The performance of the proposed chart is assessed by the ARL of the chart at different levels of shifts in both mean vector and/or covariance matrix.

6.2 The New Control Chart

Assume we have a sequence of independent and identically distributed multivariate normal random variables $\boldsymbol{X}_1$, $\boldsymbol{X}_2$, ..., where $\boldsymbol{X}_1 = (X_{11}, ..., X_{1p})'$. When the process is in-control, the variables have mean $\boldsymbol{\mu}_0$ and covariance matrix $\boldsymbol{\Sigma_0}$. Assume that the process parameters $\boldsymbol{\mu}$ and $\boldsymbol{\Sigma}$ can be expressed as $\boldsymbol{\mu} = \boldsymbol{\mu}_0 + \boldsymbol{\delta}$ and $\boldsymbol{\Sigma} = b^2\boldsymbol{\Sigma_0}$, when both the mean vector and the covariance matrix have shifted. The constants $\boldsymbol{\delta}$ and b^2 represents shifts in the mean vector and covariance matrix respectively, where $\boldsymbol{\delta} = 0$ and $b = 1$ when the process is in-control, otherwise, the process has changed due to some assignable causes.

The estimate of mean vector from a sample of n multivariate random variables is denoted by $\bar{\boldsymbol{X}}_n = (\bar{X}_1, \bar{X}_2, ..., \bar{X}_p)'$, where $\bar{X}_j = (1/n)\sum_{i=1}^{n} X_{ij}$ is the estimate of the mean for quality characteristic j made on the first n observations. The estimate of the covariance matrix is defined as

$$\mathbf{S}_n = \frac{1}{n-1}\sum_{j=1}^{n}(\mathbf{X_j} - \bar{\mathbf{X}}_\mathbf{n})(\mathbf{X_j} - \bar{\mathbf{X}}_\mathbf{n})'.$$

The sample mean vector $\bar{\boldsymbol{X}}_n$ and sample covariance matrix $\boldsymbol{S}_n$ are the uniformly minimum variance unbiased estimators for the corresponding population parameters. These statistics are also independently distributed as are the sample values. These two statistics however follow different probability distributions. The Shewhart-type multivariate charts for the mean and standard deviation are based on the following statistics:

$$T_n^2 \quad = \quad n(\bar{\mathbf{X}}_n - \boldsymbol{\mu}_0)'\boldsymbol{\Sigma}_0^{-1}(\bar{\mathbf{X}}_n - \boldsymbol{\mu}_0) \tag{6.1}$$

for monitoring the mean and the sample generalized variance, denoted by $|\mathbf{S}_n|$, is used to monitor the process dispersion. The statistic $|\mathbf{S}_n|$ is the determinant of a $p \times p$ sample variance-covariance matrix. For two quality characteristics, the sample generalized variance is given as:

$$|\mathbf{S}_n| \;=\; {s^2}_1 {s^2}_2 - {s^2}_{12}. \tag{6.2}$$

Where s_{12} is the sample covariance between two quality characteristics. Furthermore

$$\frac{2(n-1)|\mathbf{S}_n|^{1/2}}{|\Sigma_0|^{1/2}} \sim \chi^2_{2n-4}.$$

To monitor the process standard deviation, we use the $|\mathbf{S}_n|^{1/2}$ statistic.

The results discussed in this thesis are for bivariate normal random variables which can however be extended to other cases where we are monitoring more than two quality characteristics per item. Without loss of generality, we are going to consider the case where the in control mean vector is

$$\boldsymbol{\mu}_0 = \begin{bmatrix} 0 \\ 0 \end{bmatrix}$$

and the in control covariance matrix is

$$\Sigma_0 = \begin{bmatrix} 1 & \sigma_{12} \\ \sigma_{21} & 1 \end{bmatrix}$$

The performance of this multivariate chart is determined by the distance of the off-target mean vector or covariance matrix from the on-target values and not by the particular direction of the off-target mean vector or covariance matrix. Therefore only the upper control limits are considered for monitoring the significance of the magnitude of shifts for the mean vector and covariance matrix. The distance between the on-target value and the off-target value is defined as the square root of the noncentrality parameter. When the mean vector and the covariance matrix shift from their target values to $\boldsymbol{\mu} = \boldsymbol{\mu}_0 + \boldsymbol{\delta}$ and $\boldsymbol{\Sigma} = b^2\boldsymbol{\Sigma}_0$ respectively, the distance is given as:

$$D = \sqrt{n(\boldsymbol{\mu} - \boldsymbol{\mu}_0)'(\boldsymbol{\Sigma})^{-1}(\boldsymbol{\mu} - \boldsymbol{\mu}_0)}. \tag{6.3}$$

To develop our new chart, we carry out the following transformations:

$$Z_i = \Phi^{-1}\left\{H\left[n(\bar{\mathbf{X}}_n - \boldsymbol{\mu}_0)'\boldsymbol{\Sigma}_0^{-1}(\bar{\mathbf{X}}_n - \boldsymbol{\mu}_0); p\right]\right\} \tag{6.4}$$

and

$$Y_i = \Phi^{-1}\left\{H\left[\frac{2(n-1) \mid \mathbf{S}_n|^{1/2}}{\mid \boldsymbol{\Sigma}_0|^{1/2}}; 2n-4\right]\right\}, \tag{6.5}$$

where

$$\Phi(z) = P(Z \leq z),$$

for $Z \sim N(0,1)$, the standard normal distribution. The function $\Phi^{-1}(\cdot)$ is the inverse function of $\Phi(\cdot)$, and $H(w;p) = P(W \leq w|p)$ for $W \sim \chi^2_p$, the chi-square distribution with p degrees of freedom. The variables Z_i and Y_i are independent and when $\boldsymbol{\delta} = 0$ and $b = 1$, they follow the univariate standard normal distribution and their distributions do not depend on the sample size or on p, the number of factors per variable. We can construct a single chart monitoring both the process location and the process dispersion as follows.

Define

$$M_i = max\left\{\mid Z_i|, \mid Y_i|\right\} \tag{6.6}$$

When the process mean and variability remain at their target values, M_i will be small, a large value of M_i suggest that the mean vector and/or the covariance matrix have shifted from their respective target values, and thus assignable cause(s) of variation should be identified and eliminated. Since the new chart is developed using the maximum values of the two statistics, we call it the Maximum multivariate control chart (Max-Mchart).

Since Z_i and Y_i are independent and identically distributed standard normal random variables when the process is in control, the in control cumulative distribution function of M_i is found to be

$$\begin{aligned} F(y) &= P(M_i \leq y), \\ &= P(|\, Z_i| \leq y, |\, Y_i| \leq y), \\ &= P(|\, Z_i| \leq y)P(|\, Y_i| \leq y), \\ &= P(\chi_1^2 \leq y^2)^2, \qquad y \geq 0 \end{aligned} \tag{6.7}$$

Therefore, for $F(y) = 1 - \alpha$ to hold, we must have $y = \left\{\chi^2_{\sqrt{1-\alpha},1}\right\}^{1/2}$ (Chen and Cheng [21]). The upper control limit (UCL) of the Max-Mchart is then easily determined for various values of Type I error probability α; using equation (6.7), the results are given in Table 6.1.

Table 6.1: Upper control limits (UCL) of the Max-Mchart for various values of type I error probability α

α	0.0054	0.004	0.0027	0.00135
UCL	2.9995	3.0899	3.2049	3.3975

For various changes in the mean vector and/or covariance matrix, where the mean vector shifts to $\boldsymbol{\mu} = \boldsymbol{\mu}_0 + \boldsymbol{\delta}$ while the covariance matrix shifts to $\boldsymbol{\Sigma} = b^2\boldsymbol{\Sigma}_0$, the out-of-control cumulative distribution function of M_i is found to be

$$\begin{aligned} F(y; \boldsymbol{\mu}; \boldsymbol{\Sigma}; \delta) &= P(M_i \leq y), \\ &= P(|\, Z_i| \leq y, |\, Y_i| \leq y), \\ &= P(|\, Z_i| \leq y)P(|\, Y_i| \leq y), \\ &= \left\{H\left(\frac{\chi^2_{\Phi(y),p}}{b^2}; p; \delta\right) - H\left(\frac{\chi^2_{\Phi(-y),p}}{b^2}; p; \delta\right)\right\} \\ &\quad \times \left\{H\left(\frac{\chi^2_{\Phi(y),2n-4}}{b^2}; 2n-4\right) - H\left(\frac{\chi^2_{\Phi(-y),2n-4}}{b^2}; 2n-4\right)\right\}, \quad y \geq 0 \end{aligned} \tag{6.8}$$

where $\delta = \frac{n}{b^2}(\boldsymbol{\mu} - \boldsymbol{\mu}_0)'\Sigma_0^{-1}(\boldsymbol{\mu} - \boldsymbol{\mu}_0)$ is the noncentrality parameter. The ability of this chart to detect changes in the mean vector depends on $\boldsymbol{\mu} - \boldsymbol{\mu}_0$ and Σ_0 through the noncentrality parameter δ. The out-of-control ARL's for shifts in the mean vector and/or covariance matrix are computed using equation (6.8) and are shown in Tables 6.2 and 6.3.

6.3 Design of a Max-Mchart

We assess the performance of the Max-Mchart using the in control ARL of 250 runs with a corresponding 3.0899σ limit for different sample sizes at a fixed level of the correlation structure. This control limit corresponds to a probability of Type I error of 0.004. For various changes in the mean vector alone, in covariance matrix alone, and in both mean vector and covariance matrix, we calculate the ARL's which are displayed in Table 6.2 and Table 6.3. We used $p = 2$, the bivariate case and consider low and high levels of correlation.

The chart is effective in detecting both small and large shifts in both process mean vector and covariance matrix. Similar to the Max chart (Chen and Cheng [21]), as the process mean vector and covariance matrix shift , the ARL decreases and approaches one for large shifts. The Max-Mchart becomes more effective as the sample size increases as seen in Table 6.2 and Table 6.3 where the ARL decreases as sample size increases. The scheme is also more effective in detecting smaller shifts at low levels of correlation than at higher levels. However, when there is a large shift in the process, the performance of the Max-Mchart is not significantly affected by the level of correlation between observations. We have also calculated the ARLs for this chart for different values of p. We found that, the sensitivity of this scheme is not significantly affected by number of quality characteristics monitored per item (p).

Table 6.2: ARL's for the Max-Mchart with in control $ARL_0 = 250$, $\rho = 0.1$ and $n = 4$

		$\rho = 0.1$							
		a							
n	b	0.00	0.25	0.50	1.00	1.50	2.00	2.50	3.00
	1.00	250.05	171.58	54.79	5.09	1.48	1.04	1.00	1.00
	1.25	31.64	23.80	11,76	2.72	1.26	1.02	1.00	1.00
4	1.50	7.85	6.76	4.61	1.91	1.17	1.02	1.00	1.00
	2.00	2.23	2.12	1.86	1.33	1.08	1.01	1.00	1.00
	2.50	1.41	1.38	1.31	1.14	1.04	1.01	1.00	1.00
	3.00	1.17	1.16	1.14	1.07	1.02	1.00	1.00	1.00
	4.00	1.04	1.04	1.03	1.02	1.00	1.00	1.00	1.00
		$\rho = 0.8$							
n	1.00	250.05	200.11	96.18	12.73	2.91	1.36	1.05	1.00
	1.25	31.64	26.51	16.50	4.82	1.91	1.20	1.03	1.00
4	1.50	7.85	7.16	5.56	2.74	1.53	1.13	1.02	1.00
	2.00	2.23	2.16	1.98	1.53	1.21	1.06	1.01	1.00
	2.50	1.41	1.39	1.35	1.21	1.10	1.03	1.00	1.00
	3.00	1.17	1.17	1.15	1.10	1.05	1.02	1.00	1.00
	4.00	1.04	1.04	1.04	1.03	1.01	1.01	1.00	1.00

Table 6.3: ARL's for the Max-Mchart with in control $ARL_0 = 250$, $\rho = 0.1$ and $n = 6$

$\rho = 0.1$									
		a							
n	b	0.00	0.25	0.50	1.00	1.50	2.00	2.50	3.00
	1.00	250.05	140.14	29.96	2.53	1.10	1.00	1.00	1.00
	1.25	21.92	16.19	7.40	1.74	1.06	1.00	1.00	1.00
6	1.50	4.80	4.22	2.98	1.39	1.04	1.00	1.00	1.00
	2.00	1.51	1.46	1.35	1.11	1.01	1.00	1.00	1.00
	2.50	1.12	1.11	1.08	1.03	1.00	1.00	1.00	1.00
	3.00	1.03	1.03	1.02	1.01	1.00	1.00	1.00	1.00
	4.00	1.00	1.00	1.00	1.00	1.00	1.00	1.00	1.00
$\rho = 0.8$									
n	1.00	250.05	177.41	61.37	5.97	1.63	1.06	1.00	1.00
	1.25	21.92	18.20	10.78	2.92	1.33	1.04	1.00	1.00
6	1.50	4.80	4.44	3.54	1.86	1.19	1.02	1.00	1.00
	2.00	1.51	1.48	1.40	1.20	1.06	1.01	1.00	1.00
	2.50	1.12	1.11	1.10	1.05	1.02	1.00	1.00	1.00
	3.00	1.03	1.03	1.03	1.01	1.00	1.00	1.00	1.00
	4.00	1.00	1.00	1.00	1.00	1.00	1.00	1.00	1.00

6.4 The Power of a Max-Mchart

Figure 6.1 shows the power of the Max-Mchart in relation to changes in the level of correlations. The figure shows the power of this scheme for upward shifts in the mean vector and/or covariance matrix. Like the Max-MCUSUM chart discussed in chapter 5 and the T^2 chart (Wierda [101]), the performance of the Max-Mchart is not affected by the strength of the relationship, but by the direction of the correlation in relation to the shift in the parameters. If there is a strong negative correlation between the variables, increases in mean vectors and /or covariance matrices are detected quickly as opposed to decreases in these parameters. Positive correlation reduces the ability of this scheme to detect upward shifts.

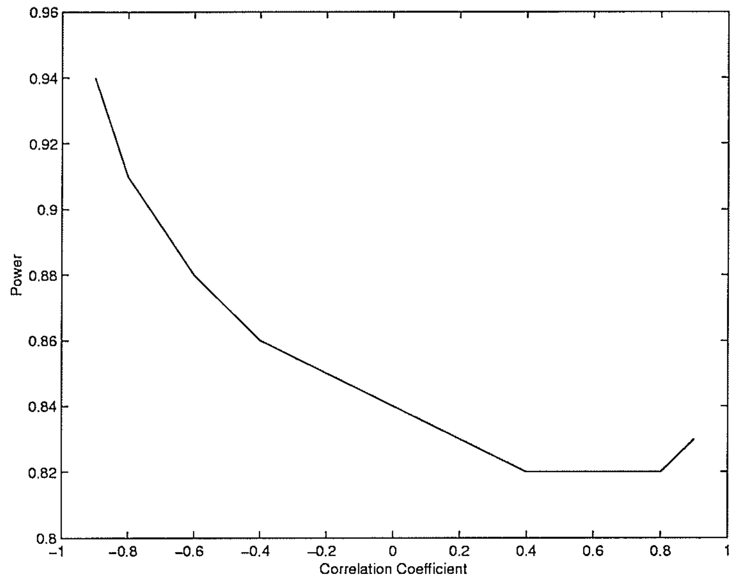

Figure 6.1: Plot of power for the Max-Mchart chart against correlation coefficients between variables.

6.5 Comparison with Other Procedures

In this section we compare the Max-Mchart with the Max-MCUSUM and Max-MEWMA (Xie [108]) charts. These charts are compared by first adjusting their respective control limits so that the in control ARL is fixed at 200. We compare the three charts by examining their ARLs for different shifts in the mean vector and/or covariance matrix. The Max-Mchart performs better than the Max-MCUSUM chart and the Max-MEWMA chart for shifts in mean that are at least 1.5σ and at least a 2σ shift in the process variability. Compared to the traditional charts, we see that these recently developed single charts are good in detecting small and large shifts in the mean vector and/or covariance matrix. Furthermore, these single charts are easy to interpret as the statistic plotting outside the control limit is indicated by a corresponding symbol defined in the design procedures.

Table 6.4: ARL's for the Max-MCUSUM chart, the Max-MEWMA chart and the Max-Mchart.

$ARL_0 = 200$ with $\rho = 0.6$							
	Max-MCUSUM						
	a						
b	0.00	0.50	1.00	1.50	2.00	2.50	3.00
1.00	200.4	4.3	2.9	2.2	1.8	1.5	1.4
1.50	8.4	3.3	2.3	1.7	1.4	1.2	1.1
2.00	5.9	2.8	1.9	1.5	1.3	1.1	1.1
2.50	4.8	2.5	1.7	1.4	1.2	1.1	1.0
3.00	4.1	2.3	1.6	1.3	1.1	1.1	1.0
	Max-MEWMA						
	a						
b	0.00	0.50	1.00	1.50	2.00	2.50	3.00
1.00	200.1	18.2	5.3	3.2	2.3	2.0	1.7
1.50	7.5	6.1	4.1	3.0	2.3	1.7	1.2
2.00	3.4	3.2	2.9	2.4	2.1	1.8	1.6
2.50	2.4	2.4	2.2	2.1	1.9	1.7	1.5
3.00	2.0	2.0	1.9	1.8	1.7	1.1	1.0
	Max-Mchart						
	a						
b	0.00	0.50	1.00	1.50	2.00	2.50	3.00
1.00	200.1	71.4	9.2	2.3	1.2	1.0	1.0
1.50	7.2	4.9	2.4	1.4	1.1	1.0	1.0
2.00	2.1	1.9	1.4	1.2	1.0	1.0	1.0
2.50	1.4	1.3	1.2	1.1	1.0	1.0	1.0
3.00	1.2	1.1	1.1	1.0	1.0	1.0	1.0

6.6 Charting Procedures

The charting procedure of a Max-Mchart is carried out as follows:

1. For each sample compute Z_i, Y_i and M_i.

2. Find the upper control limit UCL from Table 6.1 for the desired α.

3. If $\boldsymbol{\mu}$ is not known, use the sample mean vector $\bar{X}_n$ which is a p-dimensional vector of sample means. In the same manner, if the population covariance matrix is unknown, we use the sample covariance matrix $\boldsymbol{S}_n$ to estimate it.

4. When $M_i <$ UCL, plot the data point using a dot.

5. When $M_i \geq$ UCL, the following plotting procedures should be used to show the statistic that is plotting above the control limit.

   (i) If $|\ Z_i| \geq$UCL, plot $m+$. This shows a shift in the process mean.

   (ii) If $|\ Y_i| \geq$UCL, plot $V+$. This shows a shift in the process standard deviation.

   (iii) If both $|\ Z_i| \geq$UCL and $|\ Y_i| \geq$UCL, plot $B++$. This indicates shifts in both the mean and standard deviation of the process.

6. Investigate the cause(s) of the shift for each out-of-control point in the chart and carry out the remedial measures needed to bring the process back into an in control state.

If the Max-Mchart signals an out-of control state, we recommend the methods proposed by Mason, Tracy and Young ([66]) be applied to the points plotting outside the limits. This method works by decomposing the T^2 statistic into orthogonal components in order to identify the variable or set of variables causing the signal.

6.7 An Example

To demonstrate the implementation of the proposed Max-Mchart, we will use the data used by Sultan ([92]). The data is from a steel manufacturing process that measured the Brinnel hardness (x) and the tensile strength (y) for 30 samples. This data is displayed in Table 5.7. The chart is developed as follows: the sample covariance matrix is

$$\boldsymbol{S} = \begin{bmatrix} 332.13 & 69.26 \\ 69.26 & 29.97 \end{bmatrix}$$

and the sample grand mean is

$$\bar{\bar{\boldsymbol{X}}} = \begin{bmatrix} 174.67 \\ 51.67 \end{bmatrix}.$$

This control chart was constructed using the Type I error probability of 0.004. This results in an in control ARL = 250 and the upper control limit of 3.0899. The control chart shows no significant shift in the mean. Like the simultaneous chart proposed by Spiring and Cheng ([91]) and the Max-MCUSUM chart, the Max-Mchart shows a significant shift in the covariance structure for subgroup 6 as depicted in Figure 6.2.

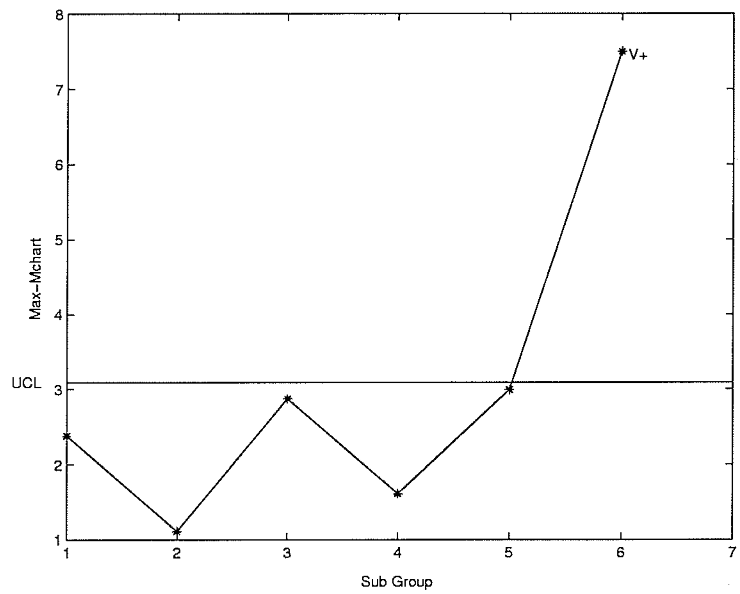

Figure 6.2: The Max-Mchart for the brinnel hardness and tensile strength data.

6.8 Conclusions and Recommendations

We have proposed a new Shewhart-type single control chart that is capable of monitoring process mean and standard deviation for multivariate normal processes. This chart is easy to use as it involves transforming the complex multivariate process to a univariate process. Then easy-to-use standard univariate procedures are used to derive the new chart. This chart also quickly detects large shifts in the process parameters.

We recommend this new chart because we can use one chart to simultaneously monitor the process location and spread unlike the traditional scheme that requires running two charts concurrently to monitor the process.

Chapter 7

Max-CUSUM Chart for Autocorrelated Processes

7.1 Introduction

In the previous 4 chapters, we proposed single univariate and multivariate control charts under the assumption that, a process being monitored will produce measurements that are independent and identically distributed over time when only the inherent sources of variability are present in the system. However, in some applications the dynamics of the process will induce correlations in observations which are closely spaced in time. If the sampling interval used for process monitoring in these applications is short enough for the process dynamics to produce significant correlation, then this correlation can have very serious effects on the properties of standard control charts, (see VanBrackle and Reynolds [96], Lu and Reynolds ([55], [56]) and Runger, Willemain and Prabhu [86]). Examples of situations where a process produces measurements that are correlated include, measured variables from tanks, reactors and recycle streams in chemical processes.

In the next two chapters, we investigate how the performance of control charts is affected by serial correlation in the observations. We will restrict our discussion to serial correlation that can be modelled using the first order autoregressive moving average ARMA(1,1) models. We propose control charts for simultaneously monitoring the process mean and variability using a single control chart in the presence of autocorrelation.

In this chapter, we propose a CUSUM control chart for autocorrelated data that can simultaneously monitor shifts in the process location and/or spread using a single plotting variable. This investigation is done for the case of processes that can be modelled as a first order autoregressive AR(1) process plus an additional random error which can correspond to sampling or measurement error. This model has been used in several charts dealing with autocorrelated data. It allows relatively accurate numerical techniques to be used to evaluate properties of the control charts and the model is frequently encountered in practice. Furthermore, it may serve as an approximation to other time series models. First order autoregressive models are also useful when a disturbance affects not only the current outcome of the process, but also (have an exponentially declining effect on) future outcomes. Such situations occur for example when a tank containing raw material is refilled from time to time with raw material of varying quality (Wieringa [102]).

7.2 Effect of Ignoring Serial Correlation

Positive autocorrelation in the process can result in severe negative bias in traditional estimators of the standard deviation. This bias produces control limits that are much tighter than desired. Lu and Reynolds ([55]) observed that tight control limits, combined with autocorrelation in the observations plotted, can result in an average false alarm rate much higher than expected. This will result in wasted effort searching for nonexisting special causes of variation in the process. This can also result in loss of confidence in the control charts and practitioners may abandon their use. Furthermore, when we use residual charts in situations when observations are positively autocorrelated, when there is a shift in the process mean only a fraction of the shift will be transferred to the residual means, this reduces the chart's ability to quickly detect such shifts. This is an undesirable situation in process monitoring particularly in the chemical industries where small shifts are commonly experienced.

When the observations are negatively correlated, the standard deviation will be overestimated and this will result in wider control limits of traditional control charts. Wide control limit makes the scheme insensitive to changes in the process mean and standard deviation. It is therefore very important to take autocorrelation among observations into consideration when designing a process monitoring scheme.

Recently, new control charts have been proposed for dealing with autocorrelated data. Two approaches have been advocated for dealing with this phenomenon. The first approach uses standard control charts on original observations, but adjust the control limits and methods of estimating parameters to account for the autocorrelation in the observations (see VanBrackle and Reynolds [96], Lu and Reynolds [56]). This approach is particularly applicable when the level of autocorrelation is low but less effective at high levels of autocorrelation.

A second approach for dealing with autocorrelated processes, fits time series model to the process observations. The procedure forecasts observations from previous values and then computes the forecast errors or residuals. These residuals are then plotted on standard control charts for process monitoring. This is because when the fitted time series model is the same as the true process model and the parameters are estimated without error, the residuals are independent and identically distributed normal random variables when the process is in control. (see Alwan and Roberts [2]; Montgomery and Mastrangelo [71]; Wadell, Moskowitz, and Plante [99]; Lu and Reynolds [57]; and Runger, Willemain and Prabhu [86]).

Yashchin ([109]) recommends charting raw data directly when the level of autocorrelation is low while for high levels of autocorrelation, they recommend transformation procedures that creates residuals. They allow for autocorrelation in the residuals due to model misspecification. The residual charts are used in process quality monitoring because a shift in the process mean and/or standard deviation results in a shift in the residual mean and/or standard deviation. Residual control charts seem to work best when the level of correlation is high. When the level of correlation is low, forecasting is more difficult and residual charts are not very effective at detecting process changes.

Most of the charts discussed in the literature monitor the process location and variability using two sets of charts. Lu and Reynolds ([57]) proposed a simultaneous EWMA control chart which uses one chart to monitor the process mean and variability by plotting two variables on the same chart. The process is deemed out of control when either of the two variables plots outside the control region. A general conclusion that can be drawn from these studies on autocorrelated processes is that correlation between observations has a significant effect on the properties of the control charts. In particular, when the observations are negatively correlated, the control chart will not quickly detect shifts in the processes while in the presence of positive correlation, the control limit will be too tight and the chart will produce a high rate of false alarm.

We acknowledge that the biased estimator of variation in serially correlated process is a serious problem when constructing control charts. We monitor the process changes by monitoring the residuals from a time series model. This is because a shift in the process mean and/or standard deviation causes a shift in the mean and/or standard deviation of the residuals. Modified Markov chain methods are used to evaluate the ARL of this chart at different levels of correlations. Our proposed chart monitors the process by simultaneously monitoring the residual means and variation. The results show that by adjusting the reference value of the standard CUSUM chart to take the autocorrelation structure into consideration, the CUSUM chart can effectively detect small shifts in the process mean and/or spread.

We assume that the underlying process model is correctly identified, and that its parameters are known. This is not a serious limitation in practice since applications where serial correlation is an issue typically arise in situations where there is a high frequency of sampling. Therefore the data are usually available to identify the model and estimate the model parameters with a high degree of accuracy.

7.3 The AR(1) Process With an Additional Random Error

Suppose that observations are taken from a process at regularly spaced time, and let X_t represent the observation taken at sampling time t. The properties of control charts are usually calculated under the assumption that the observations are independent normal random variables with constant mean and variance. When observations are independently identically distributed normal random variables, X_t can be represented as

$$X_t = \mu + \varepsilon_t, \qquad t = 1, 2, ...,$$

where μ is the process mean and the ε's are independent normal random variables with mean 0 and variance σ_ε^2. It is assumed that the process mean μ is constant at a target value when the process is in control and can change to some other values when a special cause occurs.

To model observations from an autocorrelated process, we use a model that has been discussed previously in quality control by authors such as Lu and Reynolds ([55] and [57]) and VanBrackle and Reynolds ([96]). For this model, X_t can be represented as

$$X_t = \mu_t + \varepsilon_t, \qquad t = 1, 2, ..., \tag{7.1}$$

where μ_t is the random process mean at sampling time t and ε_t's are independent normal random errors with mean 0 and variance σ_ε^2. This model accounts for correlation between samples that are close together in time, for variability in the process mean over time and for additional variability due to sampling or measurement errors. It is assumed that μ_t can be described as a first order autoregressive AR(1) process defined as

$$\mu_t \;=\; (1-\phi)\xi + \phi\mu_{t-1} + \alpha_t, \qquad t = 1, 2, ..., \tag{7.2}$$

where ξ is the overall process mean, α_t's are normally distributed random shocks with a mean 0 and variance σ_α^2. These random shocks are independent of all the random errors and of the random shocks associated with individual observations at any other time. The autoregressive parameter ϕ represents the correlation between μ_t and μ_{t-1}. The process will be stationary if $|\ \phi| < 1$. For most processes of interest in control chart application, ϕ will be nonnegative (Reynolds, Arnold and Baik [84]).

The distribution of μ_t for $t \geq 1$ depends on a starting value μ_0 for the series at time $t = 0$. If we assume that the starting value μ_0 follows a normal distribution with mean ξ and variance $\sigma_{\mu_0}^2 = \sigma_\alpha^2/(1-\phi^2)$, then μ_t will also follow a normal distribution with mean ξ and variance $\sigma_\mu^2 = \sigma_\alpha^2/(1-\phi^2)$. The random variable X_t has mean ξ and variance given as $\mathrm{Var}(X_t) = \mathrm{Var}(\mu_t) + \mathrm{Var}(\varepsilon_t)$. This variance is given as

$$\sigma_X^2 = \sigma_\mu^2 + \sigma_\varepsilon^2 \;=\; \frac{\sigma_\alpha^2}{1-\phi^2} + \sigma_\varepsilon^2, \qquad t = 1, 2, ..., \tag{7.3}$$

σ_X^2 is the true standard deviation of X since the effect of ϕ in the AR(1) process is incorporated; μ_t is the mean at time t and ξ is the overall process mean. The covariance between two observations that are i units apart is given as $\phi^i\sigma_\mu^2$ and the correlation between two adjacent observations is

$$\rho = \phi\psi, \tag{7.4}$$

where ψ is the proportion of the process variance due to variation in μ_t. We can interpret σ_μ^2 as the long-term variability and σ_ε^2 as a combination of short-term variability and the variability associated with measurement error. In situations where material is processed in batches, μ_t might represent the mean of batch t, σ_μ^2 might represent the batch-to-batch variability, and σ_ε^2 might be the within-batch variability (Lu and Reynolds [57]). When assessing processes that can be assumed to follow the model in equation (7.1) and equation (7.2), it is often convenient to consider the proportion of total process variability that is due to variation in μ_t and the proportion due to error variability. The proportion of the process variance due to μ_t is defined as

$$\psi = \frac{\sigma_\mu^2}{\sigma_X^2} = \frac{\sigma_\mu^2}{\sigma_\mu^2 + \sigma_\varepsilon^2}. \tag{7.5}$$

The proportion of the total process variation that is due to ε_t is then 1 - ψ.

Autocorrelation in the process may at times be caused by assignable causes that can be eliminated, this will reduce variability in the process. In other processes, the autocorrelations are inherent characteristics of the process and thus cannot be removed in the short-run. In these situations, the process is said to be in control when the process mean continuously wanders around the target value but within the acceptable region. Thus the process mean is not constant as in the case of independent observations.

The AR(1) process with an additional independent random error is equivalent to a first order autoregressive moving average (ARMA(1,1)) process (Box, Jenkins and Reinsel [7]), which can be written as

$$(1 - \phi B)X_t \;=\; (1 - \phi)\xi + (1 - \theta B)\gamma_t, \tag{7.6}$$

where γ_t's are the random shock components of the ARMA(1,1) process and are independent and identically distributed normal random variables with mean 0 and variance σ_γ^2, θ is the moving average parameter, ϕ is the autoregressive parameter of the AR(1) process, and B is a backshift operator such that $BX_t = X_{t-1}$. If $\phi = 0$ then the observations are independent and the parameters of the model in equation (7.6) are $\theta = 0$ and $\sigma_\gamma^2 = \sigma_\alpha^2 + \sigma_\varepsilon^2$. If $\phi > 0$, Koons and Foutz ([51]) derived θ and σ_γ^2 as

$$\theta = \frac{\sigma_\alpha^2 + (1+\phi^2)\sigma_\varepsilon^2}{2\phi\sigma_\varepsilon^2} - \frac{1}{2}\sqrt{(\frac{\sigma_\alpha^2 + (1+\phi^2)\sigma_\varepsilon^2}{\phi\sigma_\varepsilon^2})^2 - 4} \tag{7.7}$$

and

$$\sigma_\gamma^2 = \frac{\phi\sigma_\varepsilon^2}{\theta} \tag{7.8}$$

The standard time series estimation techniques can be used to estimate the parameters in the ARMA(1,1) model.

In some production processes, a large volume of items are produced in a single lot. In such situations more than one observation are sampled each time. Let X_{ti} be the i^{th} observation at sampling time t. We assume that X_{ti} can be represented as

$$X_{ti} = \mu_t + \varepsilon'_{ti} \tag{7.9}$$

where the ε'_{ti}'s are independent and identically distributed normal random variables with mean 0 and variance $\sigma_{\varepsilon'}^2$. If n sampled observations are averaged, then their average, $\bar{X}_t$ can be written as $\bar{X}_t = \mu_t + \bar{\varepsilon}'_t$, where $\bar{\varepsilon}'_t = \sum_{i=1}^n \varepsilon'_t/n$. In this case, the sample means will follow the model in equation (7.1) and equation (7.2) with mean 0 and variance $\sigma_{\varepsilon'}^2/n$.

In this chapter, we monitor the process mean and process variability by monitoring the residuals from a forecast. To do this, we first determine the distribution of the residuals when the process is in control. When the process is in control, the residual at observation t from the minimum mean square error forecast made at observation $t-1$ is

$$e_t = X_t - \xi_0 - \phi(X_{t-1} - \xi_0) + \theta e_{t-1} \tag{7.10}$$

where ϕ and θ are parameters in the ARMA(1,1) model given in equation (7.6) and ξ_0 is the overall mean when the process is in control.

If the fitted time series model is the same as the true process model and the parameters are estimated without error, then the residuals are independent and identically distributed normal random variables when the process is in control. We can then monitor the process by using standard control charts for independent observations by monitoring these residuals. If there is a step change in the process mean from the in-control value ξ_0 to ξ_1 between time $t = \tau - 1$ and $t = \tau$, the expectations of the residuals for various times are (see Lu and Reynolds [56])

$$\begin{aligned} E(e_t) &= 0, && t < \tau \\ E(e_t) &= \xi_1 - \xi_0, && t = \tau \end{aligned}$$

and

$$\begin{aligned} E(e_t) &= \left[\theta^l + (1-\phi)\sum_{i=1}^{l}\theta^{i-1}\right](\xi_1 - \xi_0) \\ &= \frac{1 - \phi + \theta^l(\phi - \theta)}{1-\theta}(\xi_1 - \xi_0) \qquad t = \tau + l, l = 1, 2, \ldots \end{aligned} \tag{7.11}$$

The asymptotic mean of the residual after the shift is

$$\frac{1-\phi}{1-\theta}(\xi_1 - \xi_0). \tag{7.12}$$

These residuals are independent and follow a normal distribution with variance σ_γ^2. The expectation of the residuals after the shift occurs is a decreasing function of time. Also, as ϕ increases, a small fraction of the shift in the process mean will be transferred to the mean of the residuals. It is evident that when the process mean shifts, only a fraction of the shift is transferred to the mean of the residuals and this fraction decreases as ϕ increases, as can be seen in equation (7.12). Since only a fraction of the process mean shift is transferred to the residual means, the chart for residuals will not quickly detect the shifts as compared to the chart for independent observations where the entire process mean shift will be monitored. On the other hand, the residuals chart is theoretically appealing because it takes the serial correlation into account, and reduces the problem to a well known, easy to use case of a shift in the process mean and/or variability of independent observations.

A change in the process variability can be attributed to a change in the autoregressive parameter, ϕ, a change in variability for the random shocks associated with individual observations σ_ε^2, and a change in variability of the random shocks associated with the autocorrelated means, σ_α^2. If between observations $t-1$ and t, σ_α^2 increases from its nominal value $\sigma_{\alpha 0}^2$ to $\sigma_{\alpha 1}^2$ and σ_ε^2 increases from its nominal value $\sigma_{\varepsilon 0}^2$ to $\sigma_{\varepsilon 1}^2$, with ϕ remaining unchanged, the model in equation (7.1) becomes

$$X_{t+l} = \mu_{t+l} + \varepsilon_{t+l} + \varepsilon_{t+l}^*, \qquad l = 0, 1, ..., \tag{7.13}$$

where $\varepsilon_t^*, \varepsilon_{t+1}^*, ...$ is a sequence of independent normal random variables with a mean 0 and variance $\sigma_{\varepsilon 1}^2 - \sigma_{\varepsilon 0}^2$, independent of the ε_{t-l}'s. The model in equation (7.2) for μ_t becomes

$$\mu_{t+l} = (1-\phi)\xi + \phi\mu_{t+l-1} + \alpha_{t+l} + \alpha_{t+l}^*, \qquad l = 0, 1, ..., \tag{7.14}$$

where $\alpha_t^*, \alpha_{t+l}^*, ...$ is a sequence of independent normal random variables with mean 0 and variance $\sigma_{\alpha 1}^2 - \sigma_{\alpha 0}^2$, independent of the α_{t+l}'s. We can write μ_{t+1}, X_{t+1}, $\hat{X}_{t+1}$ and ε_{t+1} in terms of their corresponding in-control quantities, say μ_{t+1}^0, X_{t+1}^0, $\hat{X}_{t+1}^0$

and ε^0_{t+1} respectively. Therefore using the model in equation (7.1) and equations (7.8), (7.11) and (7.12), it can be shown by induction that

$$
\begin{aligned}
\mu_{t+l} &= \mu^0_{t+l} + \sum_{i=0}^{l} \phi^{l-i}\alpha^*_{t+i}, \qquad l = 0, 1, \ldots \\
X_{t+l} &= X^0_{t+l} + \xi^*_{t+l} + \sum_{i=0}^{l} \phi^{l-i}\alpha^*_{t+i}, \qquad l = 0, 1, \ldots \\
\hat{X}_{t+l} &= \hat{X}^0_{t+l} + (\phi - \theta_0)\sum_{i=0}^{l} \theta_0^{l-i}\varepsilon^*_{t+i} + \sum_{i=0}^{l-1}(\phi^{l-i} - \theta_0^{l-i})\alpha^*_{t+i}, \qquad l = 0, 1, \ldots \\
e_t &= e^0_t + \varepsilon^*_t + \alpha^*_t \qquad (7.15)
\end{aligned}
$$

and

$$
\begin{aligned}
e_{t+l} &= e^0_{t+l} + \varepsilon^*_{t+l} - (\phi - \theta_0)\sum_{i=0}^{l-1} \theta_0^{l-i-1}\varepsilon^*_{t+i} \\
&\quad + \sum_{i=0}^{l} \theta_0^{l-i}\alpha^*_{t+i}, \qquad l = 0, 1, \ldots \qquad (7.16)
\end{aligned}
$$

where θ_0 is the in-control value of θ. This shows that e_{t+l} is a function of ε^*_{t+i} and α^*_{t+i} for $i \leq l$. Therefore the effect of a shift in the variance is to induce correlation in the residuals (Lu and Reynolds [57]).

Assuming that $\sigma^2_{\gamma 0}$ is the in-control value of σ^2_γ, then $Var(e^0_{t+l}) = \sigma^2_{\gamma 0}$. Therefore the variance of the residuals after the shift is

$$Var(e_t) = \sigma^2_{\gamma 0} + (\sigma^2_{\varepsilon 1} - \sigma^2_{\varepsilon 0}) + (\sigma^2_{\alpha 1} - \sigma^2_{\alpha 0})$$

and

$$
\begin{aligned}
Var(e_{t+l}) &= \sigma^2_{\gamma 0} + \left[1 + (\phi - \theta_0)^2 \sum_{i=0}^{l-i} \theta_0^{2(l-i-1)}\right] \\
&\quad \times(\sigma^2_{\varepsilon 1} - \sigma^2_{\varepsilon 0}) + \sum_{i=0}^{l} \theta_0^{2(l-i)}(\sigma^2_{\alpha 1} - \sigma^2_{\alpha 0}), \qquad l = 1, 2, \ldots
\end{aligned}
$$

The asymptotic variance of these residuals after the shift will increase to the limit

$$Var(e_t) = \sigma^2_{\gamma 0} + \frac{\phi^2 - 2\phi\theta_0 + 1}{1 - \theta_0^2}(\sigma^2_{\varepsilon 1} - \sigma^2_{\varepsilon 0}) + \frac{\sigma^2_{\alpha 1} - \sigma^2_{\alpha 0}}{1 - \theta_0^2}. \qquad (7.17)$$

The residuals after the shifts in the process mean and variance are correlated with the asymptotic mean given in equation (7.12) and asymptotic variance given in equation (7.17). From equation (7.17), we can see that changes in σ_α^2 and σ_ε^2 have different impact on the variability of the residual. We are therefore monitoring the effects of different shifts in these variance components separately.

In process monitoring procedures such as control charts, it is often necessary to estimate the parameters of the model given in equation (7.1) and equation (7.2) using available data. Standard time series modelling techniques can be used to estimate the parameters in the ARMA(1,1) model. Given the parameters in the ARMA(1,1) model, for $\phi > 0$, σ_α^2 and σ_ε^2 can be obtained from (see Reynolds, Arnold and Baik [84])

$$\sigma_\alpha^2 = \frac{\sigma_\gamma^2(\phi-\theta)(1-\phi\theta)}{\phi} \tag{7.18}$$

and

$$\sigma_\varepsilon^2 = \frac{\theta\sigma_\gamma^2}{\phi} \tag{7.19}$$

We can then fit the AR(1) plus random error model in equation (7.1) and equation (7.2), which is the model considered in this thesis. We consider the case of positive autocorrelation which is more prevalent than negative autocorrelation in control chart applications. The objective of monitoring the process is to detect those situations in which one or more process parameters have changed from their target values by the occurrence of a special cause. To this end, we propose a new CUSUM chart that can simultaneously monitor the effect of special causes of variation in the mean and standard deviation.

7.4 The New Control Chart

We propose a new CUSUM chart for residuals in this section. Let $X_i = X_{i1}, ..., X_{in_i}$, $i = 1, 2, ...$, denote a sequence of samples of size n_i taken on a quality characteristic X. It is assumed that, for each i, $X_{i1}, ..., X_{in_i}$ are autocorrelated and can be expressed as in the model shown in equation (7.9). We monitor the process by first fitting a time series model to the process observations and then computing the residuals. Let ξ_0 and $\sigma_{\gamma 0}$ be the nominal process mean and standard deviation of the residuals for this fitted model. Assume that the process residual parameters ξ and σ_γ can be expressed as $\xi = \xi_0 + a\sigma_{\gamma_0}$ and $\sigma_\gamma = b\sigma_{\gamma_0}$ for $b > 0$, where $a = 0$ and $b = 1$ when the process is in-control, otherwise, the process has changed due to some assignable cause. Then a represents the shift in mean and b represents the shift in standard deviation.

Let $\bar{\xi}_i = (\xi_{i1} + ... + \xi_{in_i})/n_i$ and $MSE_i = \sum_{j=1}^{n_i}(\xi_{ij} - \bar{\xi}_i)^2/n_i$ be the mean and the mean square error for the i^{th} sample residuals respectively. These statistics are independently distributed as are the sample residual values when the process is in-control. These two statistics however follow different distributions. The CUSUM charts for the mean and standard deviation are based on $\bar{\xi}_i$ and MSE_i respectively.

To develop a single CUSUM chart for simultaneously monitoring the process mean and standard deviation using residuals, we carry out the following transformations:

$$Z_i = \sqrt{n_i}\frac{(\bar{\xi}_i - \xi_0)}{\sigma_{\gamma 0}} \tag{7.20}$$

and

$$Y_i = \Phi^{-1}\left\{H\left[\frac{(n_i)MSE_i}{\sigma_{\gamma 0}^2}; n_i\right]\right\}, \tag{7.21}$$

where

$$\Phi(z) = P(Z \leq z),$$

for $Z \sim N(0,1)$, the standard normal distribution, $\Phi^{-1}(\cdot)$ is the inverse function of $\Phi(\cdot)$, the cumulative distribution function of N(0,1), and $H(w;p) = P(W \leq w|p)$ for $W \sim \chi^2_p$, the chi-square distribution with p degrees of freedom.

These variables, Z_i and Y_i are independent and when $a = 0$ and $b = 1$, they follow the standard normal distribution. The CUSUM statistics based on Z_i and Y_i are defined as

$$\begin{aligned} C_i^+ &= \max[0, Z_i - k + C_{i-1}^+], & (7.22) \\ C_i^- &= \max[0, -k - Z_i + C_{i-1}^-], & (7.23) \end{aligned}$$

and

$$\begin{aligned} S_i^+ &= \max[0, Y_i - k + S_{i-1}^+], & (7.24) \\ S_i^- &= \max[0, -k - Y_i + S_{i-1}^-], & (7.25) \end{aligned}$$

respectively, where C_0 and S_0 are starting values. Because Z_i and Y_i follow the same distribution, a new statistic for the single control chart can be defined as

$$M_i = \max[C_i^+, C_i^-, S_i^+, S_i^-] \tag{7.26}$$

If the process has gone out of control, the M_i's will plot outside the control limits, otherwise the M_i values will be within the limits. Due to nonnegative values of M_i, we plot only the upper control limit for this chart, and consider the process to be out of control if an M_i value is plotted above this upper control limit.

In SPC, we use the ARL or the average time to signal (ATS) of the chart to assess the performance of the scheme. This is the expected number of samples (or observations if we take a single observation each time) required by the chart to signal an out-of-control situation.

We investigate the AR(1) process plus a random error with four parameters namely: the autoregressive parameter, the overall mean and two variance parameters. In this case the special cause may affect any one or a combination of these four parameters. For example in a batch process, a special cause might produce an increase in within-batch variability, between-batch variability, or both (Lu and Reynolds [57]).

For a change in variability, we consider the effects of changes in σ_ε and σ_α separately to calculate the ARL. This is because the two parameters have different impacts on the level of variability of the process as shown in equation (7.17). The shifts in these parameters are considered for different values of ϕ, the correlation between μ_t and μ_{t-1}. We assume the moving average parameter, θ is fixed.

As shown previously, when the process is in-control, the residuals are independent and identically distributed normal random variables with mean $\xi_0 = 0$ and standard deviation $\sigma_{\gamma 0}$. If there is a change in the mean and the standard deviation, the residuals are correlated normal random variables with an asymptotic mean given in equation (7.12) and asymptotic variance given in equation (7.17). We will consider a situation where the occurrence of a special cause of variation results in an increase in the process mean alone, increase in the process standard deviation alone or an increase in both mean and standard deviation of the process.

7.5 Design of a Max-CUSUM Chart for Autocorrelated Process (MCAP Chart)

We use the statistic M_i to construct a new control chart. Because M_i is the maximum of four statistics, we call this new chart the Maximum Cumulative Sum chart for Autocorrelated Process (MCAP chart). Lucas ([58]) showed that a CUSUM chart for independent normal data is tuned to be most sensitive to a shift of magnitude δ by choosing the reference value, $k = \delta/2$. Runger, Willemain and Prabhu ([86]) proposed a modified procedure that takes into consideration the autocorrelation structure of the data. They proposed the reference value to be computed as $k = \delta(1-\phi)/2$ for the AR(1) process.

To calculate the ARL of the new chart we use the modified Markov chain procedure proposed by Runger, Willemain and Prabhu ([86]). For the AR(1) plus random error model when investigating shifts in mean and/or standard deviation, we use the asymptotic mean given in equation (7.12). For a given in-control ARL and a shift of the mean and/or standard deviation intended to be detected by the chart, the reference value (k) is computed as $(\frac{1-\phi}{1-\theta})\delta/2$. This guideline takes into consideration the autocorrelation structure between the variables. For these values (ARL, k), the value of the decision interval (h) is chosen to achieve the specified in-control ARL. Then we use the procedure for CUSUM chart with standard (h, k) values for a normal distribution with new mean in equation (7.12) and variance given in equation (7.17) to calculate the ARL's.

Table 7.1 and Table 7.2 give the optimal combinations of h and k for an in-control ARL fixed at 250 and the autoregressive parameter $\phi = 0.25$ with 80% of process variability due to variation in μ_t, using equation (7.4), we obtain the correlation between adjacent observations $\rho = 0.2$. Without loss of generality, we assume $\sigma^2_{X0} = \sigma^2_{\gamma_0} = 1$. We calculate the moving average parameter θ using equation (7.7) and obtain $\theta = 0.052$. We calculate the out-of-control ARL for the effect of changes in the standard deviation that are due to changes in σ_ε and σ_α respectively. The smallest value of an out-of-control ARL is calculated with respect to a pair of specified shifts in both mean and standard deviation using the optimal in-control ARL CUSUM chart parameters. For example if one wants to have in-control ARL of 250 and to guard against $3\sigma_{\gamma_0}$ increase in process mean and $2\sigma_{\gamma_0}$ increase in the process standard deviation due to an increase in σ_ε, i.e., $a = 3$ and $b = 2$, the optimal in-control chart parameter values are $h = 1.234$ and $k = 1.187$. These shifts can on average be detected on the second sample, i.e., the ARL is approximately two. We assume that the process starts in an in-control state and thus the initial value of the CUSUM statistic is set at zero.

Table 7.1: (k,h) combinations and the corresponding ARL for the MCAP chart, with $\phi = 0.25$ and $\psi = 0.8$ for shifts in the process standard deviation due to shift in σ_α.

$ARL_0 = 250$									
		a							
b	Parameter	0.00	0.25	0.50	1.00	1.50	2.00	2.50	3.00
	h	3.720	8.510	5.990	3.720	2.630	1.986	1.561	1.234
1.00	k	0.396	0.099	0.198	0.396	0.593	0.791	0.989	1.187
	ARL	250.76	29.38	11.78	4.21	2.13	1.36	1.11	1.03
	h	3.720	8.510	5.990	3.720	2.630	1.986	1.561	1.234
1.25	k	0.396	0.099	0.198	0.396	0.593	0.791	0.989	1.187
	ARL	22.78	26.50	11.07	4.01	2.03	1.33	1.10	1.03
	h	3.720	8.510	5.990	3.720	2.630	1.986	1.561	1.234
1.50	k	0.396	0.099	0.198	0.396	0.593	0.791	0.989	1.187
	ARL	16.49	23.66	10.31	3.80	1.95	1.31	1.10	1.03
	h	3.720	8.510	5.990	3.720	2.630	1.986	1.561	1.234
2.00	k	0.396	0.099	0.198	0.396	0.593	0.791	0.989	1.187
	ARL	10.57	18.79	8.83	3.40	1.82	1.28	1.09	1.02
	h	3.720	8.510	5.990	3.720	2.630	1.986	1.561	1.234
2.50	k	0.396	0.099	0.198	0.396	0.593	0.791	0.989	1.187
	ARL	7.88	15.20	7.58	3.07	1.73	1.25	1.08	1.02
	h	3.720	8.510	5.990	3.720	2.630	1.986	1.561	1.234
3.00	k	0.396	0.099	0.198	0.396	0.593	0.791	0.989	1.187
	ARL	6.39	12.61	6.58	2.82	1.66	1.23	1.08	1.02
	h	3.720	8.510	5.990	3.720	2.630	1.986	1.561	1.234
4.00	k	0.396	0.099	0.198	0.396	0.593	0.791	0.989	1.187
	ARL	4.85	9.26	5.17	2.46	1.56	1.21	1.07	1.02

Table 7.2: (k,h) combinations and the corresponding ARL for the MCAP chart, with $\phi = 0.25$ and $\psi = 0.8$ for shifts in the process standard deviation due to shift in σ_{ε}.

$ARL_0 = 250$									
		a							
b	Parameter	0.00	0.25	0.50	1.00	1.50	2.00	2.50	3.00
	h	3.720	8.510	5.990	3.720	2.630	1.986	1.561	1.234
1.00	k	0.396	0.099	0.198	0.396	0.593	0.791	0.989	1.187
	ARL	250.76	29.38	11.78	4.21	2.13	1.36	1.11	1.03
	h	3.720	8.510	5.990	3.720	2.630	1.986	1.561	1.234
1.25	k	0.396	0.099	0.198	0.396	0.593	0.791	0.989	1.187
	ARL	22.00	26.23	11.00	3.99	2.03	1.33	1.10	1.03
	h	3.720	8.510	5.990	3.720	2.630	1.986	1.561	1.234
1.50	k	0.396	0.099	0.198	0.396	0.593	0.791	0.989	1.187
	ARL	15.73	23.18	10.17	3.76	1.94	1.31	1.09	1.03
	h	3.720	8.510	5.990	3.720	2.630	1.986	1.561	1.234
2.00	k	0.396	0.099	0.198	0.396	0.593	0.791	0.989	1.187
	ARL	10.03	18.16	8.62	3.35	1.81	1.27	1.09	1.02
	h	3.720	8.510	5.990	3.720	2.630	1.986	1.561	1.234
2.50	k	0.396	0.099	0.198	0.396	0.593	0.791	0.989	1.187
	ARL	7.49	14.57	7.34	3.01	1.71	1.25	1.08	1.02
	h	3.720	8.510	5.990	3.720	2.630	1.986	1.561	1.234
3.00	k	0.396	0.099	0.198	0.396	0.593	0.791	0.989	1.187
	ARL	6.10	12.02	6.34	2.76	1.64	1.23	1.08	1.02
	h	3.720	8.510	5.990	3.720	2.630	1.986	1.561	1.234
4.00	k	0.396	0.099	0.198	0.396	0.593	0.791	0.989	1.187
	ARL	4.66	8.79	4.97	2.41	1.54	1.20	1.07	1.02

Tables 7.3 and 7.4 give the optimal combinations of h and k for an in-control ARL fixed at 250 and the autoregressive parameter $\phi = 0.75$ with 80% of process variability due to variation in μ_t, again using equation (7.4), we get the correlation between adjacent observations as 0.6. We use the same procedure to calculate the ARL for these tables as for Tables 7.1 and 7.2. Tables 7.1 and 7.3 show the chart's performance for different shifts in the process mean and/or standard deviation, with shifts in the overall process standard deviation due to shift in σ_{α} and Tables 7.2 and 7.4 correspond to shifts in these parameters with shifts in the overall process

standard deviation due to shifts in σ_ε.

Comparing these tables, it can be seen that at low level of autocorrelation, the chart quickly detects small to moderate shifts in the mean and/or standard deviation than at high level of autocorrelation. For example, as can be seen in Table 7.2, when the level of autocorrelation is 0.25, a 0.5σ shift in the mean with a 1.5σ shift in the process standard deviation, with a standard deviation shift due to shift in $\sigma_{\sigma_\varepsilon}$ will on average be detected on the $10th$ sample. When the level of autocorrelation is 0.75, the same shifts will on average be detected on the $11th$ sample as can be seen in Table 7.4.

The scheme is slightly more sensitive to shifts in the standard deviation due to shifts in σ_ε than it is to shifts in the standard deviation resulting from shifts in σ_α. This is due to the fact that an increase in σ_α, increases the level of correlation between observations while an increase in σ_ε, decreases the level of correlation between observations. This is because the variance of μ_t increases with an increase in σ_α and thus the proportion of total process variability due to variation in the autocorrelated means, μ_t increases. For example if $\phi = 0.25$, $\sigma^2_{\varepsilon 0} = 0.2$ and $\sigma^2_{\alpha 0} = 0.75$. This gives $\sigma^2_\mu = 0.8$. Using equation (7.5), we get $\psi = 0.8$. This gives $\rho = 0.2$ from equation (7.4). If σ^2_ε increases to 0.5 while σ^2_α remains at its in-control value, using equation (7.3) we get $\sigma^2_X = 1.3$ and substituting into equations (7.4) and (7.5) we get $\rho = 0.16$ and $\psi = 0.62$ respectively. If σ^2_α increases to 1.00 while σ^2_ε remains at its in-control value, using the same equations, we get $\sigma^2_X = 1.27$ and $\sigma^2_\mu = 1.07$. This gives $\psi = 0.84$ and $\rho = 0.21$. Therefore an increase in σ_ε decreases the level of correlation (ρ) between adjacent observations while the opposite is true for an increase in σ_α.

Table 7.3: (k,h) combinations and the corresponding ARL for the MCAP chart, with $\phi = 0.75$ and $\psi = 0.8$ for shifts in the process standard deviation due to shift in σ_α .

$ARL_0 = 250$									
		a							
b	Parameter	0.00	0.25	0.50	1.00	1.50	2.00	2.50	3.00
1.00	h	3.720	8.510	6.000	3.720	2.633	1.995	1.570	1.246
	k	0.164	0.041	0.082	0.164	0.246	0.329	0.411	0.493
	ARL	250.14	29.47	11.96	4.51	2.56	1.78	1.42	1.23
1.25	h	3.720	8.510	6.000	3.720	2.633	1.995	1.570	1.246
	k	0.164	0.041	0.082	0.164	0.246	0.329	0.411	0.493
	ARL	27.32	27.99	11.61	4.44	2.53	1.77	1.42	1.23
1.50	h	3.720	8.510	6.000	3.720	2.633	1.995	1.570	1.246
	k	0.164	0.041	0.082	0.164	0.246	0.329	0.411	0.493
	ARL	21.80	26.34	11.21	4.35	2.50	1.76	1.42	1.23
2.00	h	3.720	8.510	6.000	3.720	2.633	1.995	1.570	1.246
	k	0.164	0.041	0.082	0.164	0.246	0.329	0.411	0.493
	ARL	14.99	22.95	10.31	4.15	2.43	1.75	1.42	1.23
2.50	h	3.720	8.510	6.000	3.720	2.633	1.995	1.570	1.246
	k	0.164	0.041	0.082	0.164	0.246	0.329	0.411	0.493
	ARL	11.25	19.82	9.38	3.93	2.37	1.73	1.42	1.23
3.00	h	3.720	8.510	6.000	3.720	2.633	1.995	1.570	1.246
	k	0.164	0.041	0.082	0.164	0.246	0.329	0.411	0.493
	ARL	8.99	17.16	8.51	3.72	2.31	1.72	1.41	1.23
4.00	h	3.720	8.510	6.000	3.720	2.633	1.995	1.570	1.246
	k	0.164	0.041	0.082	0.164	0.246	0.329	0.411	0.493
	ARL	6.53	13.20	7.05	3.36	2.20	1.69	1.41	1.23

Table 7.4: (k,h) combinations and the corresponding ARL for the MCAP chart, with $\phi = 0.75$ and $\psi = 0.8$ for shifts in the process standard deviation due to shift in σ_{ε}.

$ARL_0 = 250$									
		a							
b	Parameter	0.00	0.25	0.50	1.00	1.50	2.00	2.50	3.00
	h	3.720	8.510	6.000	3.720	2.633	1.995	1.570	1.246
1.00	k	0.164	0.041	0.082	0.164	0.246	0.329	0.411	0.493
	ARL	250.14	29.47	11.96	4.51	2.56	1.78	1.42	1.23
	h	3.720	8.510	6.000	3.720	2.633	1.995	1.570	1.246
1.25	k	0.164	0.041	0.082	0.164	0.246	0.329	0.411	0.493
	ARL	22.13	26.69	11.05	4.32	2.49	1.76	1.42	1.24
	h	3.720	8.510	6.000	3.720	2.633	1.995	1.570	1.246
1.50	k	0.164	0.041	0.082	0.164	0.246	0.329	0.411	0.493
	ARL	17.02	23.65	10.51	4.10	2.42	1.74	1.42	1.24
	h	3.720	8.510	6.000	3.720	2.633	1.995	1.570	1.246
2.00	k	0.164	0.041	0.082	0.164	0.246	0.329	0.411	0.493
	ARL	11.85	18.96	8.74	3.71	2.30	1.71	1.42	1.23
	h	3.720	8.510	6.000	3.720	2.633	1.995	1.570	1.246
2.50	k	0.164	0.041	0.082	0.164	0.246	0.329	0.411	0.493
	ARL	9.65	15.43	8.14	3.38	2.21	1.69	1.41	1.23
	h	3.720	8.510	6.000	3.720	2.633	1.995	1.570	1.246
3.00	k	0.164	0.041	0.082	0.164	0.246	0.329	0.411	0.493
	ARL	7.47	14.03	7.17	3.13	2.13	1.67	1.41	1.23
	h	3.720	8.510	6.000	3.720	2.633	1.995	1.570	1.246
4.00	k	0.164	0.041	0.082	0.164	0.246	0.329	0.411	0.493
	ARL	6.26	11.07	6.90	2.79	2.03	1.61	1.41	1.23

CUSUM charts discussed in the literature are designed to detect small shifts in the mean. The performance of these charts is then assessed for various shifts in the mean and variability separately. In Tables 7.5 and 7.6, we assess the performance of an MCAP chart which is designed to detect a 1σ shift in the residual means. This is accomplished by fixing k and h and then calculating the ARL's at various values of residual means and standard deviations. The tables shows that this chart is sensitive to small shifts in the mean and/or standard deviation particularly at low levels of autocorrelations.

Table 7.5: ARL's for the MCAP chart with $\phi = 0.25$, $\psi = 0.8$, $k = 0.396$ and $h = 3.720$.

Changes in σ_ε								
	a							
b	0.00	0.25	0.50	1.00	1.50	2.00	2.50	3.00
1.00	250.76	11.24	6.52	4.21	3.12	2.52	2.14	1.88
1.25	22.00	7.65	5.95	3.99	2.96	2.36	1.97	1.70
1.50	15.73	6.76	5.44	3.76	2.81	2.22	1.83	1.56
2.00	10.03	5.50	4.62	3.35	2.52	1.98	1.62	1.38
2.50	7.49	4.69	4.03	3.01	2.30	1.81	1.48	1.27
3.00	6.10	4.14	3.61	2.76	2.12	1.68	1.39	1.21
4.00	4.66	3.47	3.08	2.41	1.89	1.52	1.28	1.14
Changes in σ_α								
1.00	250.76	11.24	6.52	4.21	3.12	2.52	2.14	1.88
1.25	27.16	7.74	6.00	4.01	2.98	2.38	1.99	1.72
1.50	22.78	6.89	5.51	3.80	2.83	2.24	1.85	1.58
2.00	10.57	5.65	4.72	3.40	2.56	2.01	1.64	1.39
2.50	7.88	4.83	4.13	3.07	2.34	1.84	1.50	1.29
3.00	6.39	4.27	3.71	2.82	2.17	1.71	1.41	1.22
4.00	4.85	3.57	3.16	2.46	1.92	1.54	1.29	1.15

Table 7.6: ARL's for the MCAP chart with $\phi = 0.75$, $\psi = 0.8$, $k = 0.164$ and $h = 3.720$.

Changes in σ_ε								
	a							
b	0.00	0.25	0.50	1.00	1.50	2.00	2.50	3.00
1.00	250.14	17.95	7.79	4.61	3.59	3.03	2.69	2.45
1.25	22.13	7.63	6.14	4.40	3.50	2.96	2.62	2.39
1.50	17.02	7.06	5.75	4.19	3.39	2.88	2.55	2.32
2.00	11.85	6.36	5.12	3.78	3.15	2.72	2.41	2.18
2.50	9.65	5.58	4.45	3.46	2.94	2.57	2.29	2.07
3.00	7.47	5.06	4.00	3.29	2.77	2.44	2.18	1.97
4.00	6.26	4.14	3.56	3.01	2.51	2.24	2.02	1.84
Changes in σ_α								
1.00	250.14	17.95	7.79	4.61	3.59	3.03	2.69	2.45
1.25	27.32	8.38	6.53	4.53	3.56	3.01	2.66	2.43
1.50	21.80	7.83	6.24	4.44	3.51	2.98	2.63	2.40
2.00	14.99	6.84	5.69	4.23	3.41	2.90	2.56	2.33
2.50	11.25	6.04	5.18	4.01	3.29	2.82	2.49	2.26
3.00	8.99	5.41	4.75	3.79	3.16	2.73	2.42	2.19
4.00	6.53	4.53	4.09	3.42	2.93	2.56	2.28	2.06

7.6 Comparison with Other Charts

In this section, we compare this scheme with simultaneous charts for autocorrelated processes discussed in the literature. As stated before, the performance of control charts for monitoring a process is usually assessed using the ARL. The chart that has low ARL when the process has shifted and high ARL when the process is running at the target value is considered better than the one that has high out-of-control ARL and low in-control ARL. Most of the charts discussed in the literature are for monitoring shifts in the process mean and variability for autocorrelated observations using separate charts. We compare the MCAP chart with the combined Shewhart-EWMA chart for autocorrelated data proposed by Lu and Reynolds ([57]). The combined Shewhart-EWMA chart's ARL's were obtained from Table 3 and Table 4 of Lu and Reynolds ([57]). The combined Shewhart-EWMA charts were run by simultaneously running two control charts: one chart designed primarily to detect shifts in the mean, and the other chart designed primarily to detect shifts in the process variability. The decision rule is that a signal is given if either chart signals. The value of the correlation between μ_t and μ_{t-1} considered were 0.4 and 0.8 and the proportion of variation in the process attributed to variation in μ_t, ψ, were are 0.1 and 0.9.

Comparison of ARL's of these charts are provided in Tables 7.7, 7.8, 7.9 and 7.10. The two charts are comparable, with the MCAP chart performing better than the combined Shewhart-EWMA chart for small to moderate shifts in the process mean and/or standard deviation. This is particularly more evident at high levels of autocorrelation as can be seen in Tables 7.8 and 7.10. For example when $\phi = 0.8$ and $\psi = 0.1$ as shown in Table 7.8, a 1σ shift in the mean with a 2σ shift in the process variability, with an increase in the process variability due to increase in σ_ε^2 will on average be detected on the 5^{th} sample by the MCAP chart while a combined Shewhart-EWMA chart will on average detect these shifts on the 10^{th} sample. At high levels of correlations, the combined Shewhart-EWMA chart is highly affected by the level of autocorrelation while the effect of autocorrelation is not very strong for the MCAP chart. In fact when a high proportion of process variation is attributed to variability in the autocorrelated means, the combined Shewhart-EWMA chart is not good for detecting small shift for both low and high levels of autocorrelation. For example when 90% of process variability is due to variation in μ_t with the level of autocorrelation; $\phi = 0.8$, a 1σ shift in the mean is on average detected on the $83rd$ sample by the combined Shewhart-EWMA chart while the MCAP chart on average detects this shift on the $8th$ sample. For very large shifts in the process mean and/or standard deviation, the combined Shewhart-EWMA chart performs slightly better than the MCAP chart particularly at high level of correlations and when a high percentage of process variability is due to variations in the autocorrelated means.

This is because the Shewhart chart is specifically designed for monitoring large shifts in the process parameters. We therefore recommend the use of our MCAP charts for detecting small to moderate shifts in the process mean and/or variability. For detecting large shifts, we can use a combined Shewhart-MCAP chart as the Shewhart chart is very effective in detecting large shifts in the process parameters even in the presence of autocorrelation.

Table 7.7: Comparison of the MCAP chart with a combined Shewhart-EWMA chart with $\phi = 0.4$ and $\psi = 0.1$.

		a							
		0		1		2		3	
b	Changes	MCAP	Sh-EW	MCAP	Sh-EW	MCAP	Sh-EW	MCAP	Sh-EW
1	σ_ε^2	367.0	367.9	5.0	12.0	2.8	3.7	2.0	2.0
	σ_α^2	367.0	365.8	5.0	12.1	2.8	3.8	2.2	2.0
2	σ_ε^2	12.0	30.1	4.3	8.7	2.5	3.4	2.0	2.0
	σ_α^2	12.3	25.8	4.4	9.3	2.6	3.8	2.1	2.1
3	σ_ε^2	7.0	12.6	3.8	6.6	2.3	3.3	2.0	2.0
	σ_α^2	7.1	12.0	3.8	7.4	2.4	3.7	2.0	2.2
10	σ_ε^2	2.9	3.1	2.5	2.8	2.3	2.4	2.0	2.0
	σ_α^2	2.9	3.3	2.5	3.1	2.3	2.6	2.0	2.2

MCAP: Max-CUSUM chart for autocorrelated process.
Sh-EW: Combined Shewhart-EWMA charts of residuals.

Table 7.8: Comparison of the MCAP chart with a combined Shewhart-EWMA chart with $\phi = 0.8$ and $\psi = 0.1$.

		a							
		0		1		2		3	
b	Changes	MCAP	Sh-EW	MCAP	Sh-EW	MCAP	Sh-EW	MCAP	Sh-EW
1	σ_ε^2	367.6	364.4	5.6	16.8	3.1	4.4	2.4	2.2
	σ_α^2	367.6	367.0	5.6	16.9	3.1	4.1	2.4	2.2
2	σ_ε^2	12.9	30.7	4.7	10.2	3.1	3.7	2.4	2.0
	σ_α^2	15.3	24.9	4.9	13.3	3.1	4.9	2.4	2.2
3	σ_ε^2	7.2	12.3	4.0	7.2	3.0	3.4	2.3	2.0
	σ_α^2	8.3	13.9	4.2	10.4	3.0	5.0	2.3	2.5
10	σ_ε^2	2.9	3.0	2.6	2.8	2.4	2.4	2.2	1.9
	σ_α^2	3.1	5.0	2.7	4.6	2.4	3.7	2.2	2.7

MCAP: Max-CUSUM chart for autocorrelated process.
Sh-EW: Combined Shewhart-EWMA charts of residuals.

Table 7.9: Comparison of the MCAP chart with a combined Shewhart-EWMA chart with $\phi = 0.4$ and $\psi = 0.9$.

		a							
		0		1		2		3	
b	Changes	MCAP	Sh-EW	MCAP	Sh-EW	MCAP	Sh-EW	MCAP	Sh-EW
1	σ_ε^2	370.8	368.9	6.0	23.3	3.2	5.4	2.5	2.3
	σ_α^2	370.8	370.9	6.0	22.8	3.2	5.4	2.5	2.3
2	σ_ε^2	12.6	26.0	4.9	11.2	3.2	4.2	2.5	2.1
	σ_α^2	15.2	31.2	5.1	12.5	3.2	4.8	2.5	2.3
3	σ_ε^2	6.9	10.6	4.1	7.0	3.1	3.6	2.4	2.1
	σ_α^2	8.1	12.9	4.3	8.3	3.1	4.2	2.4	2.3
10	σ_ε^2	2.9	2.9	2.6	2.6	2.4	2.3	2.2	1.9
	σ_α^2	3.0	3.2	2.7	3.0	2.5	2.6	2.3	2.1

MCAP: Max-CUSUM chart for autocorrelated process.
Sh-EW: Combined Shewhart-EWMA charts of residuals.

Table 7.10: Comparison of the MCAP chart with a combined Shewhart-EWMA chart with $\phi = 0.8$ and $\psi = 0.9$.

		a							
		0		1		2		3	
b	Changes	MCAP	Sh-EW	MCAP	Sh-EW	MCAP	Sh-EW	MCAP	Sh-EW
1	σ_ε^2	374.5	374.4	7.7	82.1	3.8	12.1	2.8	1.8
	σ_α^2	374.5	375.5	7.7	83.4	3.8	12.1	2.8	1.8
2	σ_ε^2	12.5	10.1	5.6	7.6	3.7	3.7	2.8	1.7
	σ_α^2	37.2	38.5	6.9	22.4	3.8	7.6	2.8	2.1
3	σ_ε^2	6.5	5.0	4.3	4.2	3.3	2.7	2.7	1.7
	σ_α^2	16.5	16.1	6.0	12.1	3.7	5.8	2.7	2.3
10	σ_ε^2	2.8	2.1	2.6	2.0	2.4	1.8	2.3	1.5
	σ_α^2	3.8	3.7	3.2	3.4	2.8	2.7	2.6	2.1

MCAP: Max-CUSUM chart for autocorrelated process.
Sh-EW: Combined Shewhart-EWMA charts of residuals.

7.7 Charting Procedures

Since the residuals are independent normal random variables when the process is in control, the charting procedure for the Max-CUSUM chart for Autocorrelated Process is similar to that of the Max-CUSUM for uncorrelated data. The successive CUSUM values, M_i's are plotted against the sample numbers. If a point plots below the decision interval, the process is said to be in-control and the point is plotted as a dot. An out-of-control signal is given if any point plots above the decision interval and is plotted as one of the characters defined below. The MCAP chart is a combination of two two-sided standard CUSUM charts. Use the following procedure to construct this chart:

1. Fit the time series model to the data.

2. Specify the following parameters: the in-control or target value of the mean ξ_0 and the in-control or target value of the standard deviation $\sigma_{\gamma 0}$.

3. If ξ_0 is not known, use the grand average $\bar{\bar{\xi}}$ of the data to estimate it, where $\bar{\bar{\xi}} = (\bar{\xi}_1 + ... + \bar{\xi}_m)/m$. If $\sigma_{\gamma 0}$ is unknown, use $\bar{R}/d_2$ or $\bar{S}/c_4$ to estimate it, where $\bar{R} = (R_1 + ... + R_m)/m$ is the average of the sample ranges and $\bar{S} = (S_1 + ... + S_m)/m$ is the average of the sample standard errors, $S_i = \sqrt{MSE_i}$ and $d_2 = d_2(\bar{n})$ and $c_4 = c_2(\bar{n})$ are statistically determined constants with $\bar{n} = (n_1 + ... + n_m)/m$.

4. For each sample, compute Z_i and Y_i.

5. To detect specified changes in the process mean and standard deviation, choose an optimal $(h,\ k)$ combination and calculate C_i^+, C_i^-, S_i^+ and S_i^-.

6. Compute the M_i's and compare them with h; the decision interval.

7. Denote the sample points with a dot and plot them against the sample number if $M_i \leq h$.

8. If any of the M_i's are greater than the decision interval, h, the following plotting characters should be used to show the direction as well as the statistic that is plotting above the interval.

   (i) If $C_i^+ > h$, plot $C+$. This shows an increase in the process mean.

   (ii) If $C_i^- > h$, plot $C-$. This indicates a decrease in the process mean.

   (iii) If $S_i^+ > h$, plot $S+$. This shows an increase in the process standard deviation.

   (iv) If $S_i^- > h$, plot $S-$. This shows a decrease in the process standard deviation.

   (v) If both $C_i^+ > h$, and $S_i^+ > h$, plot $B++$. This indicates an increase in both the mean and standard deviation of the process.

(vi) If $C_i^+ > h$ and $S_i^- > h$, plot $B+-$. This indicates an increase in the mean and a decrease in the standard deviation of the process.

(vii) If $C_i^- > h$ and $S_i^+ > h$, plot $B-+$. This indicates a decrease in the mean and an increase in the standard deviation of the process.

(viii) If $C_i^- > h$ and $S_i^- > h$, plot $B--$. This shows a decrease in both mean and standard deviation of the process.

9. Investigate the cause(s) of shift for each out-of-control point in the chart and carry out the remedial measure needed to bring the process back into an in-control state.

7.8 An Example

To provide a visual picture of how the MCAP chart responds to various kinds of process changes, a set of simulated data is used. Specific process changes are introduced into the data, and the chart is plotted to monitor these changes in the parameters. The data set was generated using the first order autoregressive plus random error models given in equation (7.1) and equation (7.2). The data are simulated by simulating sequences of α_t's and ε_t's.

For a fixed sequence of α_t's and ε_t's, a shift in σ_α can be simulated by multiplying α_t in equation (7.2) by a constant. A change in σ_ε can be simulated by multiplying ε_t in equation (7.1) by a constant, and a change in the mean is simulated by adding a constant to the generated observations. This approach is discussed by Lu and Reynolds ([57]). This procedure allows different types of process changes to be investigated on the same basic sequence of α_t's and ε_t's. In this example, we assume the autoregressive parameter ϕ remain constant.

We simulated 100 observations for a process following models in equation (7.1) and equation (7.2), with the following parameters: $\xi = 0$, $\phi = 0.75$, $\sigma_\alpha = 0.59$, and $\sigma_\varepsilon = 0.5$. These give $\sigma_X = 1.02$ and $\psi = 0.76$. This implies that 76% of variability in the process is due to variation in μ_t and that the correlation between the adjacent observations is $\rho = \phi\psi = 0.57$. Using equations (7.7) and (7.8), the corresponding parameters in the ARMA(1,1) model in equation (7.6) are $\theta = 0.27$ and $\sigma_\gamma = 0.83$.

The MCAP chart for these simulated observations is drawn in Figure 7.1. All points fall within the acceptable region, thus the process simulated is in control. The chart's parameters are for an in control ARL of 370 runs. The chart parameters are for detecting a 1σ increase in the parameters. They are calculated using the procedure used to derive Tables 7.1 to 7.4, this procedure takes the correlation between adjacent observations into consideration.

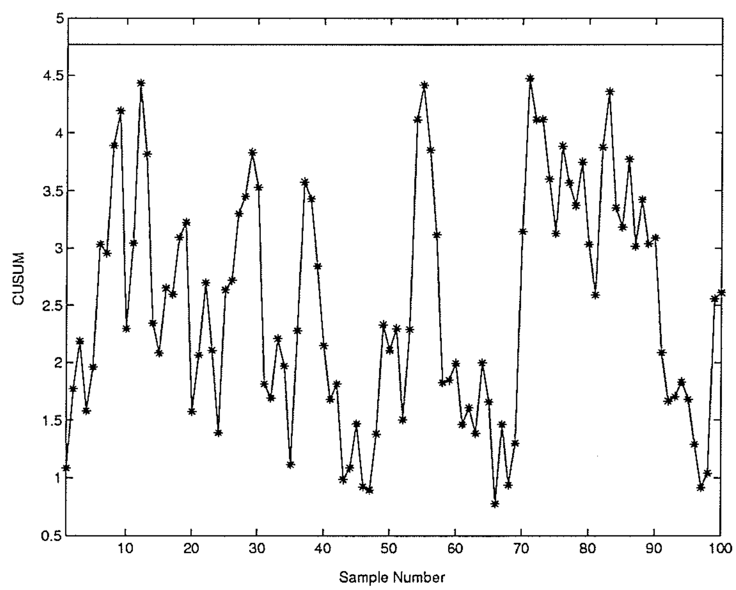

Figure 7.1: The MCAP chart for in control simulated values.

Figure 7.2 shows the performance of this chart for a shift in the process standard deviation that is due to an increase in σ_α. Suppose that, due to a special cause immediately after observation 60, σ_α increases from 0.59 to 0.97 and stays at this value for the next 40 observations. We assume that other parameters in the model remain at their in control values. This increase in σ_α results in an increase in the process standard deviation, σ_X from 1.02 to 1.56. This corresponds to a 52% increase in the process standard deviation. This also leads to an increase in ψ from 0.76 to 0.90 and an increase in the correlation between adjacent observations from 0.57 to 0.68. Therefore 90% of variation in the process is due to variation in μ_t. The increase in σ_α for the last 40 observations was accomplished by multiplying the last 40 values of α_t by the factor $0.97/0.59 = 1.644$.

When applying this to the simulated data the shift in the standard deviation is signalled at the 86^{th} observation. The delay in detecting this increase is caused by an increase in the correlation between observations which was caused by an increase in σ_α as discussed above.

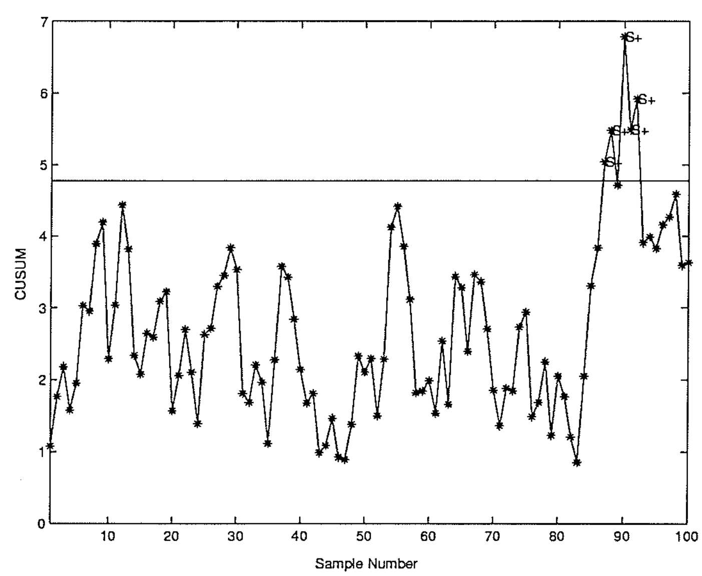

Figure 7.2: The MCAP chart for shift in the variability due to shift σ_α.

Figure 7.3 shows the performance of the MCAP chart for an increase in the process variability due to an increase in σ_ε. Due to some assignable causes, σ_ε increases from its in control value of 0.5 to 1.00 immediately after observation 60 and remains there for the rest of the process, and the rest of the process parameters remain at their in control values. This increase will result in an increase in the process standard deviation from 1.02 to 1.34 (a 30% increase). Unlike the increase in σ_α, the increase in σ_ε results in a decrease in the correlation between adjacent observations from 0.57 to 0.33, the value of the proportion of total process variability that is due to the variability in μ_t also decreases from 76% to 44%.

The increase in σ_ε for the last 40 observations was accomplished by multiplying the last 40 observations of the simulated ε_t values by $1/0.5 = 2.00$. This increase in the process standard deviation due to an increase in σ_ε is detected on the 64^{th} observation. Though this shift corresponds to only 30% increase in the process standard deviation, it is more quickly detected than for an increase in σ_α, where the process standard deviation was increased by 52%. This is due to the fact that an increase in σ_ε results in a decrease in the correlation between adjacent observations while an increase in σ_α increases this correlation. In fact, some values plotted as an increase in both mean and standard deviation, this phenomenon is discussed by Shewhart as the basic reason for always having to run an $\bar{X}$ chart with either an S or R chart as the signal of an $\bar{X}$ chart may be due to change in the process variability rather than changes in the process mean.

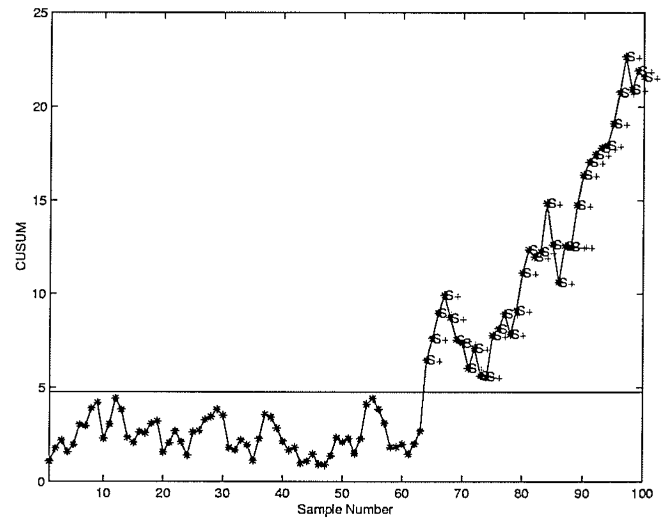

Figure 7.3: The MCAP chart for shift the variability due to shift in σ_ε.

A shift in the mean of the last 40 observations is shown in Figure 7.4. This is accomplished by adding 1 to the last 40 observations of the simulated values in Figure 7.1, for shift in the process mean from 0 to 1. We assume the variance of the process remains at its in control value. This increase in the mean is signalled for the first time at the 68^{th} observation.

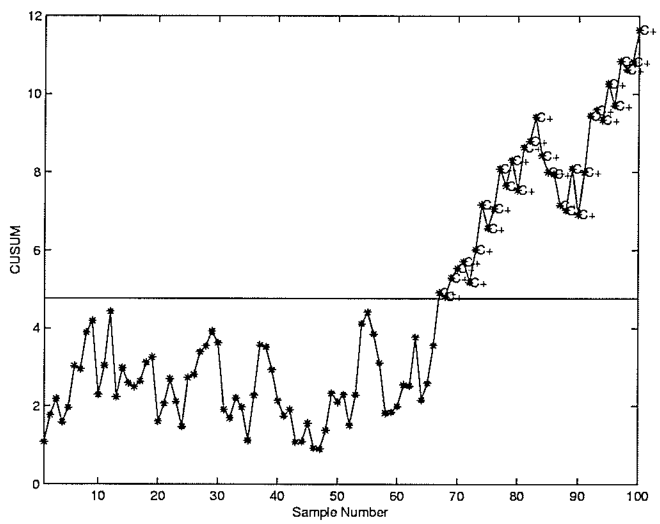

Figure 7.4: The MCAP chart for shift in the process mean.

Next we consider a simultaneous increase in the process mean and standard deviation. In Figure 7.5, we apply the MCAP chart to investigate an increase in the mean from 0 to 1 and an increase in σ_α from 0.59 to 0.97. This is accomplished by multiplying the last 40 simulated values of α_t by 1.644 as in Figure 7.2, and then adding 1 to the last 40 observations of the new process observation X_t. This is for an increase in the mean and σ_α of the last 40 observations. These shifts are signalled on the 73^{rd} observation which signals an increase in the mean only and the 76^{th} observation which signals an increase in both mean and standard deviation.

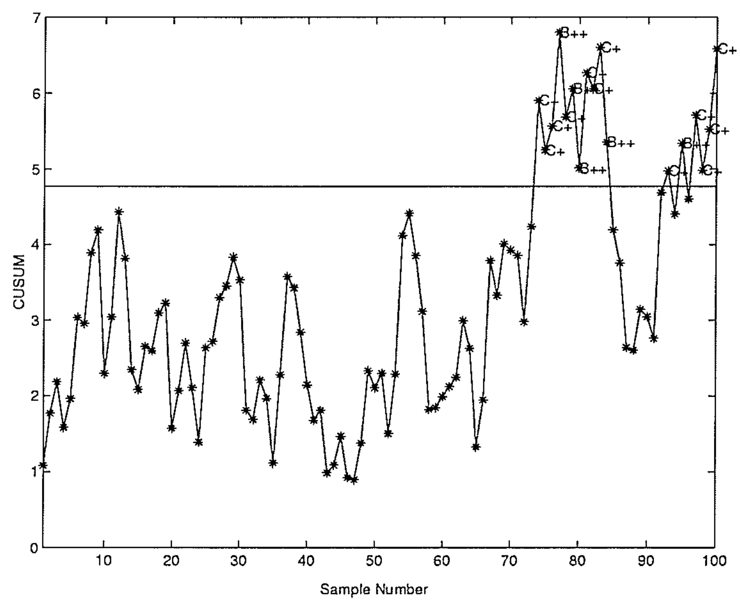

Figure 7.5: The MCAP chart for shift the mean and variability due to shift in σ_α.

An increase in both mean and σ_ε is shown in Figure 7.6. We consider an increase in mean from 0 to 1 and an increase in σ_ε from 0.5 to 1. Assume that due to some special causes, these shifts occur immediately after the 60^{th} observation and remain in effect for the rest of the process. We simulate these shifts by first multiplying the last 40 values of ε_t by 2.00 as in Figure 7.3, then we add 1 to the last 40 observations of the new process value X_t.

The chart signals a shift for the first time on the 63^{th} observation for an increase in the mean and on the 64^{th} observation for an increase in the standard deviation. It signals an increase in both parameters for the first time on the 67^{th} observation. Therefore a combination of shifts in the mean and σ_ε is more quickly detected than a combination of shifts in the mean and σ_α. This is due to variance components' effect on the level of autocorrelation.

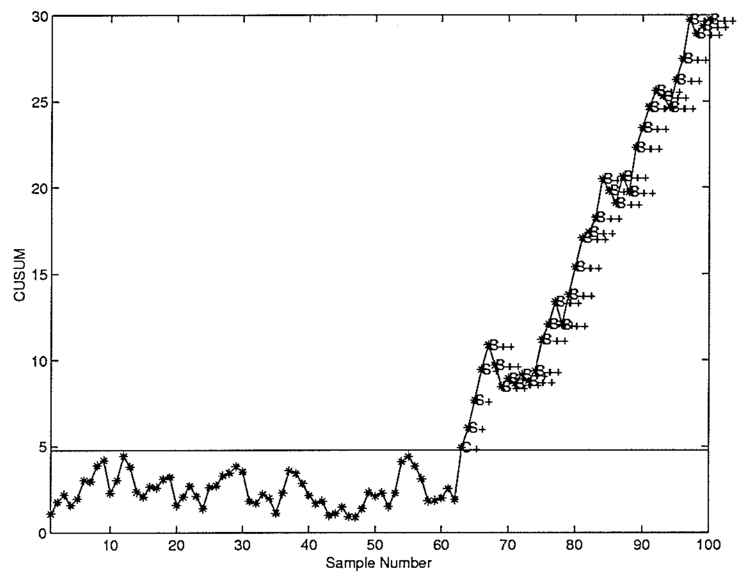

Figure 7.6: The MCAP chart for shift the mean and variability due to shift in σ_ε.

7.9 Conclusions and Recommendations

Although it is very difficult to draw general conclusions based on a single set of data corresponding to one set of process parameters, the ARL results given in this chapter together with charts plotted in Figures 7.1 to 7.6, allow some conclusions to be drawn.

The results reported here have shown that correlation among observations from a process can have significant effect on the performance of control charts. Computer simulation of individual data from a first order autoregressive plus a random error model was used to show a pictorial display of the MCAP chart. The monitoring problem in this model is very complicated as it requires more parameters than for the case when the observations are independent. We have shown how a change in any one of the two components of residual variances and the process mean impact on the overall process performance.

However, in many applications, a change in the process may be because of a combination of changes of these parameters. Therefore it becomes very difficult to diagnose the variance component that has caused the process variability to change. It might be necessary to estimate the residual variance at the point of the shift to see which component has shifted. In a process in which material is processed in batches, the process variability can be monitored by monitoring within-batch variability represented by σ_ε and between batch variability associated with σ_α. An example of such processes is a chemical process where yields are recorded in batches over time. Then σ_ε measures variability between observations in a given batch while σ_α measures variability between batches.

The MCAP chart which simultaneously monitors the process mean and standard deviation performs better than its competitors at low to moderate shifts in the process parameters and this makes it more appropriate in today's industrial application as goods are produced in large quantities within a short period of time. Furthermore, due to improvement in the production technology, low rates of defective items are observed and the MCAP chart which quickly detects small process shifts becomes more valuable in such situations. The MCAP chart for residuals is simple to construct as it uses the standard CUSUM chart parameters because residuals are independent when the process is in control, therefore, we recommend this chart for autocorrelated data. The only adjustment required is to modify the reference value to take autocorrelation among observations into consideration when calculating the ARL. Standard time series procedure discussed in Box, Jenkins, and Reinsel ([7]) can be used to fit the model and calculate the residuals.

Chapter 8

Max-Chart for Autocorrelated Processes

8.1 Introduction

In this chapter, we propose a Max-chart for autocorrelated processes. The Max chart (Chen and Cheng [21]) was proposed under the assumption that a process being monitored will produce measurements that are independent and identically distributed over time when only inherent sources of variability are present in the system. However, the independence assumption is often not reasonable for some process operations such as mining, as autocorrelation amongst the observations becomes an inherent characteristic in mineral deposit where ore grades are spatially distributed (Samanta and Bhattacherjee [87]). Autocorrelation can have very serious effects on the properties of the Shewhart control charts.

As in chapter 7, we assume that the measurements of a quality characteristic are generated by a first order autoregressive plus a random error model. Under this assumption, we propose a Shewhart-type single control chart for autocorrelated process by monitoring the residuals from the fitted time series model. We will use the design procedure developed for the Max chart by Chen and Cheng ([21]) and assume a change in the process variability is due to changes in variability of normal random errors associated with the autocorrelated observations X_t's, and changes in variability due to changes in variability of the normal random errors associated with the autocorrelated means μ_t's. We show that when the process is in control and the time series model fitted is the true model, the residuals are independently and identically distributed normal random variables. When there is a shift in the process location and spread however, the residuals are autocorrelated normal random variables.

8.2 The New Control Chart

We propose a new single Shewhart-type control chart for residuals in this section. Again we will assume that the control chart is used to detect a shift in the process mean and/or variability of a sequence of observations generated by an AR(1) plus a random error term given in model in equations (7.1) and (7.2). Under the same assumptions as for the Max-CUSUM chart, the formulas for Z_i and Y_i in this chapter are defined as in equations (7.18) and (7.19). (see sections 7.3 and 7.4 for details). To construct a single Shewhart-type control chart, we define a new statistic M_i as

$$M_i = \max[|Z_i|, |Y_i|] \tag{8.1}$$

When the process is in control, Z_i and Y_i follow a standard normal distribution. If the process has gone out-of-control, i.e, either the process mean and/or standard deviation have shifted due to the presence of some special causes, the M_i's will be plotted outside the control limits, otherwise the process is in control. Due to nonnegative values of M_i, we plot only the upper control limit for this chart, and consider the process to be out-of-control if an M_i value is plotted above the upper control limit. Because we use the maximum of the two statistics, we call this proposed single chart a Max-chart for Autocorrelated data.

8.3 Design of a Max-chart for Autocorrelated Data

To compute the control limits for this chart, we need to find the distribution of M_i. Because Z_i and Y_i are independent when the process is in control,

$$F(x; n_i, a, b) = P(M_i \leq x) = P(|Z_i| \leq x, |Y_i| \leq x)$$

$$= P(|Z_i| \leq x)P(|Y_i| \leq x)$$

When the process is in-control, $a = 0$ and $b = 1$, the distribution of M_i becomes

$$F(x; n_i, 0, 1) = \{\Phi(x) - \Phi(-x)\}^2 = P(\chi_1^2 \leq x^2)^2. \tag{8.2}$$

As shown in the Max-chart (Chen and Cheng [21]), for $F(x; n_i, 0, 1) = 1 - \alpha$ to hold, we must have $x = \left(\chi^2_{\sqrt{1-\alpha},1}\right)^{1/2}$. The center line and the upper control limits for the proposed chart are them determined for different probabilities of type I error. The center line and upper control limits for the Max-chart for autocorrelated data are shown in Table 8.1.

Table 8.1: Center line (CL) and upper control limits (UCL) of the Max-chart for autocorrelated data for various values of type I error probability α

α	0.5000	α	0.0054	0.004	0.0027	0.00135
CL	1.05176	UCL	2.9995	3.0899	3.2049	3.3975

We assess the performance of the Max-chart for autocorrelated data using the in-control ARL of 250 with a corresponding 3.09σ upper control limit for different sample sizes and autocorrelation structures. For various changes in the process mean alone, in the process standard deviation alone, and in both mean and standard deviation, we calculated the ARL for various sample sizes in Tables 8.2 to 8.5. Since there is no direct way to compute the ARL, each ARL value is obtained using 10,000 simulated values. We consider the case, where 80% of process variation is due to variability in the mean at time t, μ_t at different levels of autocorrelation. This scheme becomes more sensitive as the sample size increases as can be seen for sample sizes of 4 and 6 observations. Comparison of Tables 8.2 and 8.3 shows that, at low levels of autocorrelation, the chart is more sensitive to both small and large shifts in both process mean and standard deviation. It is however, more sensitive to changes in process variability that is due to changes in σ_ε than it is to changes due to changes in σ_α. In Tables 8.4 and 8.5, we investigate the performance of this chart at high level of autocorrelation. It can be seen that, autocorrelation in the process has a negative effect on the performance of this control chart. Shifts in both process means and standard deviations are not quickly detected when compared to the case of independent observations. This is particularly evident for small shifts in the process parameters.

A change in the process variance σ_X^2 can occur as a result of changes in ϕ, σ_ε^2 and σ_α^2. It can be seen in equations (7.4) and (7.5) that an increase in process variability due to increase in σ_ε^2, decreases the level of autocorrelations between adjacent observations, while an increase in variability due to increase in σ_α^2 results in an increase in the level of autocorrelation. Therefore, when the level of autocorrelation is high as in Tables 8.4 and 8.5, an increase in σ_α results in an increase in the level of correlation between adjacent values. This makes the chart less effective in detecting shifts in the process as only a small fraction of the shift in the process mean is transferred to the residual mean as can be deduced from equation (7.12).

However even at high level of correlation if both mean and standard deviation shift with shifts in the process standard deviation resulting from shifts in σ_ε, the Max-chart quickly detects these shifts as compared to the case when the process standard deviation shifts are due to shifts in σ_α because, as stated earlier, an increase in σ_ε results in a decrease in the correlation between observations. For example if we take a sample of $n = 4$ observations with $\phi = 0.75$, a 1σ increase in the process mean with a 1.5σ increase in the process standard deviation with variability increasing due to increase in σ_ε is detected on average on the 8^{th} sample while the same shifts will be expected to be detected on the 23^{rd} sample if the process variability increased due to increase in σ_α.

Table 8.2: ARL's for the Max-chart for autocorrelated data for shifts in σ_α with in-control $ARL_0 = 250$ with $\psi = 0.8$ and $\phi = 0.25$

		$\phi = 0.25$							
		a							
n	b	0.00	0.25	0.50	1.00	1.50	2.00	2.50	3.00
	1.00	250.05	142.86	78.13	13.77	4.19	1.88	1.26	1.05
	1.25	39.22	32.05	20.49	8.19	3.41	1.87	1.26	1.05
4	1.50	10.84	10.07	8.37	4.95	2.89	1.83	1.25	1.04
	2.00	3.16	3.07	2.89	2.46	1.94	1.59	1.23	1.04
	2.50	1.85	1.80	1.80	1.69	1.51	1.39	1.23	1.04
	3.00	1.44	1.44	1.43	1.39	1.33	1.26	1.19	1.01
	1.00	250.05	111.11	49.26	8.19	2.32	1.32	1.08	1.03
	1.25	28.74	23.64	15.60	5.22	2.18	1.31	1.05	1.01
6	1.50	7.86	7.32	6.24	3.47	1.99	1.28	1.04	1.01
	2.00	2.29	2.25	2.17	1.82	1.50	1.28	1.03	1.01
	2.50	1.45	1.43	1.40	1.34	1.24	1.17	1.03	1.01
	3.00	1.25	1.25	1.24	1.20	1.16	1.12	1.03	1.01

Table 8.3: ARL's for the Max-chart for autocorrelated data for shifts in σ_ε with in-control $ARL_0 = 250$ with $\psi = 0.8$ and $\phi = 0.25$

$\phi = 0.25$									
		a							
n	b	0.00	0.25	0.50	1.00	1.50	2.00	2.50	3.00
4	1.00	250.05	140.85	77.52	13.46	4.17	1.89	1.25	1.05
	1.25	29.94	29.07	20.24	7.72	3.35	1.87	1.21	1.04
	1.50	9.49	8.89	6.84	4.55	2.73	1.81	1.20	1.04
	2.00	2.78	2.75	2.63	2.30	1.87	1.56	1.17	1.03
	2.50	1.71	1.70	1.68	1.58	1.48	1.35	1.17	1.03
	3.00	1.38	1.39	1.38	1.35	1.29	1.23	1.14	1.02
6	1.00	250.05	111.03	49.00	8.01	2.20	1.29	1.21	1.04
	1.25	24.10	23.26	14.66	5.19	2.16	1.25	1.18	1.04
	1.50	5.04	4.99	4.44	2.89	1.85	1.23	1.13	1.03
	2.00	2.00	1.97	1.93	1.70	1.44	1.22	1.12	1.03
	2.50	1.33	1.33	1.33	1.28	1.20	1.14	1.10	1.01
	3.00	1.23	1.23	1.23	1.20	1.16	1.13	1.09	1.01

Table 8.4: ARL's for the Max-chart for autocorrelated data for shifts in σ_α with in-control $ARL_0 = 250$ with $\psi = 0.8$ and $\phi = 0.75$

$\phi = 0.75$									
		a							
n	b	0.00	0.25	0.50	1.00	1.50	2.00	2.50	3.00
4	1.00	250.05	202.03	196.08	112.36	51.02	23.75	13.40	7.32
	1.25	89.29	76.92	66.67	45.54	25.57	15.86	9.96	6.46
	1.50	33.33	28.82	26.17	22.67	16.00	10.12	7.07	4.91
	2.00	7.98	7.94	7.84	7.41	6.16	5.05	4.47	3.39
	2.50	3.71	3.65	3.63	3.46	3.29	2.94	2.71	2.43
	3.00	2.29	2.29	2.27	2.27	2.14	2.08	1.97	1.86
6	1.00	250.05	188.68	175.44	90.91	30.30	13.00	7.06	4.05
	1.25	71.94	69.44	59.88	38.46	19.57	9.61	5.73	3.56
	1.50	26.74	25.25	22.99	17.76	11.25	7.03	4.71	3.21
	2.00	5.89	5.83	5.75	4.98	4.40	3.63	2.95	2.31
	2.50	2.68	2.64	2.62	2.59	2.36	2.17	1.99	1.79
	3.00	1.71	1.71	1.71	1.68	1.65	1.59	1.52	1.45

Table 8.5: ARL's for the Max-chart for autocorrelated data for shifts in σ_ε with in-control $ARL_0 = 250$ with $\psi = 0.8$ and $\phi = 0.75$

		$\phi = 0.75$							
		a							
n	b	0.00	0.25	0.50	1.00	1.50	2.00	2.50	3.00
4	1.00	250.05	204.04	196.00	112.21	51.4	23.63	13.11	7.22
	1.25	30.49	30.13	28.65	20.92	15.08	10.62	7.17	4.91
	1.50	8.68	8.71	8.24	7.66	6.68	5.27	4.31	3.46
	2.00	2.77	2.72	2.72	2.63	2.48	2.33	2.20	2.04
	2.50	1.70	1.69	1.68	1.66	1.63	1.58	1.56	1.53
	3.00	1.39	1.39	1.38	1.38	1.36	1.36	1.34	1.31
6	1.00	250.05	186.23	175.00	90.03	30.45	12.91	6.93	3.90
	1.25	25.13	24.39	21.93	16.05	11.36	6.89	4.68	3.10
	1.50	6.36	6.31	6.15	5.54	4.39	3.74	2.99	2.49
	2.00	2.02	2.00	1.98	1.96	1.87	1.77	1.66	1.59
	2.50	1.33	1.32	1.32	1.32	1.30	1.29	1.25	1.23
	3.00	1.24	1.23	1.23	1.23	1.21	1.21	1.20	1.17

8.4 Comparison with Other Procedures

In this section, we compare the Max-chart for autocorrelated data with the simultaneous residual Shewhart chart proposed by Lu and Reynolds ([57]). These Shewhart residual charts were designed to detect simultaneous shifts in the process mean and variance. Comparisons are based on the out-of-control ARL in Tables 8.6 to 8.9. Lu and Reynolds ([57]) proposed a procedure whereby, two residual Shewhart control charts, one for monitoring the process mean and another for monitoring the process variability are run concurrently. The decision rule is that, a signal is given if either chart signals an out-of-control state. For comparison purposes, the control limits for these charts were adjusted so that the in-control ARL is fixed at 370.

The Max-chart for autocorrelated processes and simultaneous residual Shewhart chart are more effective in detecting shifts in the process mean and variability when the shifts in the process variability are due to shifts in σ_ε^2 than they are for shifts in the process variability due to shifts in σ_α^2. When the proportion of total variation attributed to variability in the autocorrelated means is high, the two charts are less effective in detecting shifts in the process parameters as compared to the case when the proportion of process variability due to variation in the autocorrelated means is small. The Max-chart is more effective than the simultaneous Shewhart chart in detecting shifts in the mean alone, standard deviation alone and simultaneous shifts in both mean and standard deviation at both low and high levels of autocorrelation.

In addition to detecting the shifts in the process parameters more quickly than the Shewhart chart, the Max-chart has an added advantage of using a single variable to monitor both process mean and standard deviation in the same chart while the simultaneous Shewhart chart requires plotting two variables in the same chart.

Table 8.6: Comparison of the Max-chart ARL against a simultaneous Shewhart chart ARL with $\phi = 0.4$ and $\psi = 0.1$.

		a							
		0		1		2		3	
b	Changes	Max	She	Max	She	Max	She	Max	She
1	σ_ε^2	370.4	371.7	18.5	49.6	2.0	7.2	1.1	2.2
	σ_α^2	370.4	370.0	18.5	50.1	2.0	7.3	1.1	2.1
2	σ_ε^2	3.1	29.1	2.4	13.3	1.6	4.5	1.2	2.1
	σ_α^2	3.3	32.2	2.5	14.4	1.6	5.1	1.2	2.3
3	σ_ε^2	1.5	12.0	1.4	7.6	1.3	3.7	1.1	2.1
	σ_α^2	1.5	13.0	1.5	8.9	1.3	4.3	1.2	2.3
10	σ_ε^2	1.3	2.9	1.3	2.7	1.3	2.4	1.2	1.9
	σ_α^2	1.3	3.1	1.3	3.0	1.3	2.5	1.3	2.1

Max: Max-chart for autocorrelated process.
She: Simultaneous residual Shewhart chart.

Table 8.7: Comparison of the Max-chart ARL against a simultaneous Shewhart chart ARL with $\phi = 0.4$ and $\psi = 0.9$.

		a							
		0		1		2		3	
b	Changes	Max	She	Max	She	Max	She	Max	She
1	σ_ε^2	370.0	370.3	40.1	96.5	3.8	17.2	1.4	3.4
	σ_α^2	370.0	369.9	40.1	96.6	3.9	17.2	1.4	3.4
2	σ_ε^2	2.8	21.9	2.5	13.7	1.8	5.7	1.4	2.4
	σ_α^2	3.9	30.6	3.3	18.0	2.1	7.2	1.4	2.8
3	σ_ε^2	1.4	9.2	1.4	7.2	1.3	4.1	1.2	2.2
	σ_α^2	1.6	12.4	1.5	9.4	1.4	4.9	1.2	2.6
10	σ_ε^2	1.3	2.6	1.3	2.5	1.3	2.2	1.3	1.8
	σ_α^2	1.3	3.0	1.3	2.8	1.3	2.5	1.2	2.1

Max: Max-chart for autocorrelated process.
She: Simultaneous residual Shewhart chart.

Table 8.8: Comparison of the Max-chart ARL against a simultaneous Shewhart chart ARL with $\phi = 0.8$ and $\psi = 0.1$.

		a							
		0		1		2		3	
b	Changes	Max	She	Max	She	Max	She	Max	She
1	σ_ε^2	370.0	370.2	23.6	78.5	2.4	11.6	1.1	2.8
	σ_α^2	370.0	369.5	23.6	78.3	2.5	11.8	1.1	2.8
2	σ_ε^2	3.1	28.1	2.5	15.1	1.7	5.2	1.3	2.2
	σ_α^2	4.4	44.6	3.3	25.1	1.9	8.6	1.3	2.9
3	σ_ε^2	1.5	11.3	1.4	8.1	1.3	3.9	1.2	2.1
	σ_α^2	1.7	20.1	1.6	15.2	1.4	7.2	1.2	3.0
10	σ_ε^2	1.3	2.8	1.3	2.7	1.3	2.3	1.2	1.9
	σ_α^2	1.3	5.2	1.3	4.9	1.3	3.9	1.3	2.8

Max: Max-chart for autocorrelated process.
She: Simultaneous residual Shewhart chart.

Table 8.9: Comparison of the Max-chart ARL against a simultaneous Shewhart chart ARL with $\phi = 0.8$ and $\psi = 0.9$.

		a							
		0		1		2		3	
b	Changes	Max	She	Max	She	Max	She	Max	She
1	σ_ε^2	370.0	369.9	171.6	217.0	69.3	51.1	24.6	4.5
	σ_α^2	370.3	370.4	172.4	207.7	70.4	50.5	24.9	4.5
2	σ_ε^2	2.2	8.3	2.2	7.1	2.0	3.9	2.0	1.8
	σ_α^2	14.3	40.6	12.6	30.3	9.6	12.6	6.4	3.0
3	σ_ε^2	1.3	4.5	1.3	4.0	1.3	2.7	1.3	1.7
	σ_α^2	3.1	16.6	3.1	13.7	2.9	7.1	2.6	2.7
10	σ_ε^2	1.2	2.0	1.2	1.9	1.2	1.7	1.2	1.5
	σ_α^2	1.3	3.5	1.3	3.3	1.3	2.6	1.3	2.0

Max: Max-chart for autocorrelated process.
She: Simultaneous residual Shewhart chart.

8.5 Charting Procedures

Because the residuals are independent normal random variables when the process is in-control, the charting procedure for the Max-chart for autocorrelated process is similar to that of the Max-chart for uncorrelated data. Successive M_i's are plotted against the sample numbers. If a point plot below the upper control limit, the process is said to be in statistical control and the plotting symbol or the point is a dot. An out-of-control signal is given if any point is plotted above the upper control limit and is plotted as one of the characters defined below. Use the following procedure to construct the Max-chart for autocorrelated data:

1. Fit the time series model to the data.

2. Find the center line (CL) and the upper control limit (UCL) from Table 8.1 for the desired α, and set up a chart with the center line and upper control limit marked.

3. If ξ_0 is not known, use the grand average $\bar{\bar{\xi}}$ of the data to estimate it, where $\bar{\bar{\xi}} = (\bar{\xi}_1 + ... + \bar{\xi}_m)/m$. If $\sigma_{\gamma 0}$ is unknown, use $\bar{R}/d_2$ or $\bar{S}/c_4$ to estimate it, where $\bar{R} = (R_1 + ... + R_m)/m$ is the average of the sample ranges and $\bar{S} = (S_1 + ... + S_m)/m$ is the average of the sample standard errors. $S_i = \sqrt{MSE_i}$, $d_2 = d_2(\bar{n})$ and $c_4 = c_2(\bar{n})$ are statistically determined constants with $\bar{n} = (n_1 + ... + n_m)/m$.

4. For each sample, compute Z_i and Y_i.

5. Compute the M_i's and compare them with the UCL.

6. Denote the sample points with a dot and plot them against the sample number if $M_i \leq UCL$.

7. If any of the M_i's are greater than the UCL, the following plotting characters should be used to show the direction as well as the statistic that is plotting above the UCL.

   (i) If only $|Z_i| > UCL$, and $Z_i > 0$, plot $C+$. This shows an increase in the process mean.

   (ii) If only $|Z_i| > UCL$, and $Z_i < 0$, plot $C-$. This indicates a decrease in the process mean.

   (iii) If only $|Y_i| > UCL$, and $Y_i > 0$, plot $S+$. This shows an increase in the process standard deviation.

   (iv) If only $|Y_i| > UCL$, and $Y_i < 0$, plot $S-$. This shows a decrease in the process standard deviation.

   (v) If $|Z_i| > UCL$ and $|Y_i| > UCL$, and both Z_i and Y_i are greater than zero, plot $B++$. This indicates an increase in both the mean and standard deviation of the process.

(vi) If $|Z_i| > UCL$ and $|Y_i| > UCL$, and both Z_i and Y_i are less than zero, plot $B--$. This shows a decrease in both mean and standard deviation of the process.

(vii) If $|Z_i| > UCL$ and $|Y_i| > UCL$, with $Z_i > 0$ and $Y_i < 0$, plot $B+-$. This indicates an increase in the mean and a decrease in the standard deviation of the process.

(viii) If $|Z_i| > UCL$ and $|Y_i| > UCL$, with $Z_i < 0$ and $Y_i > 0$, plot $B-+$. This indicates a decrease in the mean and an increase in the standard deviation of the process.

8. Investigate the cause(s) of the shift for each out-of-control point in the chart and carry out the remedial measures needed to bring the process back into an in-control state.

8.6 An Example

To provide a visual picture of how the Max-chart for autocorrelated data responds to various kinds of process changes, a set of simulated data is used. Specific process changes are introduced into the data, and the chart is plotted to monitor these changes in the parameters. The data set was generated using the first order autoregressive plus a random error term model given in equations (7.1) and (7.2). The data are simulated by simulating sequences of α_t's and ε_t's, using Matlab.

For a fixed sequence of α_t's and ε_t's, a shift in σ_α can be simulated by multiplying α_t in equation (7.2) by a constant. A change in σ_ε can be simulated by multiplying ε_t in equation (7.1) by a constant, and a change in the mean is simulated by adding a constant to the generated observations. This approach was also used to simulate the data in chapter 7. This procedure allows different types of process changes to be investigated on the same basic sequence of α_t's and ε_t's. In this example, we assume the autoregressive parameter, ϕ remains constant, and thus shifts in the process standard deviation are attributed to shifts in either σ_α or σ_ε.

We use the data generated in chapter 7 to show how the Max-chart for autocorrelated processes responds to different shifts in the process location and spread. Figure 8.1 shows the Max-chart for autocorrelated data of the 100 simulated observations. The control limit of the chart was set to achieve an in-control ARL of approximately 250.

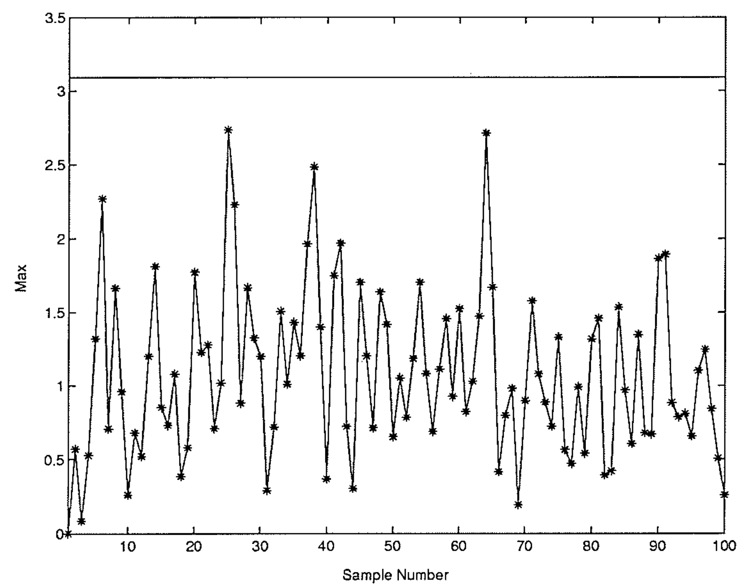

Figure 8.1: The Max-chart for in-control simulated values.

First, we investigate the performance of the Max-chart for shift in the process standard deviation attributed to shifts in σ_α. We use the data that were described in Figure 7.2. The data are displayed in Figure 8.2. The first 60 observations are the same as those in Figure 8.1 and the last 40 are for the observations after the shift. The shift in the standard deviation is signalled for the first time at the 64^{th} observation. Figure 8.3 shows the performance of the Max-chart for an increase in the process variability due to an increase in σ_ε. This data was used in Figure 7.3 and we use it here to assess the performance of the Max-chart. The Max-chart detects this shift for the first time on the 62^{nd} observation. From Figure 8.2 and Figure 8.3, we can conclude that the shift in process variability due to shifts in σ_ε is easier to detect than the shift in the process variability due to shift in σ_α. Even though σ_ε increased the process standard deviation by 30%, while the increase in σ_α resulted in a 52% increase in the process standard deviation, the scheme quickly signalled a shift in the process standard deviation when σ_ε shifted. Furthermore many points plot out-of-control for this small shift as compared to a large shift in σ_α shown in Figure 8.2. This is due to the fact that an increase in σ_ε decreases the level of autocorrelation, while the effect of an increase in σ_α is to increase in the level of autocorrelation.

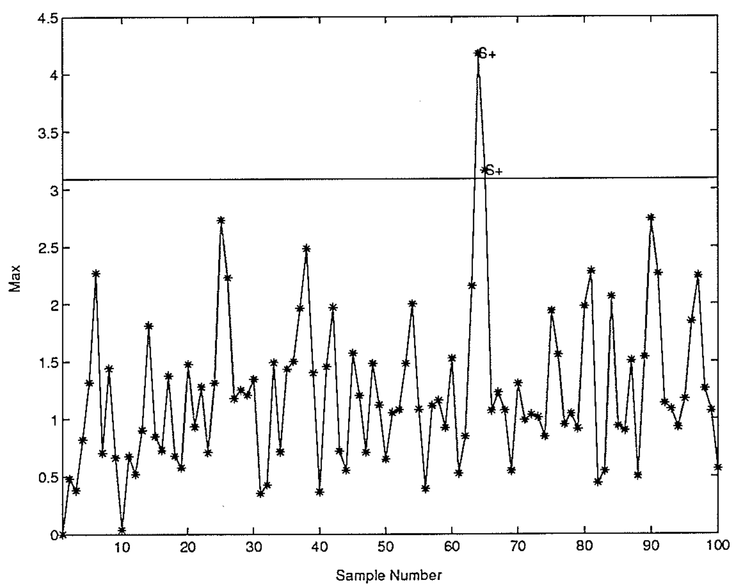

Figure 8.2: The Max-chart for shift in the process standard deviation due to shift in σ_α.

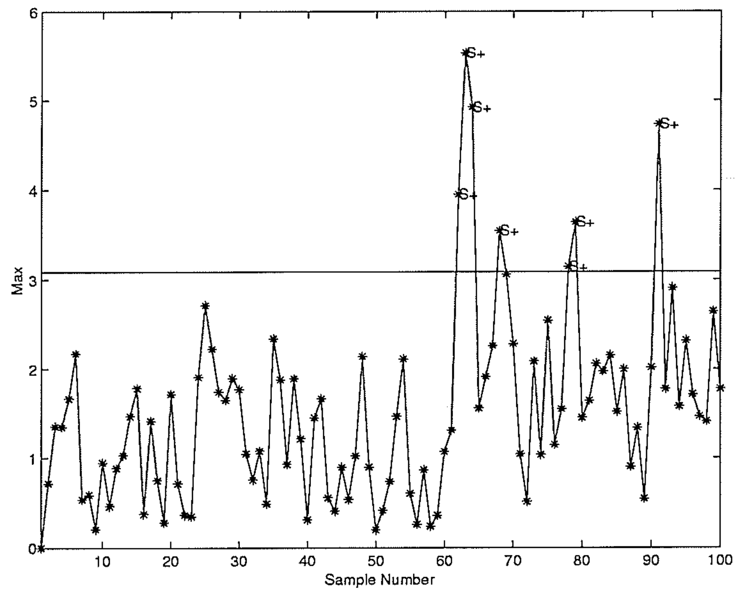

Figure 8.3: The Max-chart for shift in the process standard deviation due to shift in σ_{ε}.

The Max-chart's performance for the process mean shift of the last 40 observations is monitored in Figure 8.4. Assume that due to some special causes, the process mean increases from its target value of 0 to 3 for the last 40 observations. This is accomplished by adding 3 to the last 40 observations in Figure 8.1. This shift is detected on the 63^{rd} observation. Even though the mean increased by a large value, most of the points plot within the action limit. This is due to the fact, when the process observations are autocorrelated, only a fraction of shifts in the process means is transferred to the residual means as can be seen from equation (7.12).

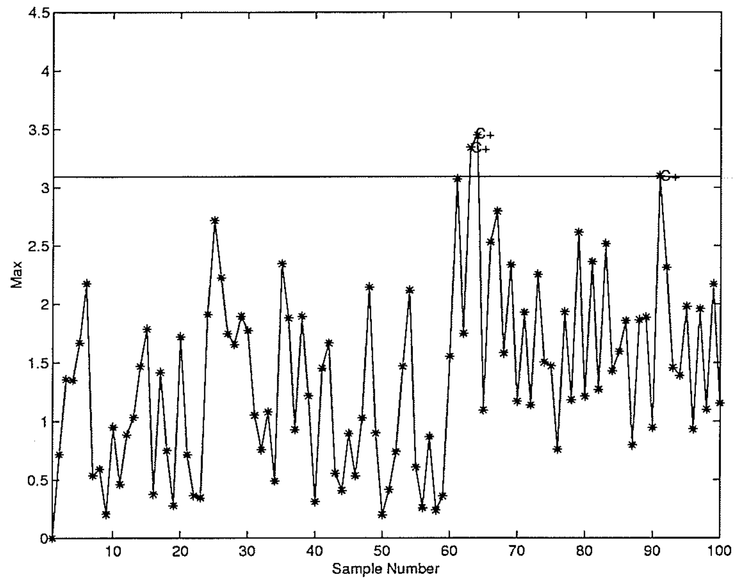

Figure 8.4: The Max-chart for shift in the process mean.

Sometimes special causes may simultaneously cause shifts in both process mean and standard deviation. The performance of the Max-chart for detecting these shifts is investigated in Figures 8.5 and 8.6 below. In Figure 8.5, we investigate the chart for shift in the process mean and standard deviation, where the shift in the standard deviation is due to shift in σ_α. The data were used in Figure 7.5. These data are shown in Figure 8.5. The Max-chart detects the mean shift on the 64^{th} observation, standard deviation shift on the 65^{th}; and a shift in both parameters on the 68^{th} observation.

In Figure 8.6, we investigate the performance of the Max-chart for cases where the special cause of variation results in an increase in both process mean and standard deviation. The shift in standard deviation, is due to shift in σ_ε only. We use the data used in Figure 7.6. The Max-chart detects the shifts in both parameters for the first time on the 61^{st} observation.

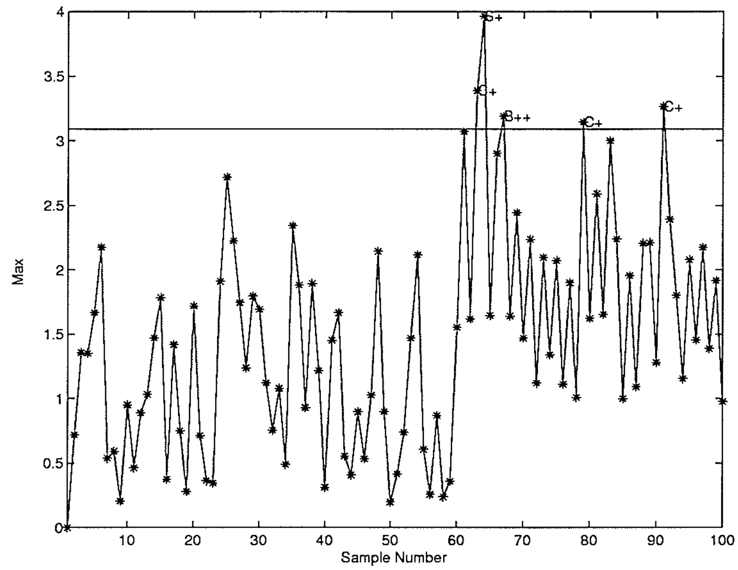

Figure 8.5: The Max-chart for shift in the process mean and standard deviation due to shift in σ_α.

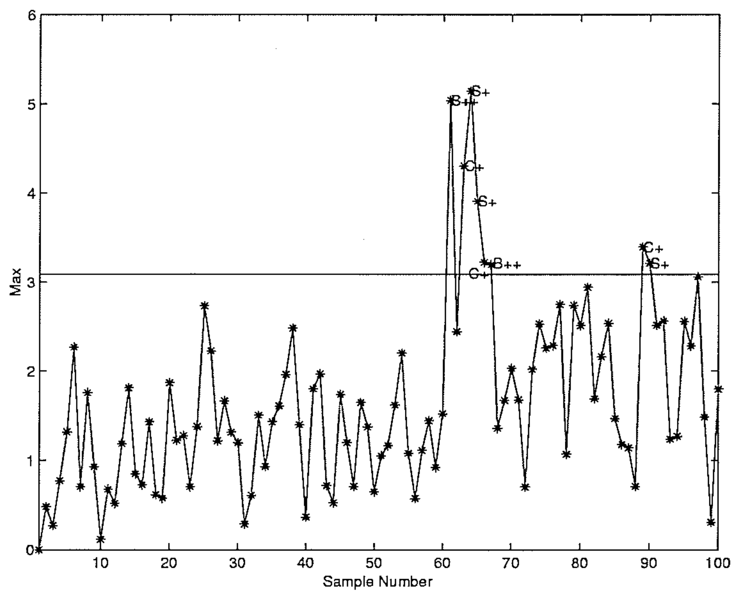

Figure 8.6: The Max-chart for shift in the process mean and standard deviation due to shift in σ_ε.

8.7 Conclusions and Recommendations

We propose a new Shewhart-type control chart for autocorrelated data that is capable of monitoring both process mean and standard deviation by plotting a single variable in a chart. This scheme clearly indicates the parameter as well as the direction of the shift. When the observations are autocorrelated, the monitoring process is very complicated because, the process has many parameters. We considered a process that can be modelled as a first order autoregressive process plus a random error with four parameters: the overall mean, ξ; two standard deviation parameters, σ_α and σ_ε; and the autoregressive parameter, ϕ. An out of control situation may occur as a result of a shift in any one of these parameters or a combination of them. Shifts in these parameters have different effects on the level of correlation between adjacent observations and thus affect the performance of the chart differently.

We have investigated the effects of shifts in the mean alone, shift in variability due to a shift in either σ_α or σ_ε and a combination of shifts in the process mean and either of the two standard deviation components. These investigations were carried out at a fixed level of the autoregressive parameter, ϕ. The conclusion that can be drawn is that this chart is more sensitive when the shift in the process standard deviation is due to shift in σ_ε, than it is to shift in σ_α. This is due to the fact that an increase in σ_α increases the level of autocorrelation while an increase in σ_ε decreases the level of autocorrelation as well as the proportion of process variation attributed to variations in the correlated means μ_t's.

The proposed chart uses the residual of the fitted time series model to monitor the process since when the process is in control the residuals are independent normal random variables. Thus procedure for the Max-chart for independent observations proposed by Chen and Cheng ([21]) can be used to calculate the control limits for our proposed chart. The proposed chart performs better than the simultaneous residual Shewhart chart proposed by Lu and Reynolds ([57]). In addition to the advantage of quickly detecting shifts in the parameters, unlike the combined residual Shewhart chart, the Max-chart for autocorrelated data uses a single variable to monitor the process. We recommend this chart for use in quality monitoring for autocorrelated processes as the effect of process autocorrelation in control charts is greatly reduced by fitting a time series model and monitoring the residuals. However, if autocorrelation is due to some special causes that can be found and eliminated, we recommend that after these special causes are removed, traditional Max chart should be used for process monitoring. The traditional Max chart uses the process observations and thus is more effective than our chart which uses residuals.

Chapter 9

Control Charts for High Yield Processes

9.1 Introduction

In this chapter, we investigate the application of control charts for monitoring processes that produce very small number of nonconforming items. Advancement in production technology particularly in the electronics industry and manufacturing automation has resulted in most of the processes experiencing low levels of nonconforming items. Modern quality assurance philosophy emphasizes the importance of building quality into the product. The fraction of nonconforming items for most processes is measured in the order of parts-per-million (ppm). These processes are referred to as *high yield processes.* To monitor a process with this very low fraction of nonconforming items, control chart procedures usually require taking very large samples or inspecting all items produced by the process.

Several procedures for monitoring high yield processes have been proposed in the past. Nelson ([74]) suggested using 3σ control charts based on a power transformation of the X (where X is the number of items sampled until a nonconforming item is found) chosen so that the transformed variable Y is approximately normal. Several authors including Quesenberry ([83]), McCool and Joyner-Motley ([69]) and Johnson and Kotz ([49]) proposed other methods based on transforming the data to normal distribution. Chang and Gan ([16]) proposed CUSUM charts for monitoring a high yield process based on nontransformed geometric and bernoulli counts.

Calvin ([12]) suggested using a control chart that plots the number of good items between defects. Hahn ([36]) proposed a method which estimate the percentage of nonconforming products in accepted lots using a zero defect acceptance sampling plan. Chen ([20]) proposed a procedure that involves adjusting the control limits for the p chart to monitor the process with very small number of nonconforming items.

Process monitoring in the case of attributes data usually uses charts for the binomial parameter p. Nelson ([75]) discussed the use of standardized p chart. This standardized p chart involves a linear transformation of the binomial distribution to the normal distribution. This transformation relies on the well known normal approximation to the binomial. Quesenberry ([83]) proposed a nonlinear transformation of the binomial distribution to normal which performs better than the linear transformation of Nelson ([75]) for cases where p is small.

In this chapter, we show that at high levels of fraction of nonconforming items, there is no significant difference between control charts based on the Poisson and normal approximation to the binomial distribution, however at very low levels of fraction nonconforming, the Poisson approximation to the binomial performs better than the normal approximations discussed by Quesenberry ([83]). This is due to the fact that when p is very small and n not very large, the binomial distribution is highly asymmetric. Improved technology in the manufacturing industry has resulted in high yields and as a result most of the control charts used in quality control are for small values of p and thus a good approximation of the distribution results in high performance of these control charts. The Poisson approximation to the binomial distribution has proven to perform well as will be shown later.

9.2 Control Charts for a Binomial Process

The Shewhart chart used for monitoring the number of nonconforming items in a sample is the np chart with control limits given as follows: we need to find the lower control limit (LCL), the center line (CL) and an upper control limit (UCL). Suppose an in control process has a target value of $p = p_0$. The 3-sigma limits for the chart for the number of nonconforming items in a sample of size n are given as

$$\begin{aligned} LCL &= np_0 - 3\sqrt{np_0(1-p_0)}, \\ CL &= np_0, \\ UCL &= np_0 + 3\sqrt{np_0(1-p_0)}. \end{aligned}$$

If p is unknown, the control chart for the number of nonconforming items is constructed by first estimating p with $\hat{p} = \frac{\sum_{i=1}^{m} x_i}{mn}$, where x_i is the number of nonconforming items in the i^{th} sample of size n and m is the number of samples taken. The np chart is constructed with control limits given as

$$\begin{aligned} LCL &= n\hat{p} - 3\sqrt{n\hat{p}(1-\hat{p})}, \\ CL &= n\hat{p}, \\ UCL &= n\hat{p} + 3\sqrt{n\hat{p}(1-\hat{p})}. \end{aligned}$$

The number of nonconforming items will be plotted on an np chart with these control limits.

9.3 Binomial Approximations for p Known

When p is very small and n very large, it is often difficult to compute the probabilities based on the binomial distribution. To overcome this difficulty, we usually use some transformation techniques to transform the binomial distribution to other distributions whose probabilities can easily be computed. In particular, we usually transform the binomial random variables to either Poisson or normal random variables. However, when p is very small and n not very large, the binomial distribution is very asymmetric and using the normal approximation to binomial is not a good approach. We show here that the Poisson approximation to binomial in case of very low values of p is the best option. We present the nonlinear transformation of the binomial random variables to Poisson random variables and nonlinear transformation of the binomial random variables to normal random variables. Let x_i denote the i^{th} observation on a binomial random variable with parameters n and p. The binomial distribution function is denoted by

$$u_i = B(x_i; n, p) \qquad i = 1, 2, ... \tag{9.1}$$

The Quesenberry procedure transforms this binomial distribution function to q_i statistics as follows:

$$q_i = \Phi^{-1}(u_i) \qquad i = 1, 2, ..., \tag{9.2}$$

where Φ^{-1} is the inverse of the standard normal cumulative distribution function.

The Shewhart chart for Quesenberry's statistics is developed by plotting the q_i values on a Q chart with control limits at

$$\begin{aligned} LCL &= -3, \\ CL &= 0, \\ UCL &= 3. \end{aligned}$$

Next we transform these binomial random variables to Poisson random variables as follows:

$$c_i = F^{-1}(u_i) \qquad i = 1, 2, ..., \tag{9.3}$$

where F^{-1} is the inverse of the Poisson cumulative distribution function.

For a Poisson distribution, the mean and variance are the same. Therefore, the c_i values are plotted on a c chart (a chart for number of nonconformities) with control limits at

$$\begin{aligned} LCL &= np_0 - 3\sqrt{np_0}, \\ CL &= np_0, \\ UCL &= np_0 + 3\sqrt{np_0}. \end{aligned}$$

We give some tables as well as graphs to compare the binomial approximations by the Poisson and normal distributions below. The normal approximation is based on the nonlinear transformation procedure proposed by Quesenberry ([83]). To study the accuracy of these approximations we considered several values of n and p. In Tables 9.1 through 9.4 we give a few of these results. The tables show the probability functions of the binomial, Poisson and normal approximations, the difference between the binomial and the Poisson approximation and the difference between the binomial and the normal approximation. We can see that the difference between the binomial probabilities and the Poisson probabilities is very small. We give tables for $p = 0.001$, 0.0003, 0.0007 and 0.00003 with $n =$ 1,000, 5,000, 10,000 and 20,000. The probability functions for these distributions are also displayed in Figures 9.1 to 9.4.

From Figures 9.1 through 9.4 we can see that when the fraction of nonconforming items is very low the Poisson approximation nicely fits the binomial while the normal approximation is not a good fit. Because the difference between the binomial and Poisson probabilities is negligible, the curve for the binomial distribution is indistinguishable from that of the Poisson distribution.

Table 9.1: The probability functions for the three distributions with n = 1,000, p = 0.001

x	Binomial (A)	Poisson (B)	Normal (C)	$\mid A-B\mid$	$\mid A-C\mid$
0	0.36770	0.36788	0.24197	0.00018	0.12572
1	0.36806	0.36788	0.39914	0.00018	0.03108
2	0.18403	0.18394	0.24197	9.202E-05	0.05794
3	0.06128	0.06131	0.05391	3.073E-05	0.00737
4	0.01529	0.01533	0.00441	3.835E-05	0.01088
5	0.00305	0.00307	0.00013	1.685E-05	0.00292
6	0.00051	0.00051	1.469E-06	4.844E-06	0.00050

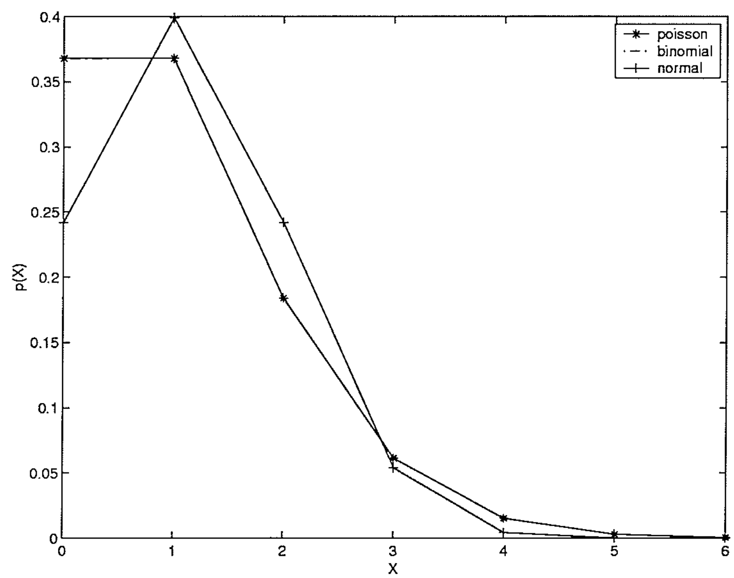

Figure 9.1: The probability functions for the three distributions with n = 1,000, p = 0.001

Table 9.2: The probability functions for the three distributions with n = 5,000, p = 0.0003

x	Binomial (A)	Poisson (B)	Normal (C)	$\mid A-B\mid$	$\mid A-C\mid$
0	0.22308	0.22313	0.15385	5.021E-05	0.06923
1	0.33472	0.33470	0.29973	2.510E-05	0.03499
2	0.25107	0.25102	0.29973	4.39E-05	0.04866
3	0.12552	0.12551	0.15385	9.412E-06	0.02833
4	0.04706	0.04707	0.04054	1.060E-05	0.00652
5	0.01412	0.01412	0.00548	1.024E-05	0.00863
6	0.00352	0.00353	0.00038	5.030E-06	0.00314

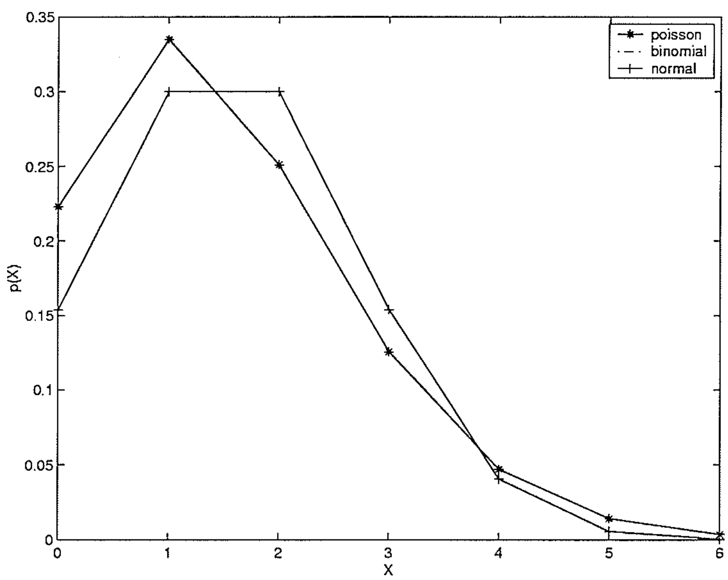

Figure 9.2: The probability functions for the three distributions with n = 5,000, p = 0.0003

Table 9.3: The probability functions for the three distributions with n = 10,000, p = 0.0007

x	Binomial (A)	Poisson (B)	Normal (C)	$\mid A-B \mid$	$\mid A-C \mid$
0	0.00090	0.00091	0.00454	2.232E-07	0.00363
1	0.00637	0.00638	0.01151	0.00001	0.00513
2	0.02232	0.02234	0.02526	0.00003	0.00294
3	0.05210	0.05213	0.04806	0.00003	0.00403
4	0.09120	0.09123	0.07927	0.00002	0.01193
5	0.12772	0.12772	0.11333	6.377E-06	0.01439
6	0.14904	0.14901	0.14043	0.00004	0.00861

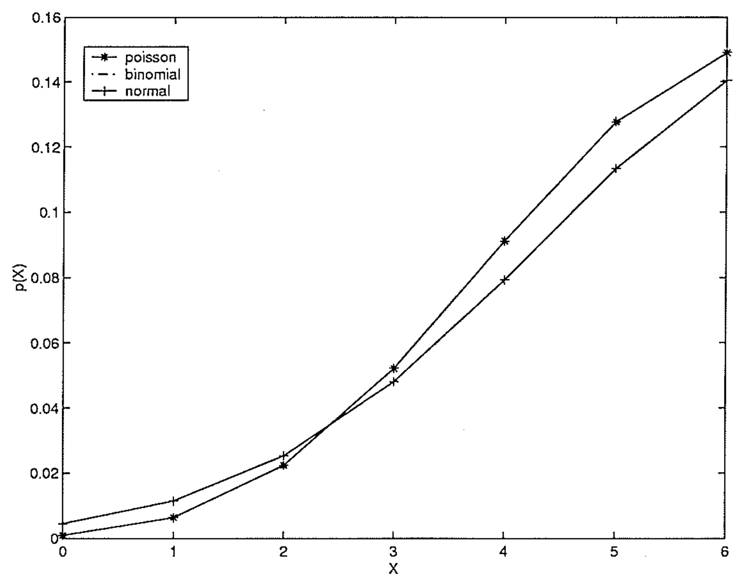

Figure 9.3: The probability functions for the three distributions with n = 10,000, p = 0.0007

Table 9.4: The probability functions for the three distributions with n = 20,000, p = 0.00005

x	Binomial (A)	Poisson (B)	Normal (C)	$\mid A-B\mid$	$\mid A-C\mid$
0	0.36787	0.36788	0.24197	9.197E-06	0.12590
1	0.36789	0.36788	0.39895	9.197E-06	0.03106
2	0.18394	0.18394	0.24197	4.599E-06	0.05803
3	0.06131	0.06131	0.05399	1.533E-06	0.00732
4	0.01533	0.01533	0.00443	1.916E-06	0.01089
5	0.00306	0.00306	0.00013	8.430E-07	0.00293
6	0.00051	0.00051	1.486E-06	2.427E-07	0.00051

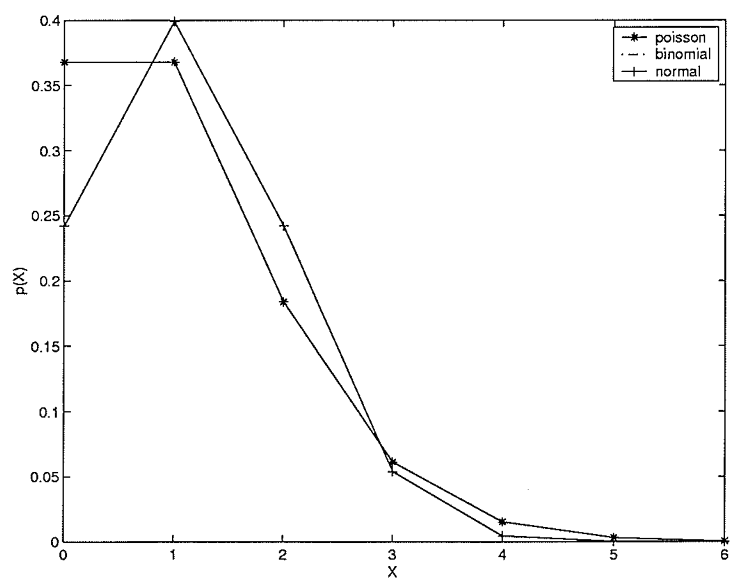

Figure 9.4: The probability functions for the three distributions with n = 20,000, p = 0.00005

9.4 Binomial Approximations for p Unknown

In this section, we consider transforming the observations from the binomial distribution to the Poisson and normal distributions for the case where p is unknown. Let x_i denote the number of nonconforming products in a sample of size n_i for $i = 1, 2, \ldots$. For the case when p is not known, Chen ([20]) showed that the Q chart by Quesenberry ([83]) can be constructed using the hypergeometric distribution function as follows:

Let $N_i = \sum_{j=1}^{i} n_j$ and $t_i = \sum_{j=1}^{i} x_j$, where x_i is an observation of a binomial random variable with parameters n_i and p. Then we define

$$u_i = \frac{\sum_{k=h_i}^{x_i} \binom{n_i}{k}\binom{t_i-k}{N_{i-1}}}{\binom{n_i+N_{i-1}}{t_i}}, \qquad i = 2, 3, \ldots \tag{9.4}$$

$$q_i = \Phi^{-1}(u_i). \tag{9.5}$$

where $h_i = max[0, t_i - N_{i-1}]$. This transformation uses the hypergeometric distribution function which is the uniform minimum variance unbiased estimating distribution function of the binomial distribution function used in equation (9.1). The Q chart is constructed by plotting the $q_2, q_3, \ldots$ values against the sample number on a chart with LCL = -3, CL = 0 and UCL = 3 . The chart is constructed by plotting the q_i values from the second sample onward because u_i is derived using N_{i-1} values.

The chart using the Poisson approximation with p unknown is constructed by transforming the u_i values in equation (9.4) as follows:

$$c_i = F^{-1}(u_i) \qquad i = 2, 3, \ldots \tag{9.6}$$

The c_i values in equation (9.6) are plotted on a c chart with control limits given as

$$\begin{aligned} LCL &= n\hat{p} - 3\sqrt{n\hat{p}}, \\ CL &= n\hat{p}, \\ UCL &= n\hat{p} + 3\sqrt{n\hat{p}}, \end{aligned}$$

where $\hat{p} = \frac{\sum_{i=1}^{m} x_i}{\sum_{i=1}^{m} n_i}$ is the estimate of the proportion of nonconforming products.

9.5 Comparison of Charts

In this section, we compare the attributes charts using the np chart, the c chart and the Q chart. We show that for small values of p, the binomial distribution is highly asymmetric and thus using a symmetric control chart to monitor the fraction nonconforming such as the Q chart is subject to more false alarms in detecting changes in p. We compared these charts for several values of n and p. We only present the results for the following values of p: 0.001, 0.0001 and 0.00001 with various sample sizes. We present in Table 9.5 the false alarm probabilities $P(X_i < LCL)$ and $P(X_i > UCL)$ for these schemes, where X_i is used to represent the plotting statistic associated with each of the three charts. We see from Table 9.5 that for small values of p, the c chart gives false alarm probabilities that are closer to those of the exact np chart than the Q chart. In particular, a chart based on Quesenberry's transformation gives high false alarm rates when p is very small. The Q chart has the same false alarm rate as the np chart for very large samples.

Under the normal distribution, the false alarm probabilities for each of the limits (UCL or LCL) are expected to be around 0.00135. Therefore a good approximation should give false alarm probabilities close to that value, however the Q chart gives values that are not close. Therefore it shows that, for small values of p a chart using normal approximation to the binomial will give misleading conclusions.

We give the in control ARL for the *np* chart, Q chart and the *c* chart in Table 9.6. It can be seen from this table that the Q chart gives in control ARL's that are different from those of the *np* chart while the *c* chart gives in control ARL's that are similar to those of the *np* chart most of the time. The Q chart performs very poorly when p is very small as its in control ARL's are very small for small sample sizes. Its use will result in more resources being wasted looking for assignable causes of variation when in fact the process is in control.

Table 9.5: The false alarm probabilities

		LCL			UCL		
p	n	Q chart	np chart	Poisson	Q chart	np chart	Poisson
0.001	10,000	0.00050	0.00050	0.00050	0.00158	0.00158	0.00159
	12,500	0.00034	0.00155	0.00155	0.00245	0.00119	0.00119
	17,500	0.00047	0.00146	0.00146	0.00221	0.00117	0.00118
	25,000	0.00058	0.00141	0.00141	0.00202	0.00117	0.00117
0.0001	17,500	0.00000	0.00000	0.00000	0.00913	0.00220	0.00220
	20,000	0.00000	0.00000	0.00000	0.00453	0.00110	0.00110
	30,000	0.00000	0.00000	0.00000	0.00380	0.00110	0.00110
	40,000	0.00000	0.00000	0.00000	0.00284	0.00091	0.00092
0.00001	20,000	0.00000	0.00000	0.00000	0.01752	0.00115	0.00115
	30,000	0.00000	0.00000	0.00000	0.0360	0.00027	0.00027
	40,000	0.00000	0.00000	0.00000	0.00793	0.00078	0.00078

Table 9.6: A comparison of in control ARL's for three procedures

		ARL_0		
p	n	Q chart	np chart	Poisson
0.001	10,000	481	481	479
	12,500	358	365	365
	17,500	373	380	379
	25,000	385	388	388
0.0001	17,500	110	455	455
	20,000	221	909	909
	30,000	263	909	909
	40,000	352	1,099	1,087
0.00001	20,000	57	870	870
	30,000	278	3,704	3,704
	40,000	571	5,882	5,882

9.6 Example 1

To provide a visual picture of the *np* chart, Q chart and the *c* chart when p is known, we simulate the data for 100 samples from a $b(X; 10,000, 0.0001)$ distribution (where $b(X; n, p)$ is the probability distribution of a binomial random variable X with parameters n and p) and then 30 more samples from a $b(x; 10,000, 0.00015)$. The Quesenberry random variables and the Poisson random variables are computed by transforming these binomial random variables using equations (9.2) and (9.3) respectively. In Table 9.7, we show the first ten values of the simulated data from a binomial random variable (u_i) with $n = 10,000$ and $p = 0.0001$ together with the corresponding q_i and c_i statistics. The q_i and c_i values are computed by substituting the u_i values into equations (9.2) and (9.3) respectively.

Table 9.7: Some data values for Examples 1

x_i	2	2	1	2	1	0	0	1	0	1
q_i	1.40	1.40	0.63	1.40	0.63	-0.34	-0.34	0.63	-0.34	0.63
c_i	3	3	2	3	2	0	0	2	0	2

A chart based on the binomial count is shown in Figure 9.5, a chart based on the Poisson approximation is shown in Figure 9.6 and a chart based on Quesenberry's normal approximation is shown in Figure 9.7. By examining these figures, we conclude that the np chart and the c chart give almost identical results while the Q chart performs differently from these other charts. The np chart and the c chart plot two values above their upper control limits after the shift while Q chart shows only one value out-of-control.

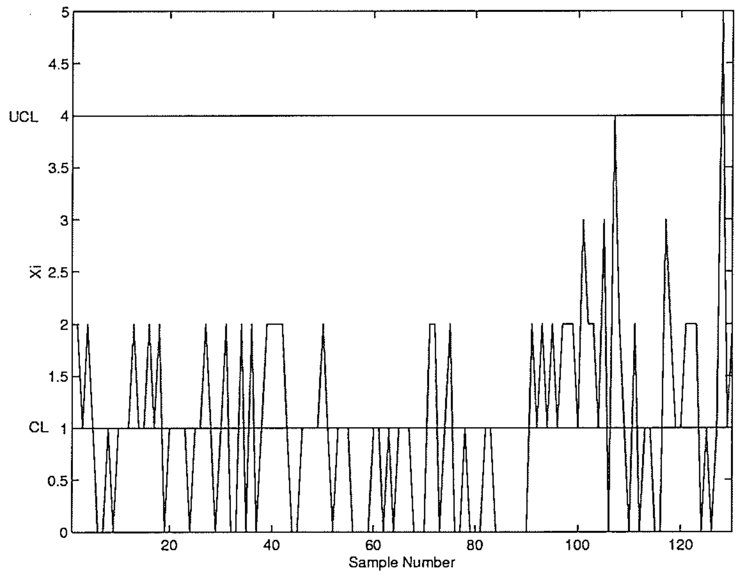

Figure 9.5: The np chart.

9.7 Example 2

To provide a visual picture of the np chart, the Q chart and the c chart when p is unknown, we use the data used in example 1. From the data we estimated p by $\hat{p} = \frac{\sum_{i=1}^{100} x_i}{\sum_{i=1}^{100} n_i} = 0.00009$ using the first 100 samples that were taken when the process was in control and used this value to compute the new control limits for the np and c charts. The Quesenberry random variables and the Poisson random variables

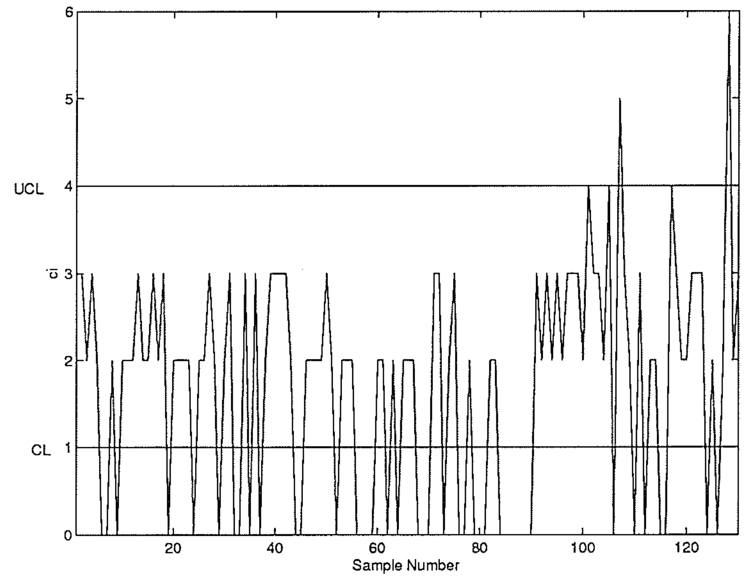

Figure 9.6: The c chart.

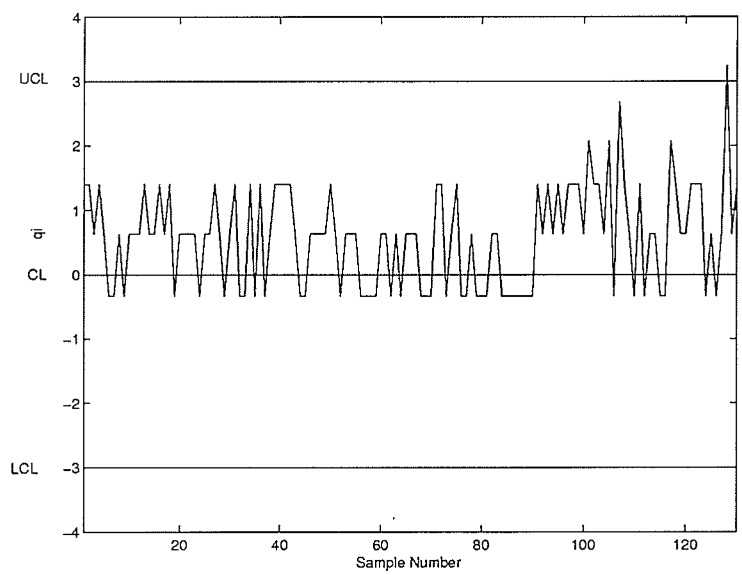

Figure 9.7: The Q chart.

are computed by transforming the data into hypergeometric random variables using equations (9.4) and then using equations (9.5) and (9.6) to obtain the q_i's and c_i's respectively. We show the first ten values of the simulated data in Table 9.8 below.

Table 9.8: Some data values for Examples 2

x_i	2	2	1	2	1	0	0	1	0	1
q_i	-	0.49	-0.10	0.69	0.01	-0.73	-0.55	0.49	-0.40	0.63
c_i	-	1	1	1	1	0	0	1	0	1

The *np* chart, *c* chart and *Q* chart are displayed in Figures 9.8, 9.9 and 9.10 respectively. Comparing these charts to the corresponding charts for known value of p, we can conclude that the point patterns for these charts are very similar. This is because we have used the best (UMVU) estimator of the binomial probability density function, namely the hypergeometric distribution.

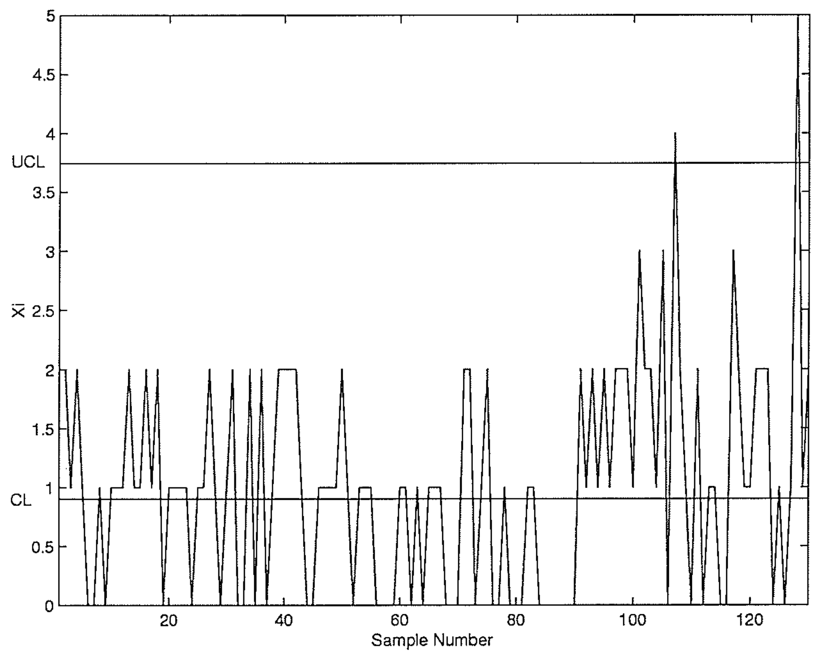

Figure 9.8: The np chart.

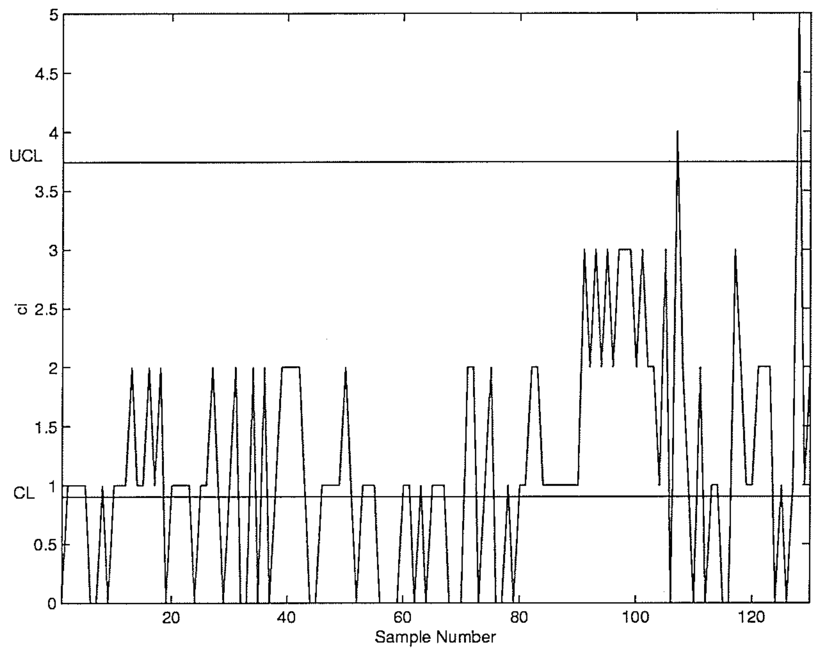

Figure 9.9: The c chart.

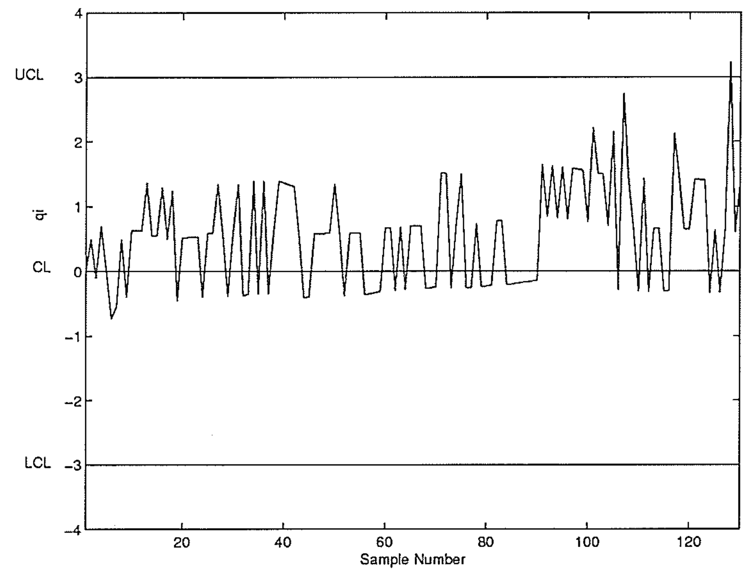

Figure 9.10: The Q chart.

9.8 Conclusion and Recommendations

We have shown that when the number of nonconforming items is measured in the order of parts-per-million, control charts based on Poisson approximation to binomial perform better than those based on the normal approximation to binomial. The in control ARL's for the Poisson chart are closer to those of the binomial np chart. Due to the asymmetric nature of the binomial distribution for low fraction nonconforming, the chart based on normal approximation to binomial gives high false alarm rates. Since the c chart is simple to construct and easier to interpret than the np chart and the Q chart, we recommend that for small values of p, practitioners should use the c chart.

Chapter 10

Conclusions

10.1 Summary

In any production process, there are always some forms of variability in products. If the process produces items that are independent and identically distributed over time, we expect the mean of the process output to be constant over time even though individual observations are not exactly identical. However when the observations are autocorrelated, the mean will vary with time even when the process is in-control. The usual process monitoring procedure for variables data requires running two control charts concurrently, one chart for monitoring the process location and another one for monitoring the process spread.

The major objective of this thesis is to develop single control charts that can simultaneously monitor both process location and spread. Under the normality assumption, we propose six new single control charts for univariate and multivariate processes with variables data. Four of the charts are developed under the assumption that individual observations are independent over time while the other two are developed for the case where the observations are serially correlated. When an out-of-control signal is issued, plotting characters are used to indicate the source as well as the direction of the detected shift. We further proposed the use of Poisson based control chart for the case when the process produces very low number of nonconforming units. These processes are referred to as high yield processes. We show that charts based on the normal approximation are not effective due to the asymmetric nature of the binomial distribution when the sample size is not very large and the proportion of nonconforming products is very small.

The single charts proposed in chapters 3 to 8 are compared with the recently developed single charts by adjusting their control limits so that both charts have the same in control ARL. Comparison of the new single CUSUM charts with the single EWMA charts shows that the single CUSUM charts performs better than the single EWMA charts for very small shifts in the mean and/or standard deviation while the EWMA charts performs better than our CUSUM charts for moderate to large shifts. These charts are compared in Chapters 3 to 5. In Chapter 6 we proposed a single Shewhart-type multivariate chart. This chart more quickly detects large shifts in the process mean vector and/or covariance matrix than the single multivariate CUSUM and EWMA charts. Our proposed multivariate charts are developed by transforming the multivariate observations into univariate observations so that simple univariate charts procedure could be used to monitor these multivariate observations.

In Chapters 7 and 8, we develop new single CUSUM and Shewhart-type charts for autocorrelated processes. These charts are developed by fitting a time series model to the data and then monitoring the estimated residuals. These charts are developed by taking the process autocorrelation into consideration when computing their control limits. This procedure significantly reduces the effect of autocorrelation in control charts. These charts are compared with the simultaneous charts developed by Lu and Reynolds ([57]). Our new charts performs better than their competitors for both small and large shifts in the process mean and/or standard deviation. In addition to this advantage of quickly detecting shifts, our new charts use a single variable to asses both mean and standard deviation.

10.2 Future Research

There are some extensions of the work done in this thesis that can be investigated. These include the following:

1. Developing single multivariate charts for autocorrelated processes.

2. Developing single CUSUM charts for processes following other distributions.

3. Developing single EWMA charts for autocorrelated processes.

Bibliography

[1] Alt, F. B. and Smith, N. D. (1988). Multivariate Process Control. *Handbook of Statistics*, Volume 7, North-Holland, Amsterdam, 333-351.

[2] Alwan, L. C. and Roberts, H. V. (1988). Time Series Modelling for Statistical Process Control. *Journal of Business and Economic Statistics*, **6**, 87-95.

[3] Atienza, O. O., Tang, L. C. and Ang, B. W. (2002). A CUSUM Scheme for Autocorrelated Observations. *Journal of Quality Technology*, **34**, 188-199.

[4] Barnard, G. A. (1959). Control Charts and Stochastic Processes. *Journal of the Royal Statistics Society*, **XXI**, 240-271.

[5] Bissell, A. F. (1969). CUSUM Technigues for Quality Control. *Applied Statistics*, **18**, 1-30.

[6] Bissell, A. F. (1979). A Semi-parabolic Mask for CUSUM Charts. *Applied Statistics*, **28**, 1-7.

[7] Box, G. E. P., Jenkins G. M. and Reinsel, G. C. (1994). *Time Series Analysis, Forcasting and Control*, 3rd edition. Prentice-Hall, Englewood Cliffs, NJ.

[8] Box, G. E. P. and Ramirez, J. G. (1991a). Sequential Methods in Statistical Process Monitoring. Report No. 65, Center for Quality and Productivity Improvement, University of Wisconsin-Madison, Madison, WI.

[9] Box, G. E. P. and Ramirez, J. G. (1991b). Sequential Methods in Statistical Process Monitoring. Report No. 66, Center for Quality and Productivity Improvement, University of Wisconsin-Madison, Madison, WI.

[10] Box, G. E. P. and Ramirez, J. G. (1991c). Sequential Methods in Statistical Process Monitoring. Report No. 67, Center for Quality and Productivity Improvement, University of Wisconsin-Madison, Madison, WI.

[11] Brook, D. and Evans, D. A. (1972). An Approach to the Probability Distribution of CUSUM Run Length. *Biometrika*, **59**, 539-549.

[12] Calvin, T. W. (1983). Quality Control Techniques for "Zero Defects". IEEE *Transactions on Components, Hybrids and Manufacturing Technology*, **6**, 323-328.

[13] Champ, C. W. and Rigdon, S. E. (1991). A Comparison of the Markov Chain and the Integral Equation Approaches for Evaluating the Run Length Distribution of Quality Control Charts. *Communications in Statistics-Simulation*, **20**, 191-204.

[14] Champ, C. W. and Woodall, W. H. (1987). Exact Results for Shewhart Control Charts with Supplementary Runs Rules. *Technometrics*, **29**, 393-399.

[15] Chan, L. K. and Zhang, J. (2001). Cumulative Sum Control Charts for the Covariance Matrix. *Statistica Sinica*, **11**, 767-790.

[16] Chang, T. C. and Gan, F. F. (2001). Cumulative Sum Charts for High Yield Processes *Statistica Sinica*, **11**, 791-805.

[17] Chang, T. C. and Gan, F. F. (1995). A Cumulative Sum Control Chart for Monitoring Process Variance. *Journal of Quality Technology*, **27**, 109-119.

[18] Chantraine, P. M. R. (1987). Geometric Moving Average Charts in a Manufacturing Environment. Paper Presented at the 31st Annual Fall Technical Conference, Atlantic City, NJ.

[19] Chao, M. T. and Cheng, S. W. (1996). Semicircle Control Chart for Variables Data. *Quality Engineering*, **8**, 441-446.

[20] Chen, G. (1998). An Improved p Chart Through Simple Adjustments. *Journal of Quality Technology*, **30**, 142-151.

[21] Chen, G. and Cheng, S. W. (1998). Max-chart: Combining X-Bar Chart and S Chart. *Statistica Sinica*, **8**, 263-271.

[22] Chen, G., Cheng, S. W. and Xie, H. (2004). A new EWMA control chart for monitoring both location and dispersion. *International Journal of Quality and Quantitative Management*, **1**, (To appear: Sept. 2004).

[23] Chen, G., Cheng, S. W. and Xie, (2001). Monitoring Process Mean and Variability With One EWMA Chart. *Journal of Quality Technology*, **33**, 223-233.

[24] Cheng, S. W. and Li, G. Y. (1993). A Single Variables Control Chart. Technical Report, University of Manitoba, Winnipeg, Canada.

[25] Cox, M. A. A. (1999). Toward the Implementation of a Universal Control Chart and Estimation of its Average Run Length using a Spreadsheet. *Quality Engineering*, **11**, 511-536.

[26] Crosier, R. B. (1988). Multivariate Generalizations of Cumulative Sum Quality-Control Schemes. *Technometrics*, **30**, 291-303.

[27] Crowder, S. V. (1987). A Simple Method for Studying Run-Length Distributions of Exponentially Weighted Moving Average Charts. *Technometrics*, **29**, 401-407.

[28] Crowder, S. V. (1989). Design of Exponentially Weighted Moving Average Scheme. *Journal of Quality Technology*, **21**, 155-162.

[29] Crowder, S. V. and Hamilton, M. D. (1992). An EWMA for Monitoring a Process Standard Deviation. *Journal of Quality Technology*, **24**, 12-21.

[30] Devor, R. E., Chang, T. and Sutherland, W. (1992). *Statistical Quality Design and Control.* West Publishing Company, St. Paul, MN.

[31] Domangue, R. and Patch, S. C. (1991). Some Omnibus Exponentially Weighted Moving Average Statistical Process Monitoring Schemes. *Technometrics*, **33**, 299-313.

[32] Duncan, A. J. (1974). *Quality Control and Industrial Statistics.* Homewood, IL: Richard D. Irwin.

[33] Ewan, W. D. (1963). When and How to Use CUSUM Charts. *Technometrics*, **5**, 1-22.

[34] Gan, F. F. (1991). An Optimal Design of CUSUM Quality Control Charts. *Journal of Quality Technology*, **23**, 279-286.

[35] Gibra, I. N. (1975). Recent Developments in Control Chart Techniques. *Journal of Quality Technology*, **7**, 183-192.

[36] Hahn, G. J. (1986). Estimating the Percent Nonconforming in the Accepted Product After Zero Defect Sampling. *Journal of Quality Technology*, **18**, 182-188.

[37] Harris, T. J. and Ross, W. H. (1991). Statistical Process Control Procedures for Correlated Observations. *The Canadian Journal of Chemical Engineering*, **69**, 48-57.

[38] Hawkins, D. M. (1993). Cumulative Sum Control Charting: An Underutilized SPC Tool. *Quality Engineering*, **5**, 463-477.

[39] Hawkins, D. M. (1981). A CUSUM for Scale Parameter. *Journal of Quality Technology*, **13**, 228-231.

[40] Hawkins, D. M. and Olwell, D. H. (1997). *Cumulative Sum Charts and Charting for Quality Improvement.* Springer-Verlag New York Berlin Heidelberg.

[41] Healy, J. D. (1987). A Note on Multivariate CUSUM Procedures. *Technometrics*, **29**, 409-412.

[42] Hotelling, H. (1947). Multivariate Quality Control. *Techniques of Statistical Analysis*, McGraw-Hill, New York, 113-184.

[43] Hunter, J. S. (1986). The Exponentially Weighted Moving Average. *Journal of Quality Technology*, **18**, 203-210.

[44] Jackson, J. E. (1985). Multivariate Quality Control. *Communications in Statistics-Theory and Methods*, **14**, 2657-2688.

[45] Jackson, J. E. (1959). Quality Control methods for several Related Variables. *Technometrics*, **1**, 359-377.

[46] Jackson, J. E. and Morris, R.H. (1957). An Application of Multivariate Quality Control to Photographic Processing. *Journal of the American Statistics Association*, **52**, 186-199.

[47] Jensen, D. R. and Solomon, H. (1972). A Gaussian Approximation to the Distribution of a Definite Quadratic Form. *Journal of the American Statistical Association*, **67**, 898-902.

[48] Johnson, R. A. and Bagshaw, M. (1974). The Effect of Serial Correlation on the Performance of CUSUM Tests. *Technometrics* , **16**, 103-112.

[49] Johnson, N. L. and Kotz, S. (1970). *Continuous Univariate Distributions 1.* Houghton Mifflin, Boston, MA.

[50] Khoo, M. B. C. and Quah, S. H. (2002). Proposed Short Runs Multivariate Control Charts for the Process Mean. *Quality Engineering*, **14**, 603-621.

[51] Koons, B. K. and Foutz, R. V. (1990). Estimating Moving Average Parameters in the Presence of Measurement Error. *Communications in Statistics-Theory and Methods*, **19**,3179-3187.

[52] Kourti, T. and MacGregor, J. F. (1996). Multivariate SPC Methods for Process and Product Monitoring. *Journal of Quality Technology*, **28**, 409-428.

[53] Lowry, C. A. and Montgomery, D. C. (1995). A review of Multivariate Control Charts. IIE *Transactions*, **27**, 800-810.

[54] Lowry, C. A. and Woodall, W. H. (1992). A Multivariate Exponentially Weighted Moving Average Control Chart. *Technometrics*, **34**, 46-53.

[55] Lu, C. W. and Reynolds, JR. M. R. (2001). CUSUM Charts for Monitoring an Autocorrelated Process. *Journal of Quality Technology*, **33**, 316-334.

[56] Lu, C. W. and Reynolds, JR. M. R. (1999). EWMA Control Charts for Monitoring the Mean of Autocorrelated Processes. *Journal of Quality Technology*, **31**, 166-187.

[57] Lu, C. W. and Reynolds, JR. M. R. (1999). Control Charts for Monitoring the Mean and Variance of Autocorrelated Processes. *Journal of Quality Technology*, **31**, 259-274.

[58] Lucas, J. M. (1982). Combined Shewhart-CUSUM Quality Control Schemes. *Journal of Quality Technology*, **14**, 51-59.

[59] Lucas, J. M. (1973). Large Differences Between Partial Correlation Coefficients. *The American Statistician*, **27**, 77-78.

[60] Lucas, J. M. and Crosier, R. B. (2000). Fast Initial Response for CUSUM Quality Control Scheme: Give Your CUSUM a Head Start. *Technometrics*, **42**, 102-107.

[61] Lucas, J. M. and Crosier, R. B. (1982a). Fast Initial Response for CUSUM Quality Control Schemes. *Technometrics*, **24**, 199-144.

[62] Lucas, J. M. and Saccucci, M. S. (1990). Exponentially Weighted Moving Average Control Schemes: Properties and Enhancements. *Technometrics*, **32**, 1-12.

[63] MacGregor, J. F. and Harris, T. J. (1993). The Exponentially Weighted Moving Variance. *Journal of Quality Technology*, **23**, 106-118.

[64] Maragah, H. D. and Woodall, W. H. (1992). The Effect of Autocorrelation on the Retrospective X-Charts. *Journal of Statistical Computing Simulation*, **40**, 29-42.

[65] Marquardt, D. W. (1984). New Technical and Educational Directions for Managing Product Quality. *The American Statistician*, **38**, 8-14.

[66] Mason, R. L., Tracy, N. D. and Young, J. C. (1997). A Practical Approach for Interpreting Multivariate T^2 Control Chart Signals. *Journal of Quality Technology*, **29**, 396-405.

[67] Mason, R. L., Tracy, N. D. and Young, J. C. (1996). Monitoring a Multivariate Step Process. *Journal of Quality Technology*, **28**, 39-50.

[68] Mason, R. L., Champ, C. W., Tracy, N. D., Wierda, S. J. and Young, J. C. (1997). Assessment of Multivariate Process Control Techniques. *Journal of Quality Technology*, **29**, 140-143.

[69] McCool, J. I. and Joyner-Motley, T. (1998). Control Charts Application When the Fraction Nonconforming is Small. *Journal of Quality Technology*, **30**, 240-247.

[70] Montgomery, D. C. (2001). *Introduction to Statistical Quality Control.* 4th edition. John Wiley and Sons, Inc., New York.

[71] Montgomery, D. C. and Mastrangelo, C. M. (1991). Some Statistical Process Control Methods for Autocorrelated Data. *Journal of Quality Technology*, **23**, 179-193.

[72] Moore, P. G. (1958). Some Properties of Runs in Quality Control Procedures. *Biometrika*, **45**, 89-95.

[73] Muirhead, R. J. (1982). *Aspects of Multivariate Statistical Theory.* John Wiley and Sons: New York.

[74] Nelson, L. S. (1994). A Control Chart for Parts-Per-Million Nonconforming Items. *Journal of Quality Technology*, **26**, 239-240.

[75] Nelson, L. S. (1989). Standardization of Shewhart Control Charts. *Journal of Quality Control*, **21**, 287-289.

[76] Nelson, L. S. (1984). The Shewhart Control Chart-Tests for Special Causes. *Journal of Quality Technology*, **16**, 237-239.

[77] Page, E.S. (1963). Controlling the Standard Deviation by CUSUM and Warning Lines. *Technometrics*, **5**, 307-315.

[78] Page, E. S. (1962). Cumulative Sum Schemes Using Gauging. *Technometrics*, **4**, 97-109.

[79] Page, E. S. (1961). Cumulative Sum Charts. *Technometrics*, **3**, 1-9.

[80] Page, E. S. (1954). Continuous Inspection Schemes. *Biometrika*, **41**, 100-115.

[81] Prabhu, S. S. and Runger, G. C. (1997). Designing a Multivariate EWMA Control Chart. *Journal of Quality Technology*, **29**, 8-15.

[82] Prins, J. and Mader, D. (1997). Multivariate Control Charts for Grouped and Individual Observations. *Quality Engineering*, **10**, 49-57.

[83] Quesenberry, C. P. (1991). SPC Q Charts for a Binomial Parameter p: Short or Long Runs. *Journal of Quality Technology*, **3**, 239-246.

[84] Reynolds, JR. M. R., Arnold, J. C. and Baik, J. W. (1996). Variable Sampling Interval $\bar{X}$ Charts in the Presence of Correlation. *Journal of Quality Technology*, **28**, 12-30.

[85] Roberts, S. W. (1959). Control Charts tests Based on Geometric Moving Averages. *Technometrics*, **1**, 239-250.

[86] Runger, G. C., Willemain, T. R. and Prabhu, S. (1995). Average Run Lengths for CUSUM Control Charts Applied to Residuals. *Communications in Statistics -Theory and Methods*, **24**, 273-282.

[87] Samanta, B. and Bhattacherjee, A. (2001). An Investigation of Quality Control Charts for Autocorrelated Data. *Mineral Resources Engineering*, **10**, 53-69.

[88] Shewhart, W. A. (1931). *Economic Control of Quality of Manufactured Product.* Van Nostrand Inc., New York.

[89] Snee, R. D. (1990). Statistical Thinking and its Contribution to Total Quality. *American Statistician*, **44**, 116-121.

[90] Sparks, R. S. (2000). CUSUM Charts for Signalling Varying Location Shifts. *Journal of Quality Technology*, **32**, 157-171.

[91] Spiring, F. A. and Cheng, S. W. (1998). An Alternate Variables Control Chart: The Univariate and Multivariate Case. *Statistica Sinica*, **8**, 273-287.

[92] Sultan, T. I. (1986). An Acceptance Chart for Raw Materials of two Correlated Properties. *Quality Assurance*, **12**, 70-72.

[93] Sweet, A. L. (1986). Control Chart Using Coupled EWMA. *Institute of Industrial Engineers Transactions*, **18**, 239-250.

[94] Taguchi, G. and Wu, Y. (1980). *Introduction to Off-line Quality Control.* Romulus, MI: American Supplier Institute.

[95] Tracy, N. D., Young, J. C. and Mason, R. L. (1992). Multivariate Control Charts for Individual Observations. *Journal of Quality Technology*, **24**, 88-95.

[96] VanBrackle III, L. N. and Reynolds, JR. M. R. (1997). EWMA and CUSUM Control Charts in the Presence of Correlation. *Communications in Statistics -Simulation*, **26**, 979-1008.

[97] Van Nuland, Y. (1992-93). ISO 9002 and the Circle technique. *Quality Engineering*, **5**, 269-291.

[98] Vasilopoulus, A. V. and Stamboulis, A. P. (1978). Modification of Control Chart Limits in the Presence of Data Correlation. *Journal of Quality Technology*, **10**, 22-30.

[99] Wardeall, D. G., Moskowitz, H. and Plante, R. D. (1994). Run-Length Distributions of Special-Cause Control Charts for Correlated Processes. *Technometrics*, **36**, 3-17.

[100] Weindling, J. I., Littauer, S. B. and Tiago, D. J. (1970). Mean Action Time of the X-bar Control Chart with Warning Limits. *Journal of Quality Technology*, **2**, 79-85.

[101] Wierda, S. J. (1994). Multivariate Statistical Process Control. PhD. thesis, University of Groningen, The Netherlands.

[102] Wieringa, J. (1998). Statistical Process Control for Serially Correlated Data. PhD. thesis, University of Groningen, The Netherlands.

[103] White, E. M. and Schroeder, R. (1987). A Simultaneous Control Chart. *Journal of Quality Technology*, **19**, 1-10.

[104] Woodall, W. H. (1986). The Design of CUSUM Quality Control Charts. *Journal of Quality Technology*, **18**, 99-102.

[105] Woodall, W. H. (1983). The Distribution of the Run Length of One-Sided CUSUM Procedure for Continuous Random Variables. *Technometrics*, **25**, 295-301.

[106] Woodall, W. H. and Ncube, M. M. (1985). Multivariate CUSUM Quality Control Procedures. *Technometrics*, **27**, 285-292.

[107] Wortham, A. W. and Ringer, L. J. (1971). Control via Exponential Smoothing. *The Logistics Review*, **7**, 33-40.

[108] Xie, H. (1999). Contributions to Qualimetry. PhD. thesis, University of Manitoba, Winnipeg, Canada.

[109] Yashchin, E. (1993). Performance of CUSUM Control Schemes for Serially Correlated Observations. *Technometrics*, **35**, 37-52.

[110] Yeh, A. B., Lin, D. K. -J., Zhou, H. and Venkataraamani, C. (2001). A Multivariate Exponentially Weighted Moving Average Control Chart for Monitoring Process Variabilty. Submitted for publcation, Bowling Green State University, Bowling Green, Ohio.

Appendix A

Computer Programs for the New Charts

A.1 Markov Chain Approach

The CUSUM statistic has the Markov chain property because when given the n^{th} value of the CUSUM statistic, the previous values have no effect on the $(n+1)^{th}$ value of the CUSUM statistic. The ARL's of the CUSUM procedures presented in this thesis are approximated by using a discrete Markov chain proposed by Brook and Evans ([11]) for processes that produce independent observations over time. For autocorrelated processes we use the Markov chain approach of Runger, Willemain and Prabhu ([86]). The possible values of the CUSUM statistic M_i are represented by $t+1$ states. One state is an absorbing state representing $M_i > h$. The remaining t transient states are numbered 0, 1, 2, ..., (t-1) and represent values of M_i between 0 and h. We used a transition matrix of size 100 in our computation but due to space limitation, we provide programs for transition matrix of size 5 below, we assume the mean shift by a and the standard deviation shifts by b. We use matlab Version 6.1 and JMP IN 4 to compute the ARL for the charts proposed in this thesis.

A.1.1 Matlab Program for Computing ARL for CUSUM Charts for Independent Observations

This program computes the ARL of the Max-CUSUM chart with in-control ARL = 250.

h = 3.813;

t = 5;

a = 0;

d = 1;

b = 1;

m = a*d;

s = b*d;

k = a*d/2;

w = 2*h/(2*t-1);

f0 = normcdf(w/2+k,m,s);

f1 = normcdf(-w+w/2+k,m,s);

f2 = normcdf(-2*w+w/2+k,m,s);

f3 = normcdf(-3*w+w/2+k,m,s);

f4 = normcdf(-4*w+w/2+k,m,s);

p0 = normcdf(w/2+k,m,s)-normcdf(-w/2+k,m,s);

p1 = normcdf(w+w/2+k,m,s)-normcdf(w-w/2+k,m,s);

p2 = normcdf(2*w+w/2+k,m,s)-normcdf(2*w-w/2+k,m,s);

p3 = normcdf(3*w+w/2+k,m,s)-normcdf(3*w-w/2+k,m,s);

p4 = normcdf(4*w+w/2+k,m,s)-normcdf(4*w-w/2+k,m,s);

pm1 = normcdf(-w+w/2+k,m,s)-normcdf(-w-w/2+k,m,s);

pm2 = normcdf(-2*w+w/2+k,m,s)-normcdf(-2*w-w/2+k,m,s);

pm3 = normcdf(-3*w+w/2+k,m,s)-normcdf(-3*w-w/2+k,m,s);

$$\mathrm{P}=\begin{bmatrix} f0 & p1 & p2 & p3 & p4 \\ f1 & p0 & p1 & p2 & p3 \\ f2 & pm1 & p0 & p1 & p2 \\ f3 & pm2 & pm1 & p0 & p1 \\ f4 & pm3 & pm2 & pm1 & p0 \end{bmatrix};$$

A = eye(5, 5);

B = [1;1;1;1;1];

x = [1 0 0 0 0];

ARL = x*inv(A-P)*B

A.1.2 JMPIN Simulation Program for Computing the ARL for the SS-CUSUM chart

The following program computes the ARL for the SS-CUSUM chart. For a given in-control ARL of 250, each ARL value is obtained using 10,000 simulations of sample size 4.

h = 3.841

k = 0.5

a = 0

b = 1

c = 0

mu = a*1

s = 1

S = b*1

Add 10,000 rows

$$\text{If Row} = \begin{cases} 1 & RandomSeed(1254237) \\ else & RandomNormal()S + mu \end{cases}$$

Do this for columns 1, 2, 3 and 4

xbar = Mean(1,2,3,4)

std = Std Dev(1,2,3,4)

$z_i = \sqrt{4}\frac{(xbar-c)}{s}$

$y_i = NormalQuantile(ChiSquareDistribution(\frac{n*std^2}{s^2}, n))$

$c_i^+ = Maximum(0, z_i - k + Lag(c_i^+, 1))$

$c_i^- = Maximum(0, Lag(c_i^-, 1) - z_i - k)$

$s_i^+ = Maximum(0, y_i - k + Lag(s_i^+, 1))$

$s_i^- = Maximum(0, Lag(s_i^-, 1) - y_i - k)$

$m_i = Maximum(c_i^+, c_i^-)$

$v_i = Maximum(s_i^+, s_i^-)$

$ss_i = {m_i}^2 + v_i^2$

If $ss_i > h^2$; r $= \begin{cases} 1 \\ else \;\; 0 \end{cases}$

rl = Col Sum(r)

ARL = $\frac{10{,}000}{rl}$

A.1.3 Matlab Program for Computing the ARL for Max-MCUSUM Chart

This program computes the ARL of our single multivariate CUSUM chart where the quality of a product is determined by 5 correlated quality characteristics. The mean vector is assumed to change from good value (Mg) to bad value (Mb). The in-control ARL = 250.

h = 2.037;

t = 5;

b = 1;

a = 0;

$$S = \begin{bmatrix} 1 & 0.1 & 0.1 & 0.1 & 0.1 \\ 0.1 & 1 & 0.1 & 0.1 & 0.1 \\ 0.1 & 0.1 & 1 & 0.1 & 0.1 \\ 0.1 & 0.1 & 0.1 & 1 & 0.1 \\ 0.1 & 0.1 & 0.1 & 0.1 & 1 \end{bmatrix};$$

Mg = [0; 0; 0; 0; 0];

A = [1;1;1;1;1];

Mb = a*A;

m = ((Mb-Mg)'*inv(b*S)*(Mb-Mg))$^{0.5}$;

k = m/2;

s = b;

w = 2*h/(2*t-1);

f0 = normcdf(w/2+k,m,s);

f1 = normcdf(-w+w/2+k,m,s);

f2 = normcdf(-2*w+w/2+k,m,s);

f3 = normcdf(-3*w+w/2+k,m,s);

f4 = normcdf(-4*w+w/2+k,m,s);

p0 = normcdf(w/2+k,m,s)-normcdf(-w/2+k,m,s);

p1 = normcdf(w+w/2+k,m,s)-normcdf(w-w/2+k,m,s);

p2 = normcdf(2*w+w/2+k,m,s)-normcdf(2*w-w/2+k,m,s);

p3 = normcdf(3*w+w/2+k,m,s)-normcdf(3*w-w/2+k,m,s);

p4 = normcdf(4*w+w/2+k,m,s)-normcdf(4*w-w/2+k,m,s);

pm1 = normcdf(-w+w/2+k,m,s)-normcdf(-w-w/2+k,m,s);

pm2 = normcdf(-2*w+w/2+k,m,s)-normcdf(-2*w-w/2+k,m,s);

pm3 = normcdf(-3*w+w/2+k,m,s)-normcdf(-3*w-w/2+k,m,s);

$$\mathrm{P} = \begin{bmatrix} f0 & p1 & p2 & p3 & p4 \\ f1 & p0 & p1 & p2 & p3 \\ f2 & pm1 & p0 & p1 & p2 \\ f3 & pm2 & pm1 & p0 & p1 \\ f4 & pm3 & pm2 & pm1 & p0 \end{bmatrix};$$

A = eye(5, 5);

B = [1;1;1;1;1];

x = [1 0 0 0 0];

ARL = x*inv(A-P)*B

A.1.4 Matlab Program for Computing the ARL for Max-CUSUM Chart for Autocorrelated Observations

This program computes the ARL for a single Max-CUSUM chart for autocorrelated processes when the autocorrelation among observations is equal to 0.4 and 90% of process variation is due to variations in the autocorrelated means. The in-control ARL = 250.

```
h = 3.813;
t = 5;
e = 1;
b=1;
sx = b^2*e;
a = 0;
c = 0.4;
psi = 0.9;
s2 = 1-psi;
s4 = (e-s2)*(1-c^2);
s1 = sx-s4/(1-c^2);
s3 = (sx-s2)*(1-c^2);
d = ((s4+(1+c^2)*s2))/(2*c*s2)-0.5*((((s4+(1+c^2)*s2)/(c*s2))^2-4)^0.5);
k = (1-c)/(1-d)/2;
ka = (a*e)/2;
ma = ((1-c)/(1-d))*a*e;
m = a*e;
S = (e+((c^2-2*c*d+1)/(1-c^2))*(s1-s2)+(s3-s4)/(1-c^2))^0.5;
s = b*e;
w = 2*h/(2*t-1);
f0 = normcdf(w/2+k,m,s);
```

f1 = normcdf(-w+w/2+k,m,s);

f2 = normcdf(-2*w+w/2+k,m,s);

f3 = normcdf(-3*w+w/2+k,m,s);

f4 = normcdf(-4*w+w/2+k,m,s);

p0 = normcdf(w/2+k,m,s)-normcdf(-w/2+k,m,s);

p1 = normcdf(w+w/2+k,m,s)-normcdf(w-w/2+k,m,s);

p2 = normcdf(2*w+w/2+k,m,s)-normcdf(2*w-w/2+k,m,s);

p3 = normcdf(3*w+w/2+k,m,s)-normcdf(3*w-w/2+k,m,s);

p4 = normcdf(4*w+w/2+k,m,s)-normcdf(4*w-w/2+k,m,s);

pm1 = normcdf(-w+w/2+k,m,s)-normcdf(-w-w/2+k,m,s);

pm2 = normcdf(-2*w+w/2+k,m,s)-normcdf(-2*w-w/2+k,m,s);

pm3 = normcdf(-3*w+w/2+k,m,s)-normcdf(-3*w-w/2+k,m,s);

$$\mathrm{P} = \begin{bmatrix} f0 & p1 & p2 & p3 & p4 \\ f1 & p0 & p1 & p2 & p3 \\ f2 & pm1 & p0 & p1 & p2 \\ f3 & pm2 & pm1 & p0 & p1 \\ f4 & pm3 & pm2 & pm1 & p0 \end{bmatrix};$$

F0 = normcdf(w/2+ka,ma,S);

F1 = normcdf(-w+w/2+ka,ma,S);

F2 = normcdf(-2*w+w/2+ka,ma,S);

F3 = normcdf(-3*w+w/2+ka,ma,S);

F4 = normcdf(-4*w+w/2+ka,ma,S);

P0 = normcdf(w/2+ka,ma,S)-normcdf(-w/2+ka,ma,S);

P1 = normcdf(w+w/2+ka,ma,S)-normcdf(w-w/2+ka,ma,S);

P2 = normcdf(2*w+w/2+ka,ma,S)-normcdf(2*w-w/2+ka,ma,S);

P3 = normcdf(3*w+w/2+ka,ma,S)-normcdf(3*w-w/2+ka,ma,S);

P4 = normcdf(4*w+w/2+ka,ma,S)-normcdf(4*w-w/2+ka,ma,S);

Pm1 = normcdf(-w+w/2+ka,ma,S)-normcdf(-w-w/2+ka,ma,S);

Pm2 = normcdf(-2*w+w/2+ka,ma,S)-normcdf(-2*w-w/2+ka,ma,S);

Pm3 = normcdf(-3*w+w/2+ka,ma,S)-normcdf(-3*w-w/2+ka,ma,S);

$$\text{Pa} = \begin{bmatrix} F0 & P1 & P2 & P3 & P4 \\ F1 & P0 & P1 & P2 & P3 \\ F2 & Pm1 & P0 & P1 & P2 \\ F3 & Pm2 & Pm1 & P0 & P1 \\ F4 & Pm3 & Pm2 & Pm1 & P0 \end{bmatrix};$$

A = eye(5, 5);

B = [1;1;1;1;1];

x = [1 0 0 0 0];

ARL = 1+x*P*inv(A-Pa)*B

A.2 ARL for Shewhart-type maximum Charts

The following programs computes the ARL's for the Shewhart-type maximum control charts developed in this thesis.

A.2.1 Matlab Program for Computing the ARL for Max-Mchart

This program computes the ARL for Max-Mchart for bivariate normal processes. Changes in the mean vector and covariance matrix are a and b respectively. For a given in-control ARL of 250, each ARL value is obtained using the distribution of M_i.

$$\text{S}=\begin{bmatrix} 1 & 0.6 \\ 0.6 & 1 \end{bmatrix};$$

M = [1 1];

n = 4;

```
b = 1;
a = 0;
m = a*M;
ucl = 3.023;
l = n*(m*inv(b*s)*m');
c = ncx2cdf(chi2inv(normcdf(ucl),2)/b^2,2,l)
    -ncx2cdf(chi2inv(normcdf(-ucl),2)/b^2,2,l);
d = chi2cdf((chi2inv(normcdf(ucl),2*n-4))/b^2,2*n-4)
    -chi2cdf((chi2inv(normcdf(-ucl),2*n-4))/b^2,2*n-4);
e = c*d;
ARL = 1/(1-e)
```

A.2.2 JMPIN Simulation Program for Computing the ARL for Max-chart for Autocorrelated Data

The following program computes the ARL for the Max-chart for autocorrelated processes. For a given in-control ARL of 250, each ARL value is obtained using 10,000 simulations of sample size 4. This program is for the case when autocorrelation among observations is equal to 0.4 and 90% of process variation is due to variations in the autocorrelated means.

```
UCL = 3.2049
e = 1
b=1
sx = b^2*e
a = 0
c = 0.4
psi = 0.9
s2 = 1-psi
```

s4 = (e-s2)*(1-c^2)

s1 = sx-s4/(1-c^2)

s3 = (sx-s2)*(1-c^2)

d = ((s4+(1+c^2)*s2))/(2*c*s2)-0.5*((((s4+(1+c^2)*s2)/(c*s2))^2-4)$^{0.5}$)

mu = ((1-c)/(1-d))*a*e

S = (e+((c^2-2*c*d+1)/(1-c^2))*(s1-s2)+(s3-s4)/(1-c^2))$^{0.5}$

Add 10,000 rows

If Row = $\begin{cases} 1 & RandomSeed(1254237) \\ else & RandomNormal()S + mu \end{cases}$

Do this for columns 1, 2, 3 and 4

xbar = Mean(1,2,3,4)

std = Std Dev(1,2,3,4)

$Z_i = \sqrt{4}\frac{(xbar-mu)}{e}$

$Y_i = NormalQuantile(ChiSquareDistribution(\frac{n*std^2}{e^2}, n))$

m = Maximum($\mid z \mid, \mid y \mid$)

If $m > UCL$; r = $\begin{cases} 1 \\ else \;\; 0 \end{cases}$

rl = Col Sum(r)

ARL = $\frac{10{,}000}{rl-1}$

A.2.3 Matlab Program for Computing the In-control ARL's for Attributes Charts

This program computes the in-control ARL by first computing the false alarm rates and then computing the in-control ARL as the reciprocal of the false alarm rates.

n = 40000;

p = 0.00001;

```
x = n*p-3*sqrt(n*p*(1-p));
xb = n*p+3*sqrt(n*p*(1-p));
xp = n*p-3*sqrt(n*p);
xup = n*p+3*sqrt(n*p);
xn = n*p-3*sqrt(n*p*(1-p));
norl = norminv(binocdf(xn,n,p));
lclnor = normcdf(norl,0,1);
xun = n*p+3*sqrt(n*p*(1-p));
noru = norminv(binocdf(xun,n,p));
uclnor = 1-normcdf(noru,0,1);
ARL(normal) = 1/(lclnor+uclnor);
lclbino = binocdf(x,n,p);
uclbino = 1-binocdf(xb,n,p);
ARL(binomial) = 1/(lclbino+uclbino);
lclpois = poisscdf(xp,n*p);
uclpois = 1-poisscdf(xup,n*p);
ARL(poisson) = 1/(lclpois+uclpois);
```